AD NUMBER

AD864702

LIMITATION CHANGES

TO:

Approved for public release; distribution is unlimited.

FROM:

**Distribution authorized to U.S. Gov't. agencies and their contractors;
Administrative/Operational Use; FEB 1970. Other requests shall be referred to Arnold Engineering Development Center, Arnold AFB, TN.**

AUTHORITY

AEDC ltr 26 Apr 1973

FLOW FIELD CHARACTERISTICS BENEATH THE F-4C AIRCRAFT AT MACH NUMBERS 0.50 AND 0.85

Ronald E. Davis

ARO, Inc.

February 1970

PROPULSION WIND TUNNEL FACILITY
ARNOLD ENGINEERING DEVELOPMENT CENTER
AIR FORCE SYSTEMS COMMAND
ARNOLD AIR FORCE STATION, TENNESSEE

NOTICES

When U. S. Government drawings specifications, or other data are used for any purpose other than a definitely related Government procurement operation, the Government thereby incurs no responsibility nor any obligation whatsoever, and the fact that the Government may have formulated, furnished, or in any way supplied the said drawings, specifications, or other data, is not to be regarded by implication or otherwise, or in any manner licensing the holder or any other person or corporation, or conveying any rights or permission to manufacture, use, or sell any patented invention that may in any way be related thereto.

Qualified users may obtain copies of this report from the Defense Documentation Center.

References to named commercial products in this report are not to be considered in any sense as an endorsement of the product by the United States Air Force or the Government.

FLOW FIELD CHARACTERISTICS BENEATH THE F-4C AIRCRAFT AT MACH NUMBERS 0.50 AND 0.85

Ronald E. Davis
ARO, Inc.

FOREWORD

The work reported herein was sponsored by the Air Force Armament Laboratory (AFATL), Air Force Systems Command (AFSC), under Program Element 63716F, System 670A.

The test results presented were obtained by ARO, Inc. (a subsidiary of Sverdrup & Parcel and Associates, Inc.), contract operator of the Arnold Engineering Development Center (AEDC), AFSC, Arnold Air Force Station, Tennessee, under Contract F40600-69-C-0001. The tests were conducted during the period September 18 to 23, 1969, under ARO Project No. PC0017, and the manuscript was submitted for publication on December 8, 1969.

This technical report has been reviewed and is approved.

George F. Garey
Lt Colonel, USAF
AF Representative, PWT
Directorate of Test

Roy R. Croy, Jr.
Colonel, USAF
Director of Test

ABSTRACT

Tests were conducted to investigate the flow field characteristics beneath the F-4C aircraft at high subsonic speeds. A conical-tip probe was used to measure the velocity-vector components in the region near the aircraft at Mach numbers 0.50 and 0.85. Aerodynamic force and moment data were obtained on a model of the M-117 bomb both near the aircraft and in the free stream to further evaluate the flow field. Data were obtained with a clean-wing aircraft configuration and with several combinations of M-117 bombs on the inboard wing-pylon station plus a fuel tank on the outboard wing-pylon station. Results of the test indicated that a larger region of the flow beneath the F-4C model wing is affected by store addition at Mach number 0.85 than at Mach number 0.50. Also, in some regions of the curvilinear flow field near the wing, a pitching-moment couple was produced on the store model when the model was aligned for zero normal force.

CONTENTS

APPENDIXES

I. ILLUSTRATIONS

Figure

Page

II. TABLES

NOMENCLATURE

BL	Aircraft buttock line from plane of symmetry, model scale (Fig. 12), in.
C_m	Pitching-moment coefficient, pitching moment/$q_\infty Sd$
C_N	Normal-force coefficient, normal force/$q_\infty S$
d	Model diameter, 0.80 in.
ℓ	Model length, 4.375 in.
MS	Model station from nose aircraft, model scale, in. (Fig. 12)
M_∞	Free-stream Mach number
q_∞	Free-stream dynamic pressure, psf
S	Model cross-sectional area, 0.00349-in.^{2} model scale
V_{YZ}	Velocity component in plane normal to tunnel free-stream flow direction, ft/sec
V_∞	Free-stream velocity, ft/sec
WL	Aircraft waterline from reference horizontal plane, model scale (Fig. 12), in.
X	M-117 bomb model cg location measured from bomb carriage position in a direction parallel to the F-4C model longitudinal axis, positive direction upstream, model scale, in.
Y	M-117 bomb model cg location measured from bomb carriage position in a direction perpendicular to the F-4C model plane of symmetry, positive direction to the right looking upstream as seen by pilot, model scale, in.

Z M-117 bomb model cg location measured from bomb carriage position in a direction normal to the F-4C model longitudinal and lateral axes, positive direction down as seen by pilot, model scale, in.

ϵ Probe indicated angle between projection of local flow velocity vector onto vertical plane through tunnel longitudinal axis, and tunnel longitudinal axis, positive for a velocity-vector component in the negative Z_W direction, deg

η Store model angle of yaw, positive nose right as seen by pilot measured from vertical plane through the tunnel longitudinal axis, deg

$\overline{\eta}$ $\eta - \eta_N$, deg

η_N Store model null angle of yaw; angle for which side-force coefficient is zero, deg

ν Store model angle of attack positive nose up as seen by pilot measured from tunnel X-axis, deg

$\overline{\nu}$ $\nu - \nu_N$, deg

ν_N Store model null angle of attack; angle for which normal-force coefficient is zero, deg

σ Probe indicated angle between local velocity vector and projection of local velocity vector onto a vertical plane through tunnel longitudinal axis, positive for a velocity-vector component in negative Y_W direction, deg

WIND-AXIS SYSTEM

X_W Parallel to the wind tunnel centerline, positive forward

Y_W Perpendicular to the X_W-axis in the horizontal plane of the wind tunnel, positive to the right looking upstream

Z_W Perpendicular to the X_W- and Y_W-axes in the vertical plane of the wind tunnel, positive down

SECTION I
INTRODUCTION

The static stability characteristics of aircraft store payloads as determined from free-stream wind tunnel tests may differ from the store stability characteristics in the curvilinear flow field beneath the aircraft wing. An investigation concerning the above phenomenon was conducted in Propulsion Wind Tunnel, Transonic (4T) at AEDC. Velocity-vector flow field data and M-117 bomb static stability data were obtained in the vicinity of the F-4C aircraft. The velocity-vector data provide a description of the flow field beneath the wing when the M-117 bomb payload is in the carriage position. The static-force and moment data in the presence of the F-4C aircraft are compared with corresponding free-stream data to determine the effect of the curvilinear flow field on store stability characteristics.

To simulate the flow field beneath the F-4C aircraft wing, a 1/20-scale model of the F-4C aircraft was mounted on the primary model support system. The velocity-vector data were obtained by mounting a 40-deg conical flow probe on a sting attached to the Captive Trajectory System (CTS), which positioned the probe at points in a three-dimensional space beneath the F-4C model wing. The static stability data in the presence of the F-4C model were obtained by mounting the M-117 bomb model on a six-component strain-gage balance and sting combination attached to the CTS which also positioned the store cg at points in a three-dimensional space beneath the F-4C model. The free-stream static stability data were obtained with the 1/20-scale F-4C model removed from the test section and with the M-117 bomb model positioned on the tunnel centerline.

SECTION II
APPARATUS

2.1 TEST FACILITY

Tunnel 4T is a closed-loop, continuous flow, variable density tunnel. It is capable of operating at Mach numbers from 0.10 to 1.40 with a variable stagnation pressure from 300 to 3700 psfa at all Mach numbers. The test section is 4 ft square and 12.5 ft long with variable porosity walls (0.5 to 10 percent). The test section is completely enclosed in a plenum chamber from which the air can be evacuated, thus allowing part of the tunnel airflow to be removed through the test section

walls. This design allows control of wave attenuation and blockage effects. A more complete description of the test facility can be found in the Test Facilities Handbook.[1]

2.2 TEST ARTICLES

The general arrangement of the 1/20-scale F-4C model and CTS sting used during the flow field investigation is shown in Fig. 1 (Appendix I). The F-4C model was pitched to an angle of attack of 0.30 deg. The sting-mounted store represents either the flow probe or the M-117 bomb model. A typical dual-model installation is shown in Fig. 2, although not specifically one of the present configurations tested. For flow field definition testing, the F-4C configurations consisted of various combinations of the inboard pylon, Triple Ejection Rack (TER), M-117 dummy stores, and a 370-gal dummy outboard fuel tank. Shown in Figs. 3, 4, 5, and 6 are dimensional sketches of models of the inboard and outboard pylons, TER, sting-mounted M-117 bomb, and 370-gal fuel tank, respectively, used for this investigation. The M-117 bomb model which is mounted on the CTS sting is slightly different in shape from the TER-supported, dummy M-117 bomb models in the afterbody region. The dummy stores represent the actual M-117 bomb shape. The three configurations used to obtain the velocity-vector flow field data are shown in Fig. 7, and the two configurations used to obtain the F-4C flow field effects on the bomb model stability data are shown in Fig. 8. A sketch of the M-117 bomb installation as used in Configuration C, with various MS locations indicated, is shown in Fig. 9.

2.3 INSTRUMENTATION

The 40-deg conical probe used to obtain the flow field velocity-vector data was designed and calibrated using established methods.[2] A view of the probe is shown in Fig. 10, and dimensional details of the probe tip are shown in Fig. 11.

A five-component, internal, strain-gage balance was used to obtain the force and moment data on the M-117 bomb store model. Both the

---

[1]Test Facilities Handbook (Eighth Edition). "Propulsion Wind Tunnel Facility, Vol. 5." Arnold Engineering Development Center, December 1969.

[2]Black, J. A., Carleton, W. E., and Anderson, C. F. "Calibration of Four Conically Tipped Flow Survey Rakes at Transonic Speeds." AEDC-TDR-63-134 (AD409079), July 1963.

probe and M-117 store model were mounted on the CTS sting support, which had an electrical fouling circuit to indicate contact with the F-4C model or tunnel wall.

SECTION III
TEST DESCRIPTION

3.1 TEST PROCEDURE

The regions beneath the F-4C aircraft wing where velocity-vector (Phase I) and M-117 bomb static stability (Phase II) data were obtained are shown in Fig. 12. For both Phase I and II testing, the flow-angle probe and M-117 bomb were traversed in the F-4C model-axis system which, as stated earlier, was pitched a positive 0.30 deg. During testing for these two phases, tunnel conditions were established, and the probe tip or the M-117 bomb model cg was positioned at a known coordinate point relative to the F-4C model. At this position, initial-point data were taken which oriented the computer program controlling the CTS sting movement in the F-4C model-axis system. The initial data point for Phase II testing was the carriage position of the M-117 bomb model for the configuration of interest, as shown in Fig. 8. The dynamic pressure was held constant at 500 and 300 psf during the Phase I and II tests, respectively.

After the initial data point was recorded, the computer automatically positioned the CTS sting at desired positions in the region of interest for a given configuration.

At each coordinate point, during the Phase II test period, the M-117 bomb model was simultaneously pitched and yawed until the normal- and side-force coefficients were approximately zero. Data were then recorded while moving the model through pitch polars from -5 to 5 deg at each of several constant yaw angles from -5.0 to 5.0 deg. The M-117 bomb model free-stream static stability data (Phase III) were recorded while moving the model through a pitch polar from -10 to 10 deg at each of several constant yaw angles from 0 to 10 deg.

3.2 CORRECTIONS

Balance and sting deflections caused by the aerodynamic loads on the store model were accounted for in the data reduction program to determine the true model angle of attack. Corrections were also made for model weight tares to calculate net aerodynamic forces on the model.

3.3 PRECISION OF MEASUREMENTS

Uncertainties in the data were calculated taking into consideration probable inaccuracies in balance measurements and tunnel conditions. The uncertainties are based on a 95-percent confidence level and are listed below.

C_N	C_m	q_∞, psfa	V_∞, ft/sec	V_{YZ}, ft/sec	X, in.	Y, in.	Z, in.	ν, deg	η, deg	ϵ, deg	σ, deg
±0.02	±0.004	±8.0	±5.0	±2.0	±0.05	±0.05	±0.05	±0.15	±0.15	±0.15	±0.15

The estimated uncertainty in setting Mach number was no greater than ±0.005. Tunnel calibrations indicate that the Mach number variation in the area of the tunnel occupied by the model is no greater than ±0.004.

SECTION IV
RESULTS AND DISCUSSION

The primary purpose of this investigation was to obtain velocity-vector flow field and M-117 bomb static stability data to be used in conjunction with the development of a theoretical and empirical method for the prediction of store trajectories while the store is in the aircraft-influenced flow field. Some representative results of the present investigation will be presented here.

The most extreme flow deflection conditions beneath the wing were obtained with aircraft Configuration C. The projection (V_{YZ}) of the local flow velocity vector onto a plane normal to the tunnel flow will reflect the direction and magnitude of the transverse forces acting on a separating store. The V_{YZ} magnitudes and directions for Configuration C as compared to Configuration A are shown in Figs. 13 through 22 for Mach number 0.50 and in Figs. 23 through 32 for Mach number 0.85 for model stations (MS) 9 through 18. The cross section at MS 15 of the pylons, TER, bombs, and fuel tank for Configuration C is shown in the figures. The presence of velocity-vector components transverse to the aircraft-model plane of symmetry for Configuration A is caused by the collective uncertainties in pressure measurement, CTS sting orientation, F-4C model orientation and symmetry, tunnel flow angularity, and flow-probe calibration. Inspection of the flow field data of Figs. 13, 14, 23, and 24 indicates an engine-inlet spillage effect at MS 9 and 10 in the region near the wing. In general, the flow patterns at Mach numbers 0.50 and 0.85 are similar for a given configuration. Between MS 9

and 15, the overall effect of the Configuration C store additions to the wing is a more pronounced downwash in the region from WL -1.0 to WL -4.5 at Mach number 0.50 and correspondingly from WL -1.0 to WL -8.5 for Mach number 0.85. The effect of the M-117 bomb stores on the flow field at both Mach numbers is clearly illustrated by observing the flow patterns at successive MS positions.

The effect of a curvilinear flow field on store stability characteristics can be demonstrated by comparisons of force and moment coefficient data obtained on the store model in the F-4C model flow field with the same data obtained in the uniform free-stream flow. As mentioned in Section 3.1, the Phase II stability data were obtained after first orienting the M-117 bomb model in the position that reduced the normal force and side force to zero (null position). The null orientation of the model was taken as zero pitch and yaw, and data were obtained by pitching and yawing the model from the null position. The null pitch and yaw angles for Configurations D and E are given in Table I (Appendix II) and are seen to vary considerably with both Mach number and store position relative to the aircraft. The existence of nonzero moments acting on the model under conditions of zero forces indicates the existence of a couple acting on the model produced by the curvilinear flow field about the aircraft model.

The normal-force coefficient data for the M-117 bomb in the free stream and in the flow field beneath aircraft Configuration D at Mach numbers of 0.50 and 0.85 are shown in Figs. 33 and 34, respectively. The M-117 bomb model roll angle was 45 deg (fins in vertical and horizontal planes) for the free-stream and Configuration D tests but was zero for the Configuration E test. Therefore, direct comparisons can only be made between free-stream and Configuration D data. The data show that the flow field beneath the F-4C model does not produce any significant change in the variation of normal-force coefficient with pitch angle. Note that the data have been plotted against $\overline{\nu}$ to accentuate the similarity in slopes.

The pitching-moment coefficient data for the M-117 bomb in the free stream and in the flow field beneath aircraft Configuration D at Mach numbers of 0.50 and 0.85 are shown in Figs. 35 and 36, respectively. The effects of the flow field on the M-117 bomb model pitching-moment data are most pronounced at X = 0 and small values of Z, which correspond to bomb cg locations directly below and near the bomb carriage position on the TER and consist primarily of a small negative (nose down) shift in the trim angle (C_m = 0) with little or no change in slope. The effects decrease as the model moves out of the nonuniform flow field. At X = -5.00, the pitching-moment coefficients, relative to

those in free stream, are not affected significantly by the flow field under the F-4C model wing.

Since Configurations B and E have identical wing stores, the flow angles determined at similar positions beneath aircraft Configuration B should be in general agreement with the null angles obtained beneath aircraft Configuration E. Shown in Table II is a comparison of indicated flow and null angles for Configurations B and E at three probe and cg locations that are close to each other. The data in the table indicate general agreement between the flow and null angles in the region where the M-117 bomb model is located.

The data presented herein show that the flow field near the aircraft is rather complex, particularly when external stores are carried. However, it does appear possible to develop a rather simple method of predicting store loads from free-stream store aerodynamic data, once the flow field has been described. The prediction method would require an adjustment in effective pitch and yaw angles related to the local flow direction and an increment in the pitching- and yawing-moment coefficients related to the local streamline curvature.

SECTION V
SUMMARY

The following observations were made from the significant results of this investigation:

1. The flow field data indicate that the addition of stores to the F-4C model wing affects a greater region of the flow beneath the wing at Mach number 0.85 than at 0.50. Specifically, the addition of stores to the wing produces a general increase in downwash from WL -1.00 to -4.50 at Mach number 0.50 and correspondingly from WL -1.00 to -8.50 at Mach number 0.85.

2. The curvilinear flow field beneath the F-4C model wing produced two effects on the aerodynamic data for the M-117 bomb. The null pitch and yaw angles ($C_N = C_Y = 0$) varied with position of the store relative to the aircraft, and the trim pitch angle ($C_m = 0$) did not in general correspond to the null pitch angle. These conditions were most significant when the store was near the carriage position on the TER and diminished with store movement rearward and downward.

3. The flow field and aerodynamic data comparisons indicate the possibility of developing an empirical method for predicting store loads based on local flow field velocity-vector data and free-stream store aerodynamic data.

APPENDIXES
I. ILLUSTRATIONS
II. TABLES

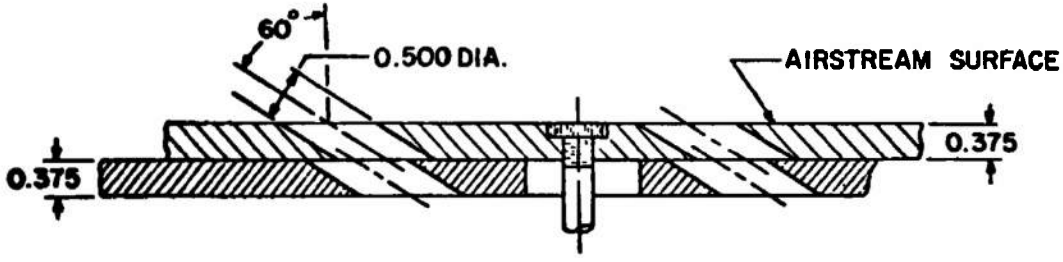

TYPICAL PERFORATED WALL CROSS SECTION

NOTE: TUNNEL STATIONS AND DIMENSIONS ARE IN INCHES

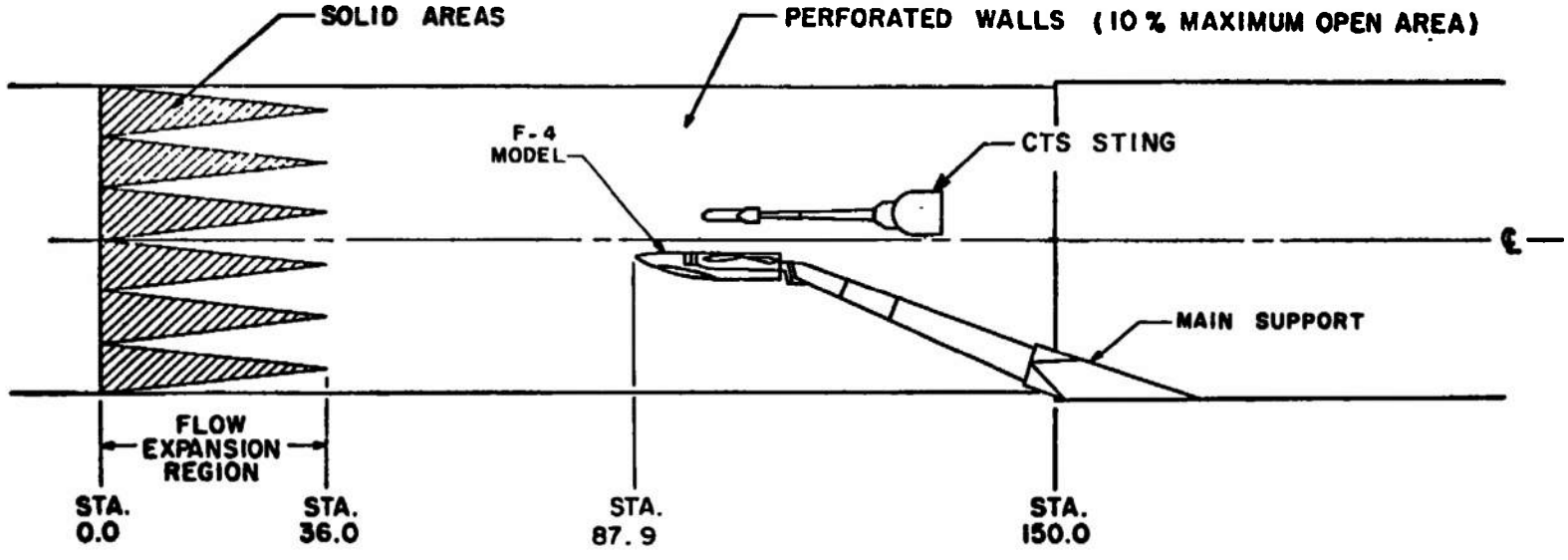

Fig. 1 Schematic of the Tunnel Test Section Showing Model Location

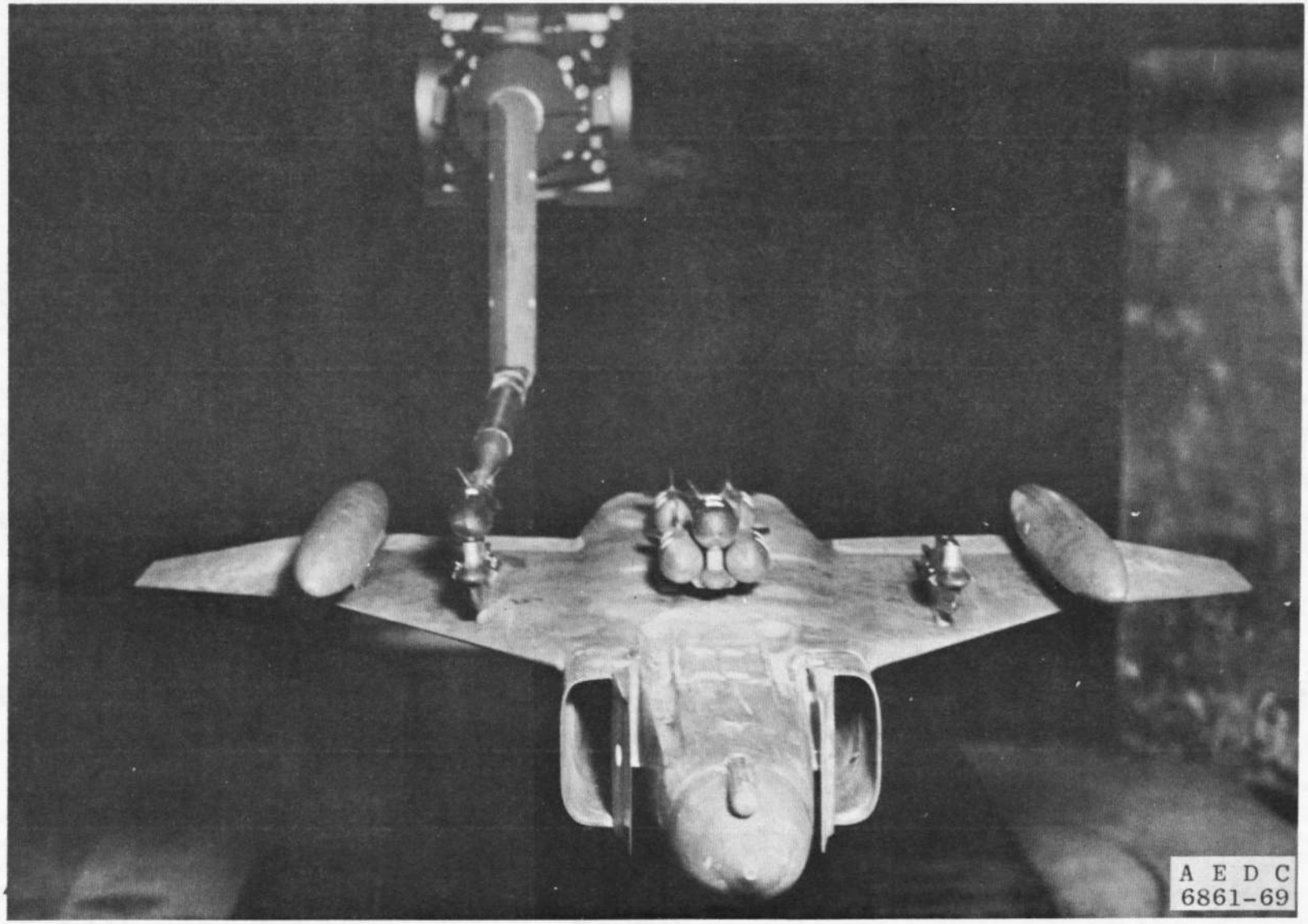

Fig. 2 Typical Tunnel Installation of 1/20-Scale F-4C Aircraft and CTS Sting-Mounted Store

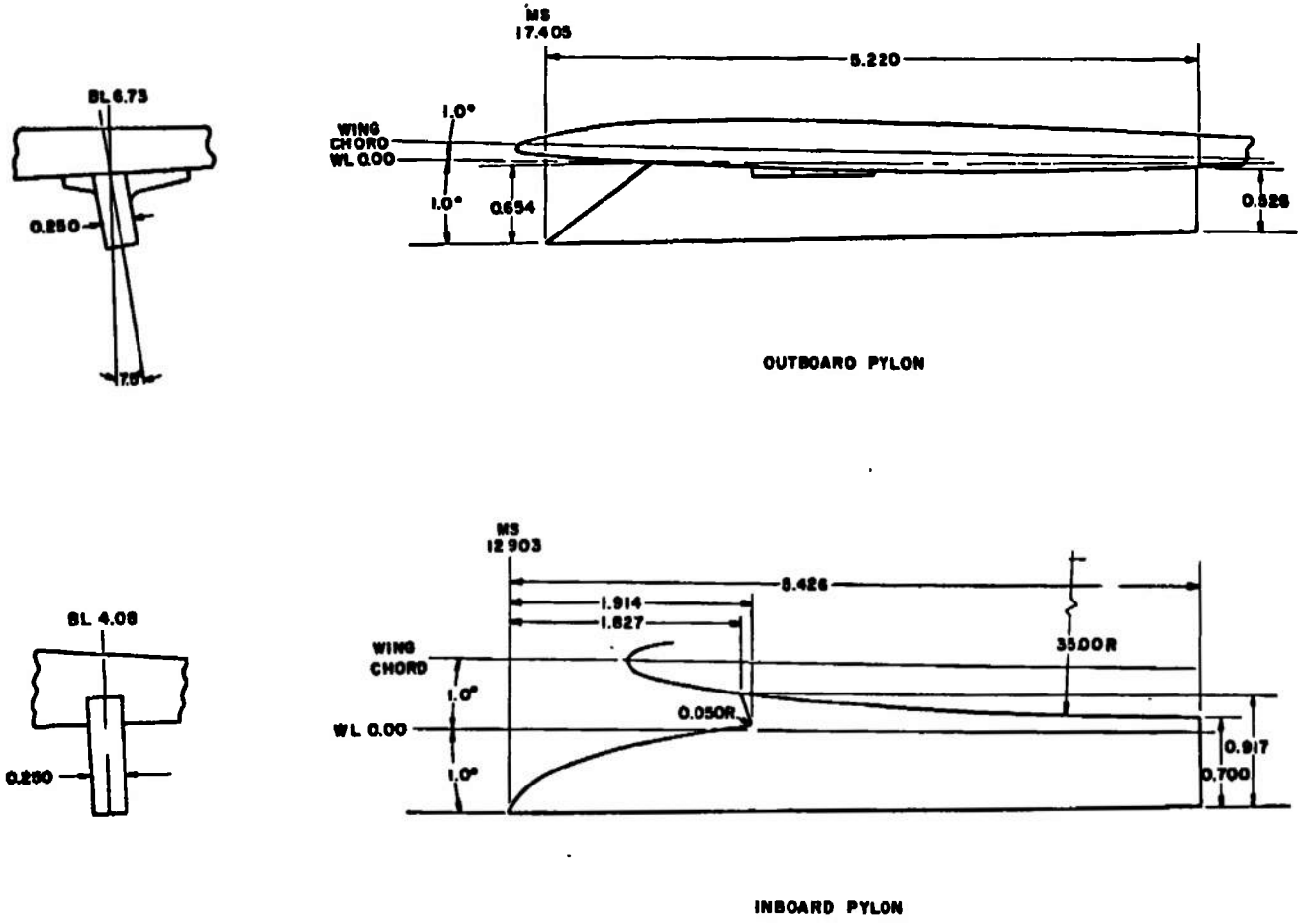

NOTE: All dimensions in inches

Fig. 3 Dimensional Sketch of Inboard and Outboard Pylon Models

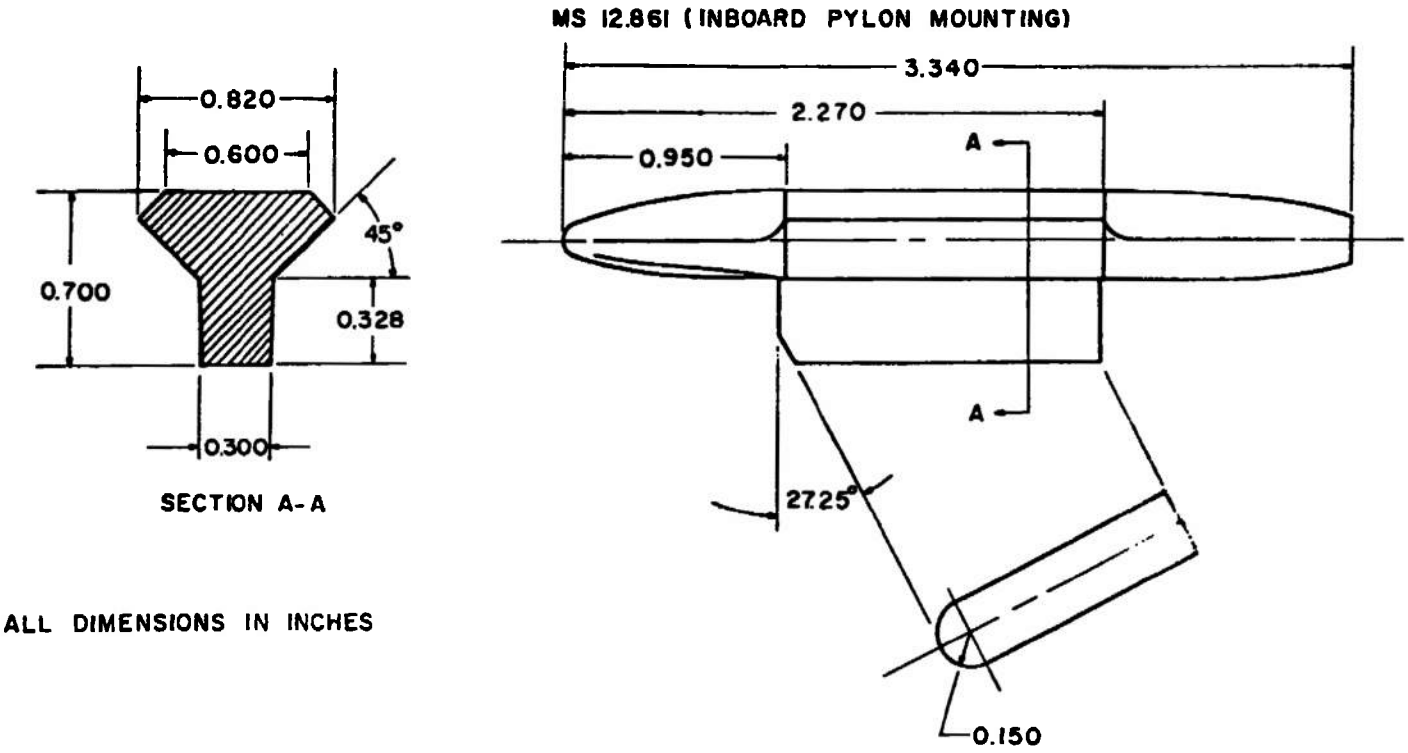

Fig. 4 Dimensional Sketch of TER Model

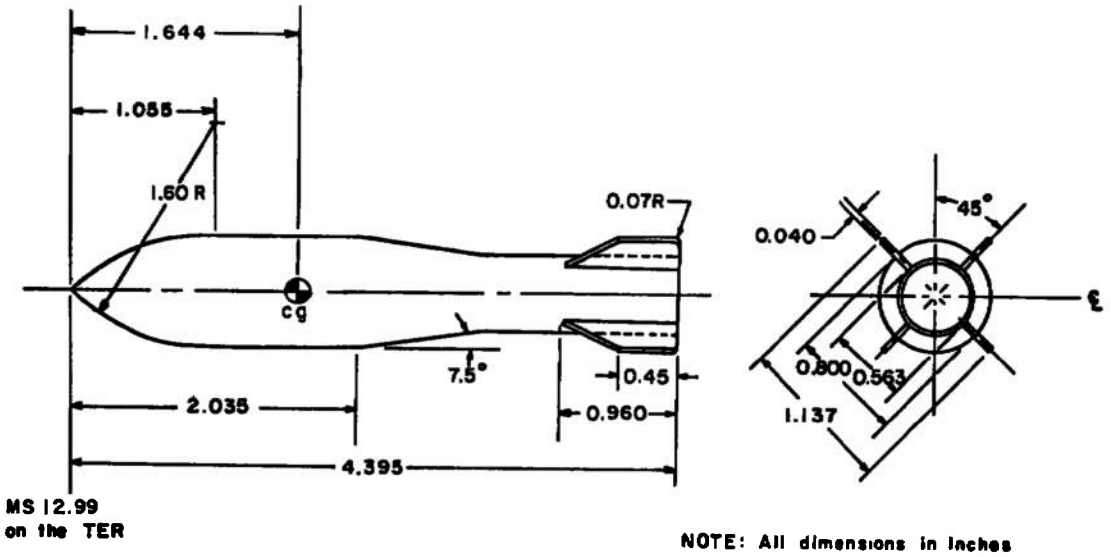

Fig. 5 Dimensional Sketch of 1/20-Scale M-117 Bomb Model

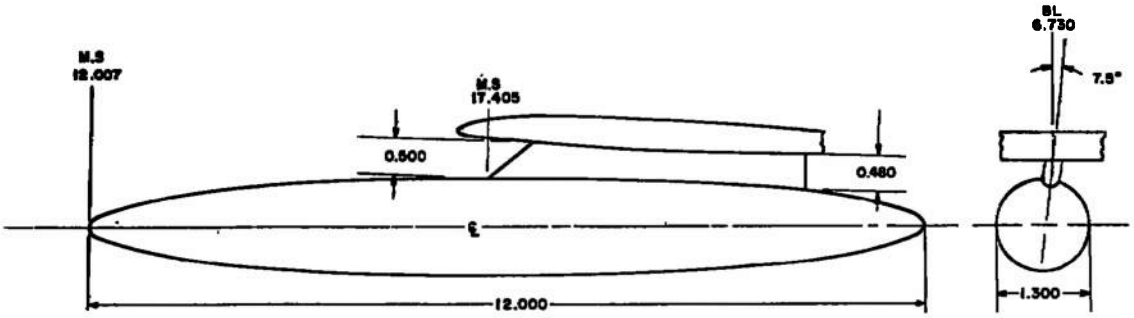

BODY CONTOUR, TYPICAL BOTH ENDS

STATION	BODY DIAM	STATION	BODY DIAM
0.000	0.000	2.500	1.118
0.025	0.100	2.750	1.156
0.050	0.144	3.000	1.190
0.150	0.258	3.250	1.218
0.250	0.340	3.500	1.242
0.500	0.498	3.750	1.260
0.750	0.622	4.000	1.274
1.000	0.724	4.250	1.286
1.250	0.812	4.500	1.294
1.500	0.890	4.750	1.298
1.750	0.958	5.000	1.300
2.000	1.016	6.000	1.300
2.250	1.070		

Fig. 6 Dimensional Sketch of 370-gal Fuel Tank Model

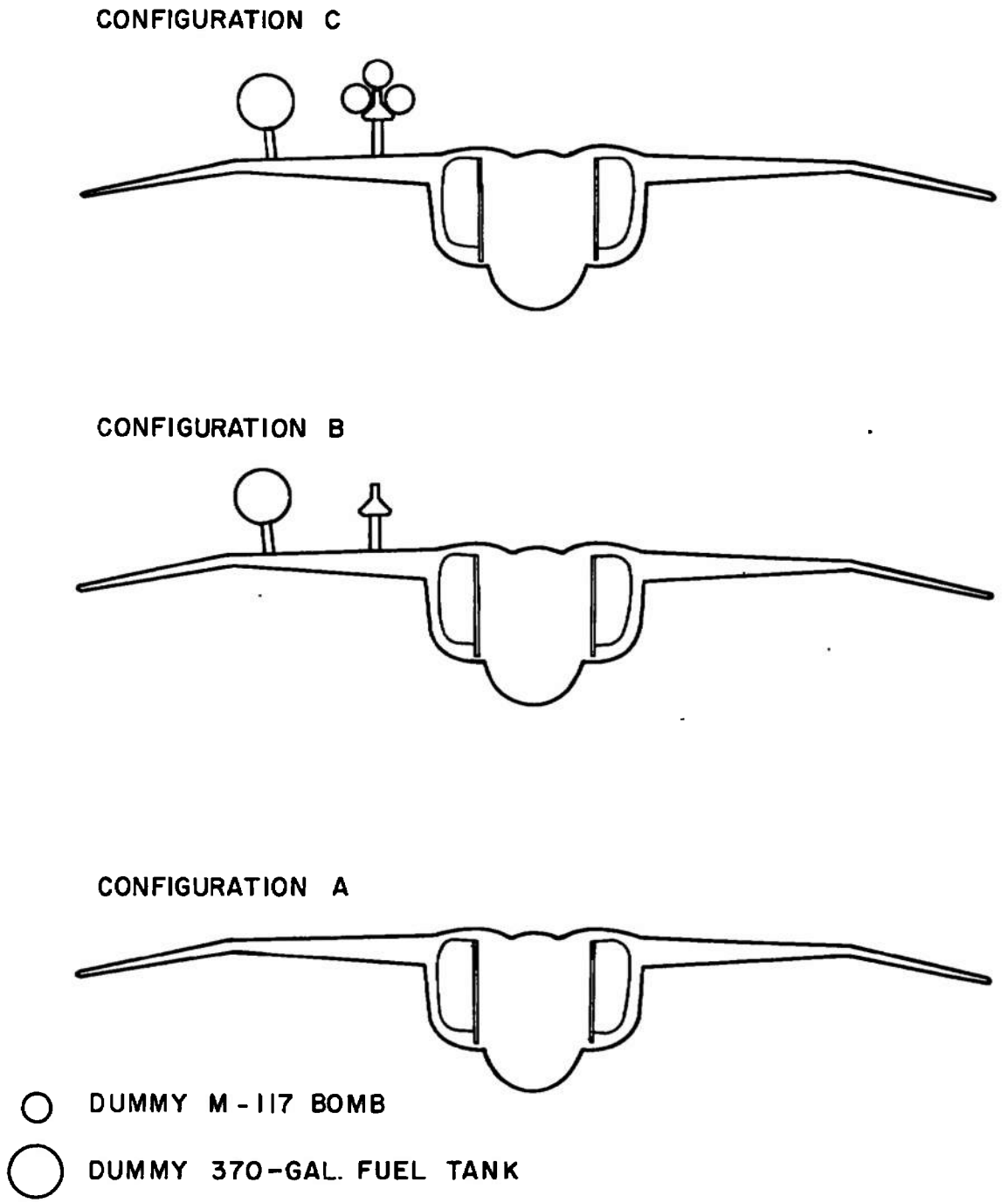

Fig. 7 1/20-Scale F-4C Aircraft Configurations Used for Flow Field Definition Testing

CONFIGURATION E

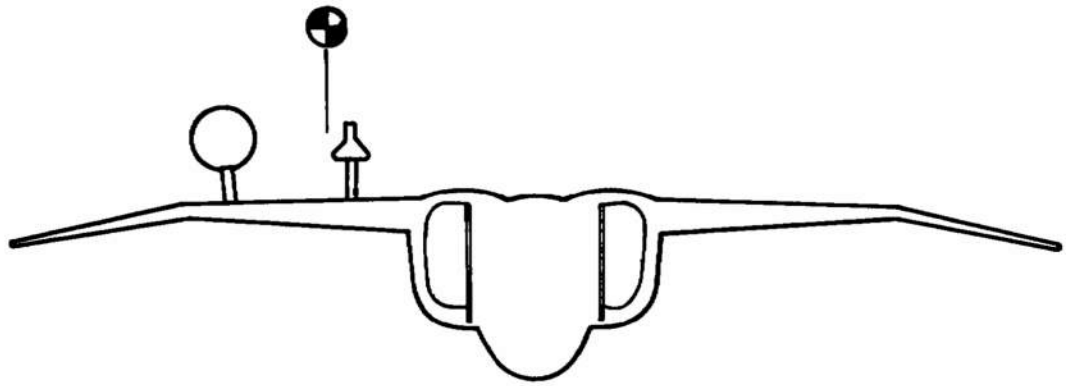

CONFIGURATION D

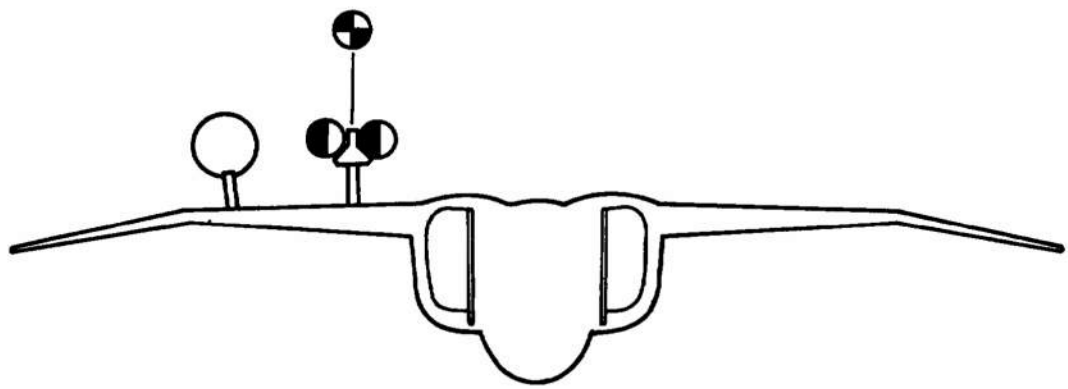

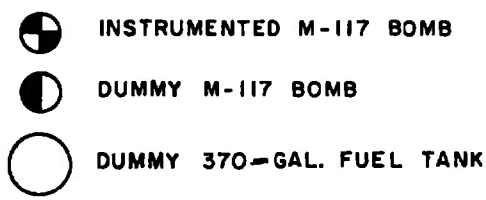

Fig. 8 1/20-Scale F-4C Aircraft Wing Configurations Used for Aerodynamic Testing

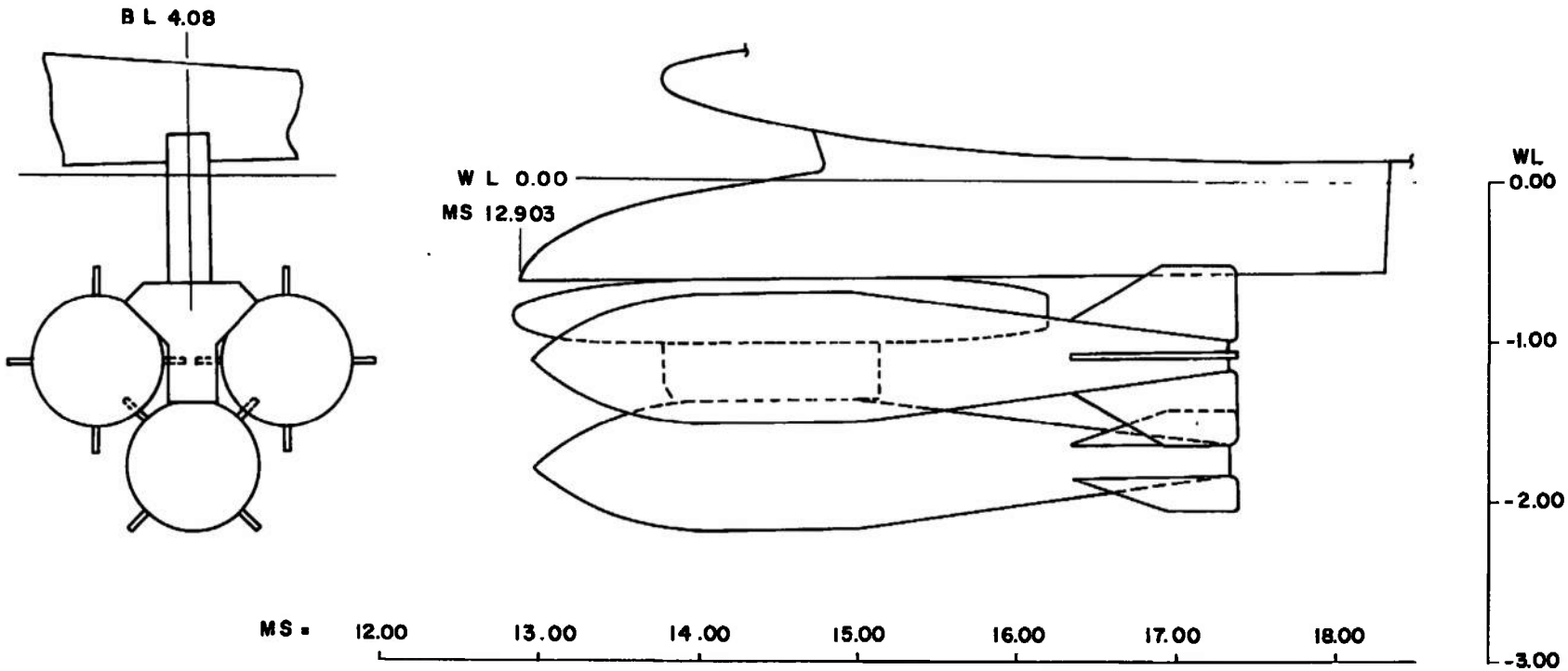

NOTE: All dimensions in inches

Fig. 9 Sketch of M-117 Bomb Store Installation for Configuration C

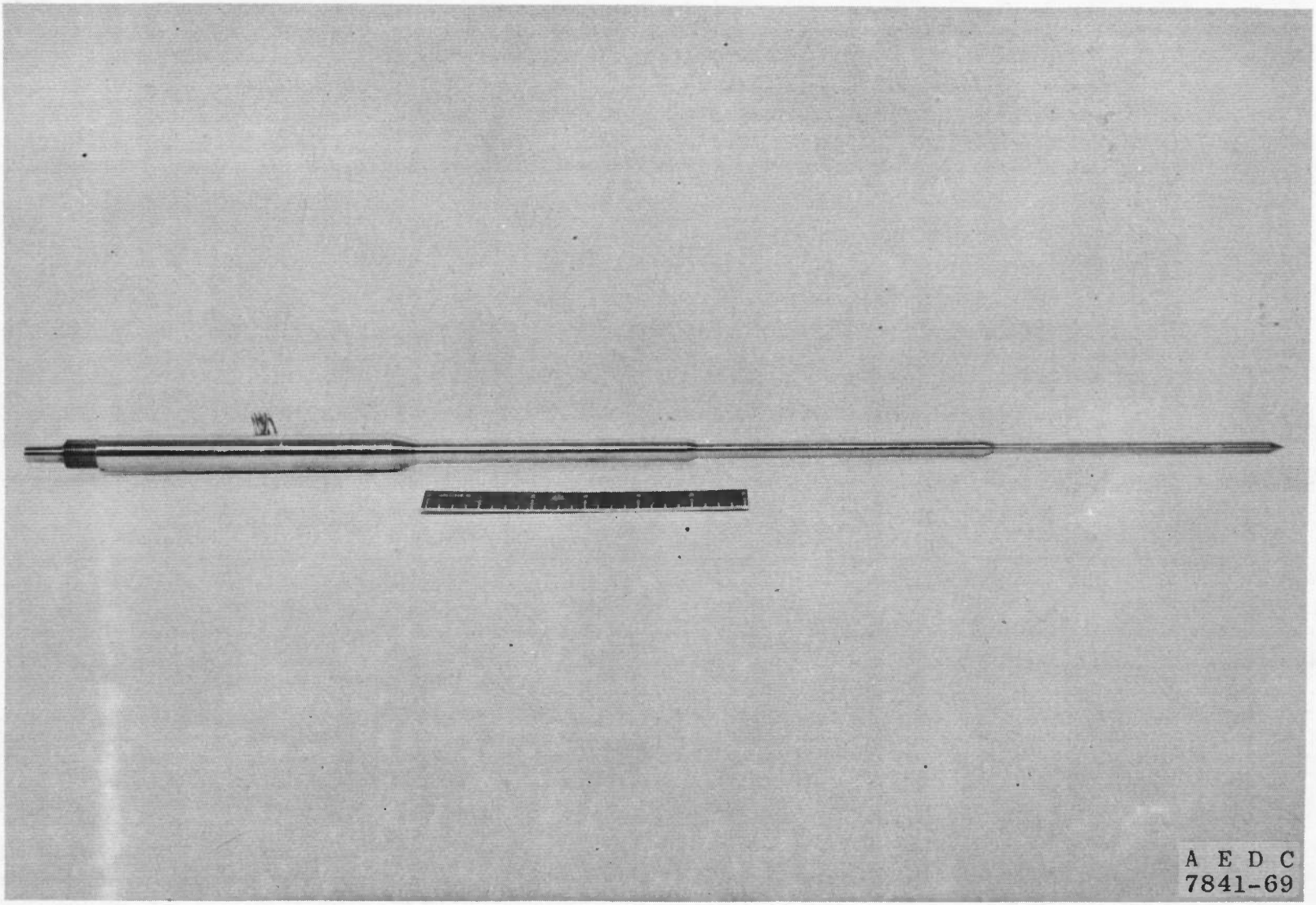

Fig. 10 View of 40-deg Conical Probe Used for Flow Field Definition Testing

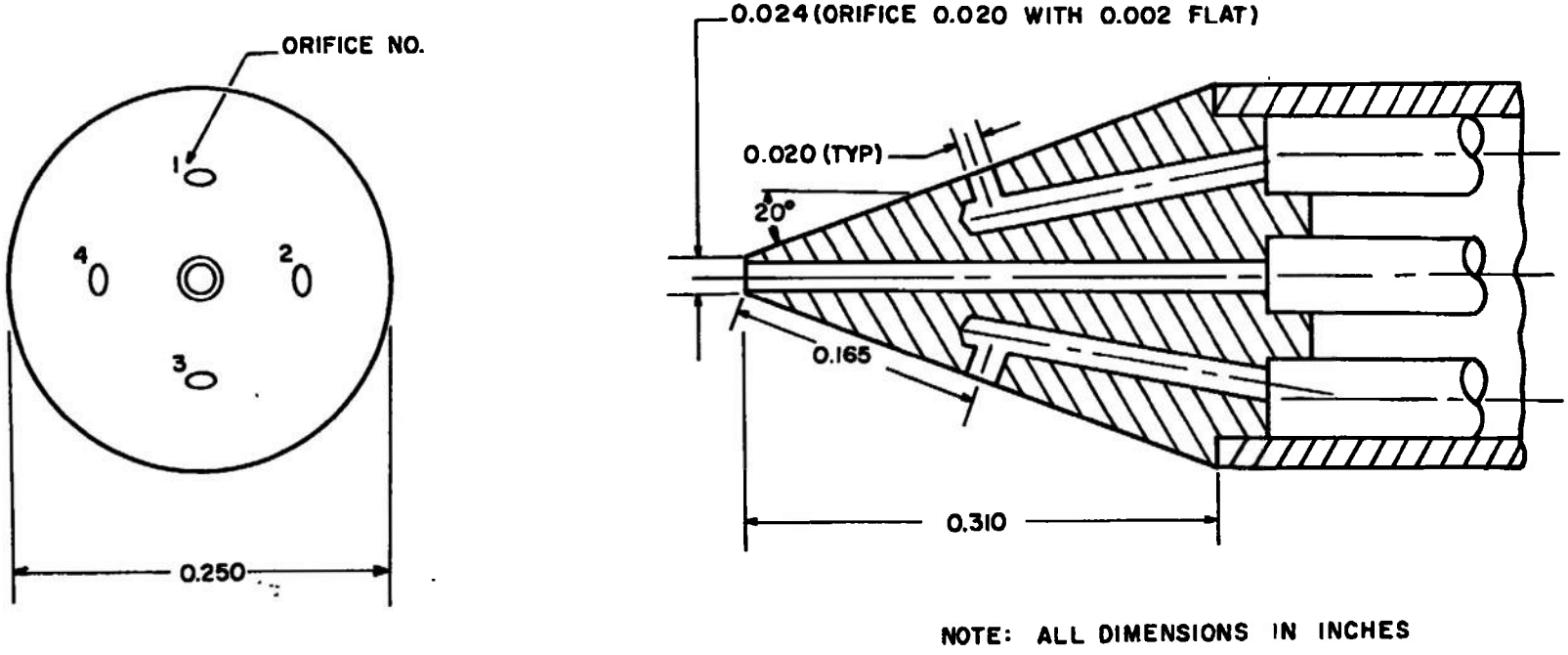

Fig. 11 Details of 40-deg Conical Probe Tip

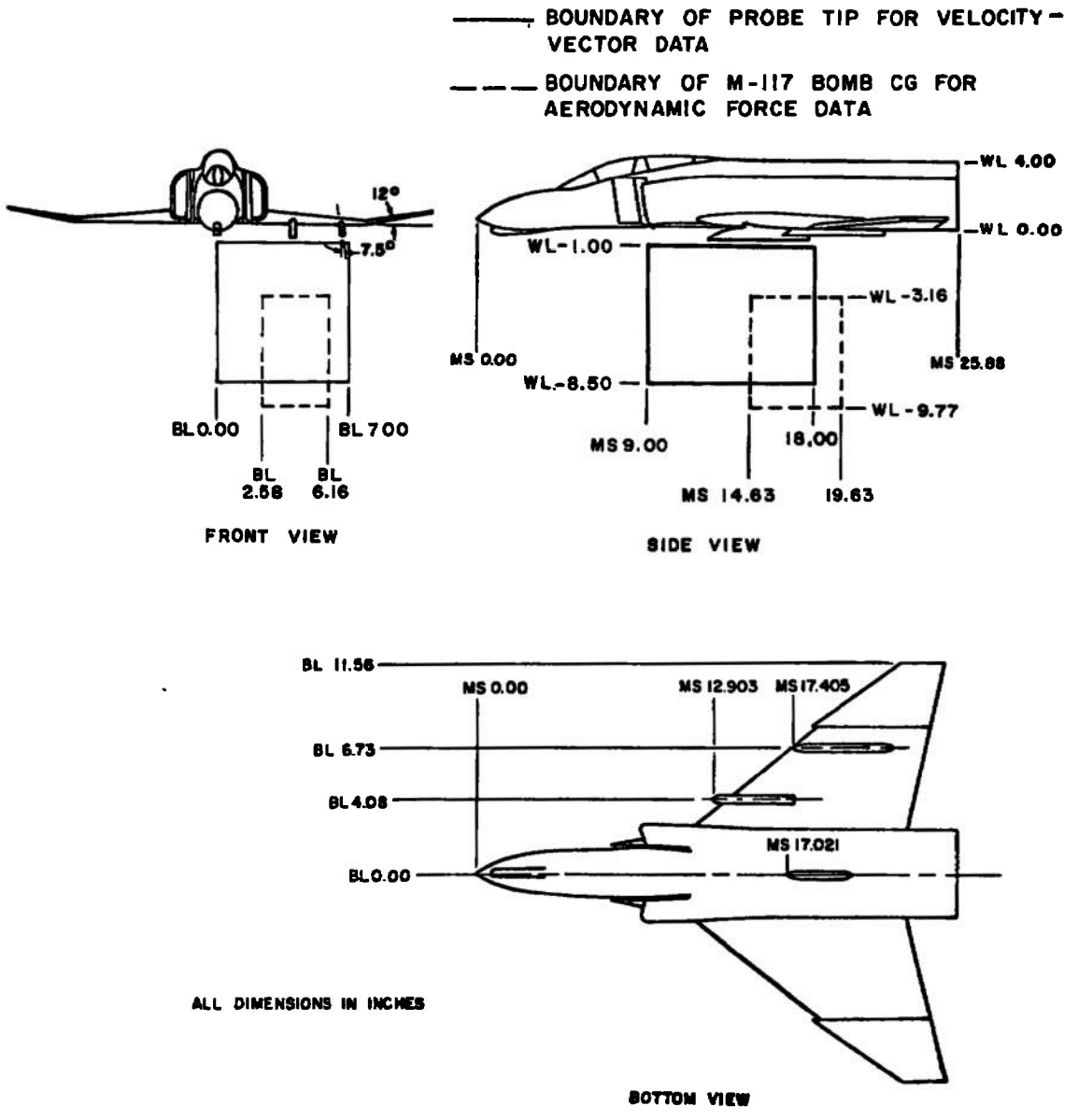

Fig. 12 Sketch of F-4C Model Illustrating the Flow Regions Surveyed

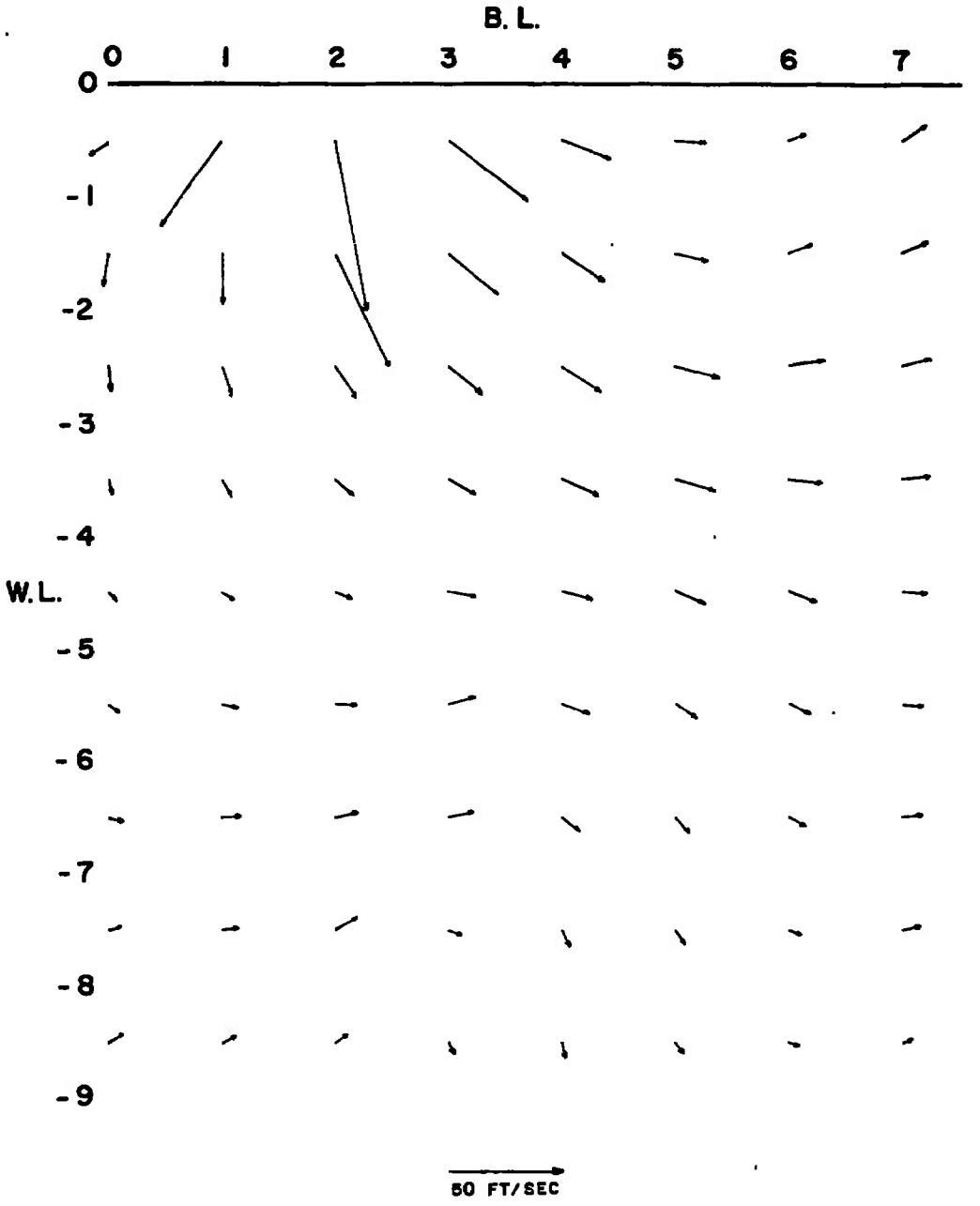

a. Configuration A

Fig. 13 Effect of External Stores on the Transverse Velocity Components of the Flow Field at M_∞ = 0.50, V_∞ = 578, MS 9

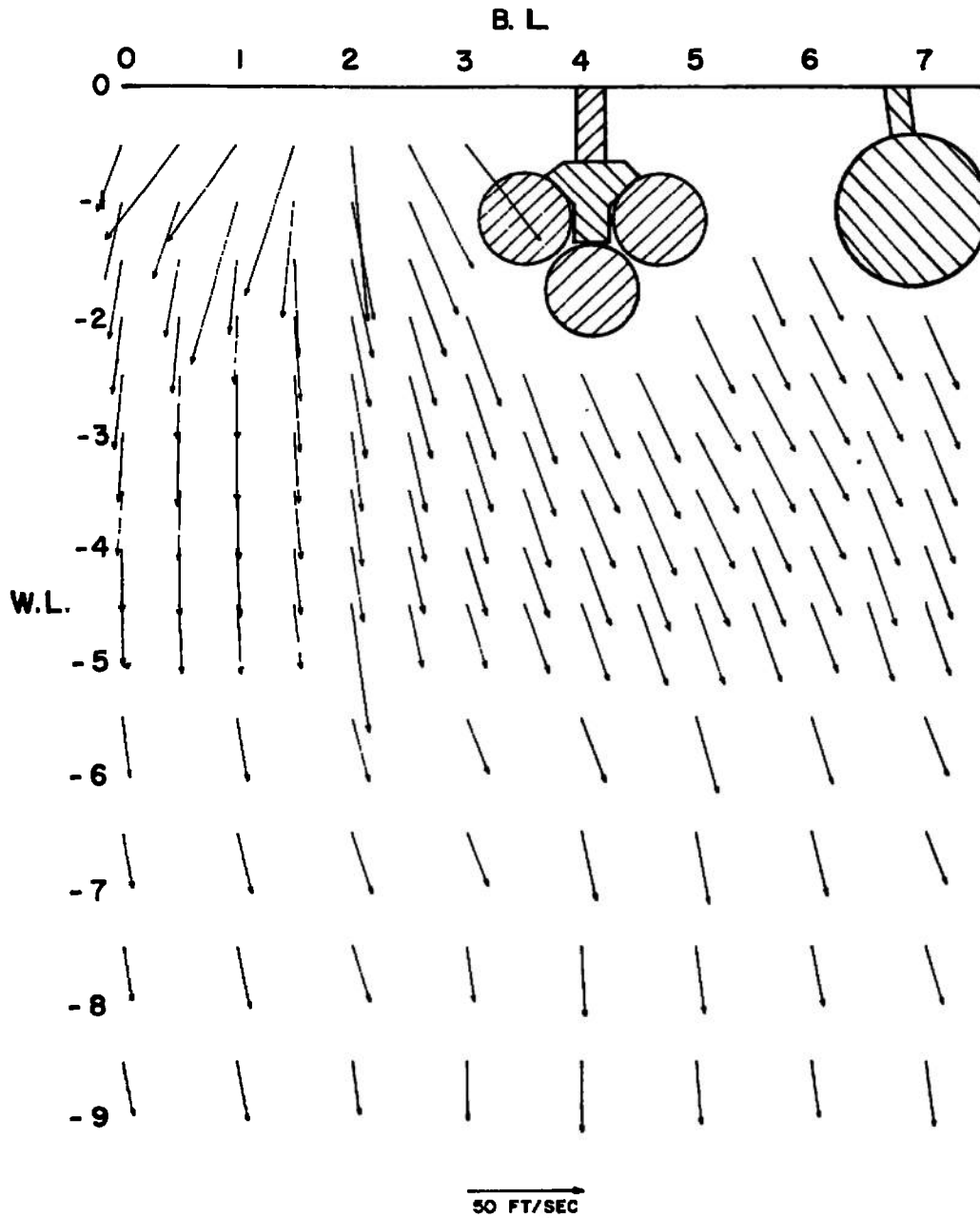

b. Configuration C
Fig. 13 Concluded

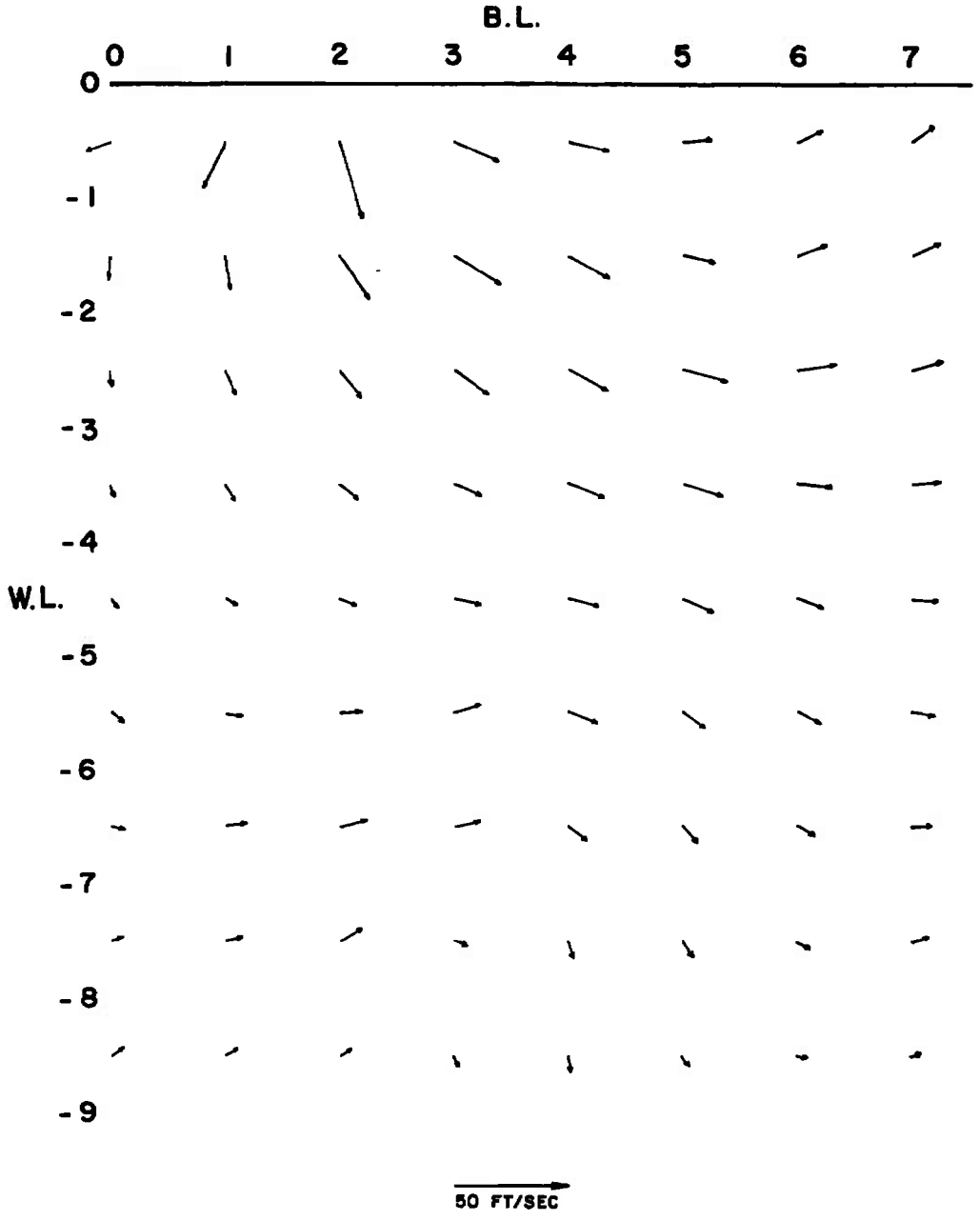

a. Configuration A

Fig. 14 Effect of External Stores on the Transverse Velocity Components of the Flow Field at M_∞ = 0.50, V_∞ = 578, MS 10

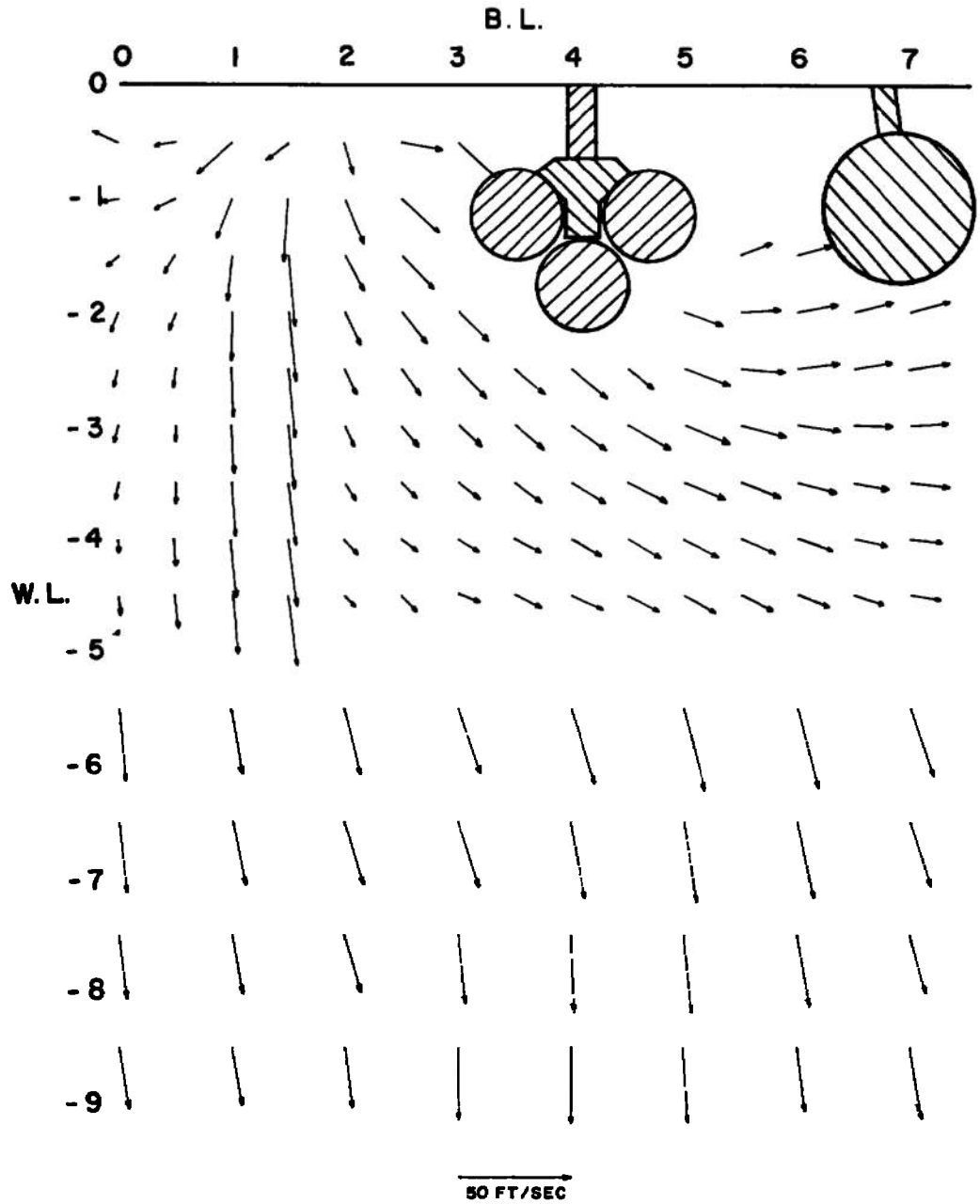

b. Configuration C
Fig. 14 Concluded

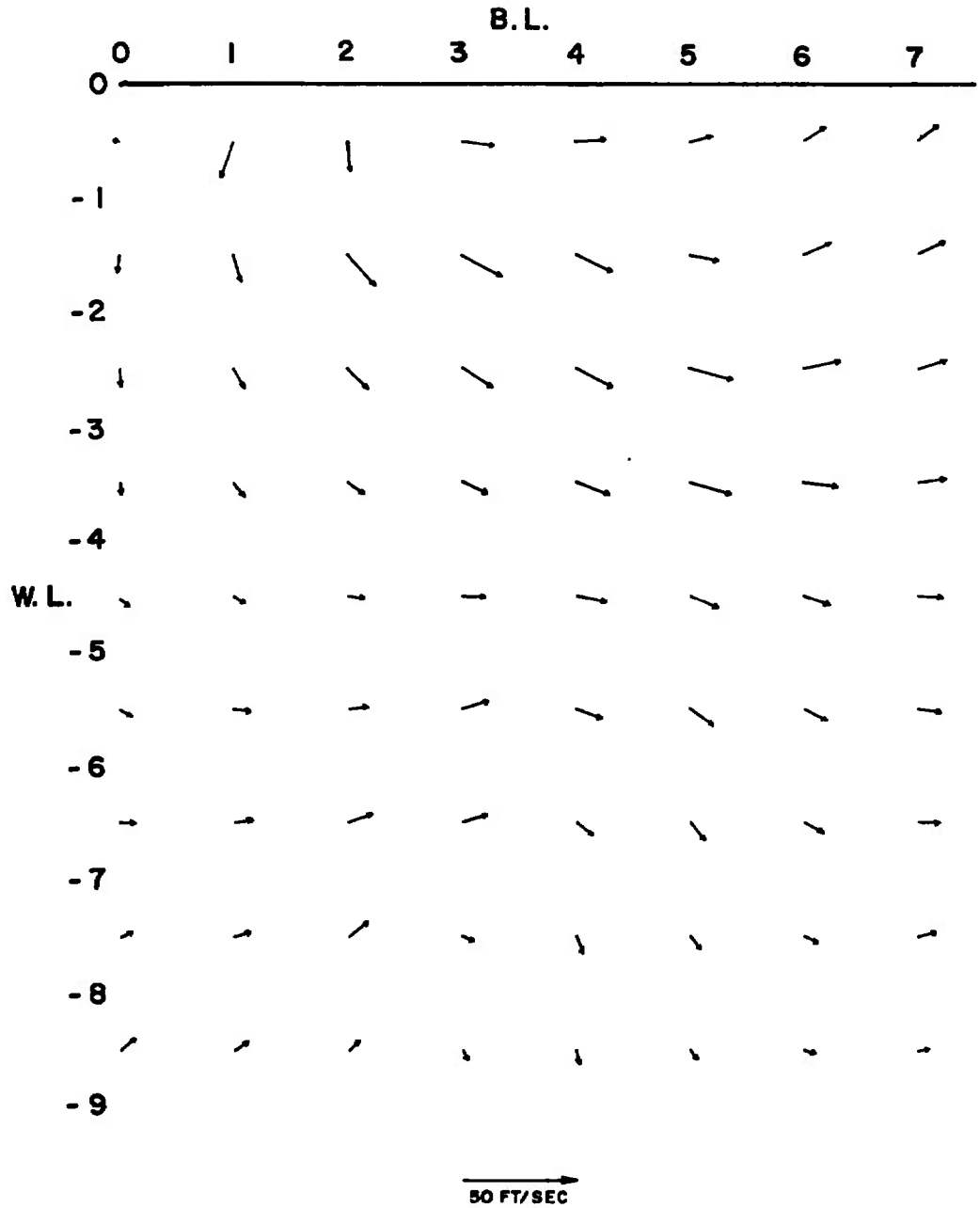

a. Configuration A

Fig. 15 Effect of External Stores on the Transverse Velocity Components of the Flow Field at M_∞ = 0.50, V_∞ = 578, MS 11

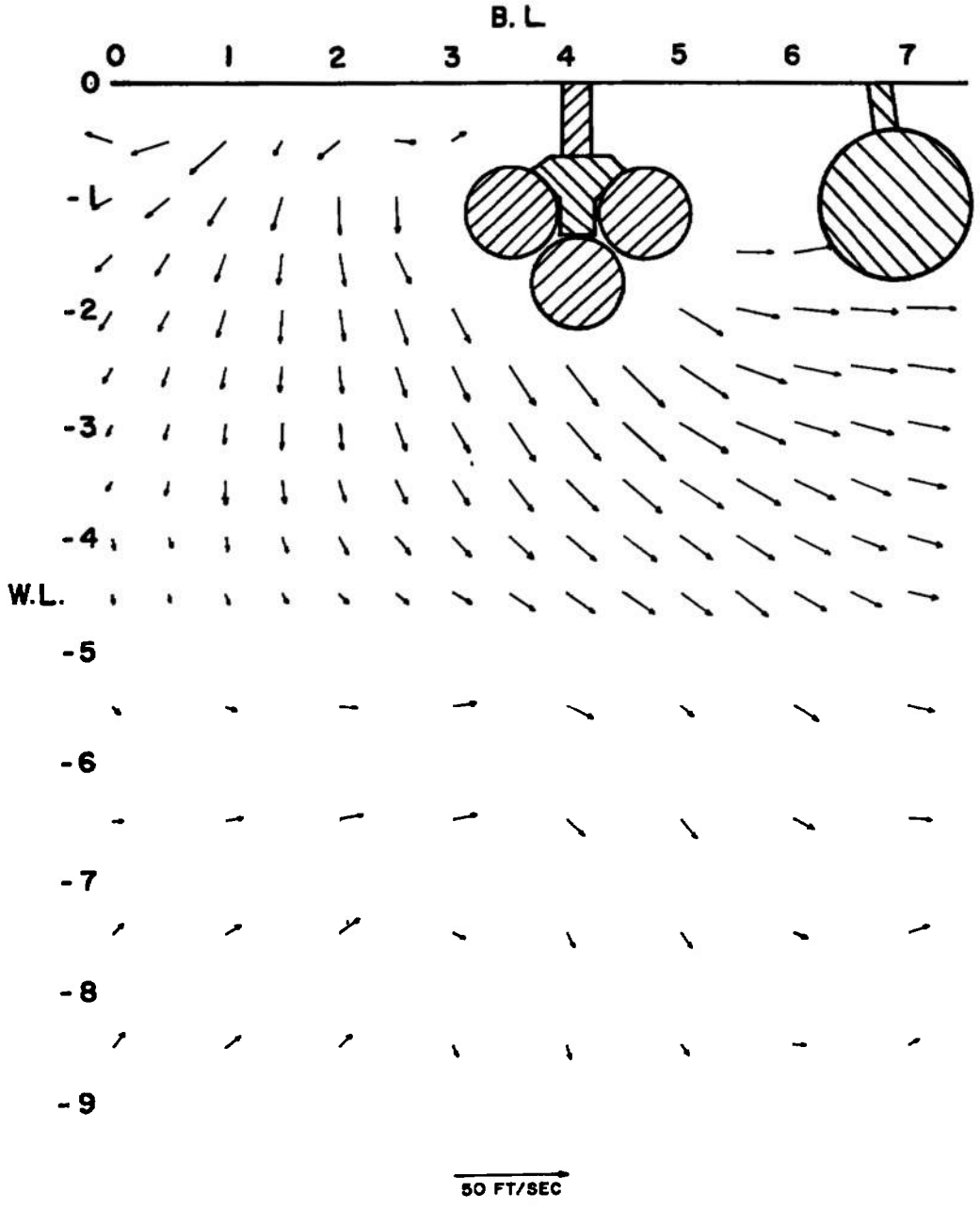

b. Configuration C
Fig. 15 Concluded

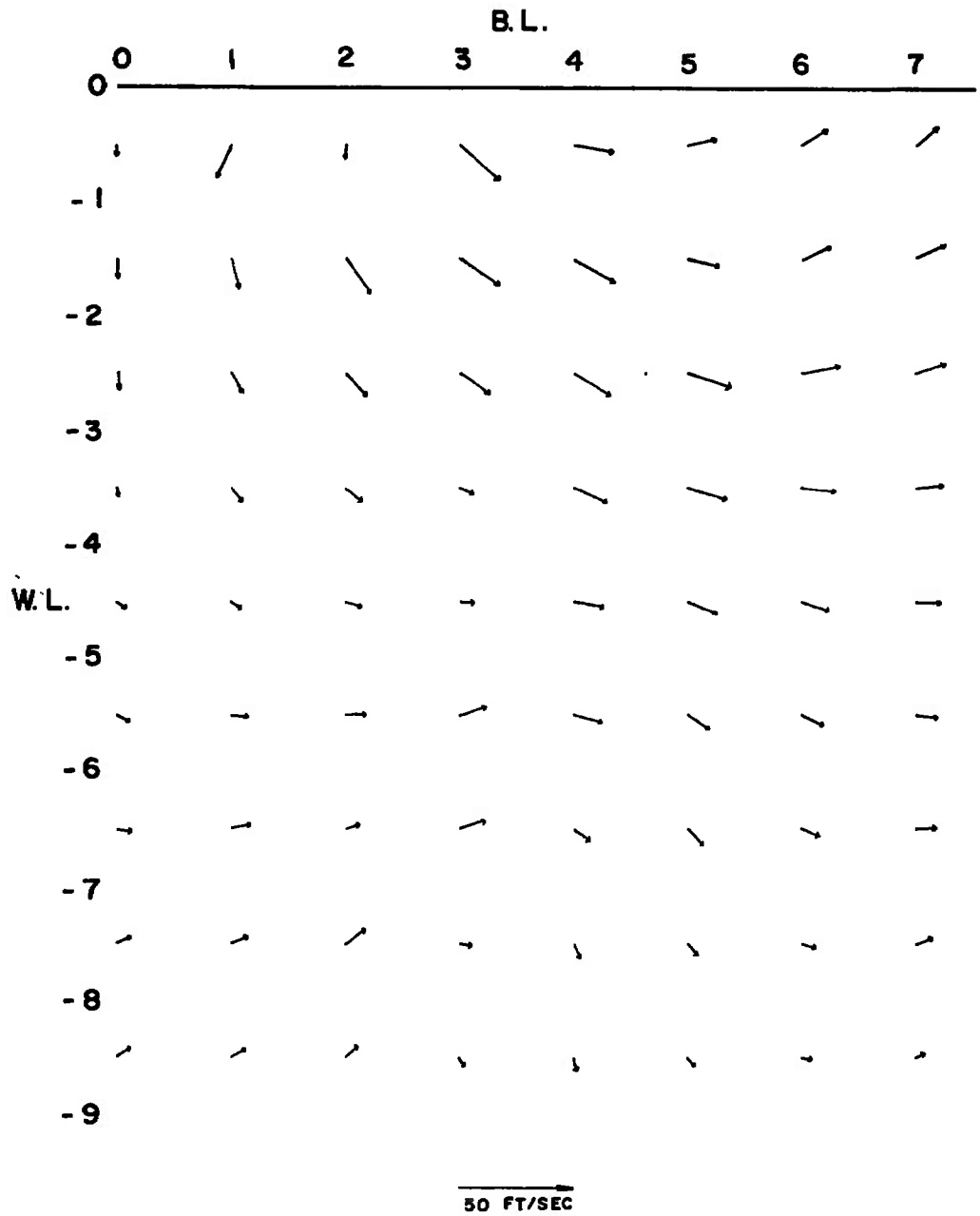

a. Configuration A

Fig. 16 Effect of External Stores on the Transverse Velocity Components of the Flow Field at M_∞ = 0.50, V_∞ = 578, MS 12

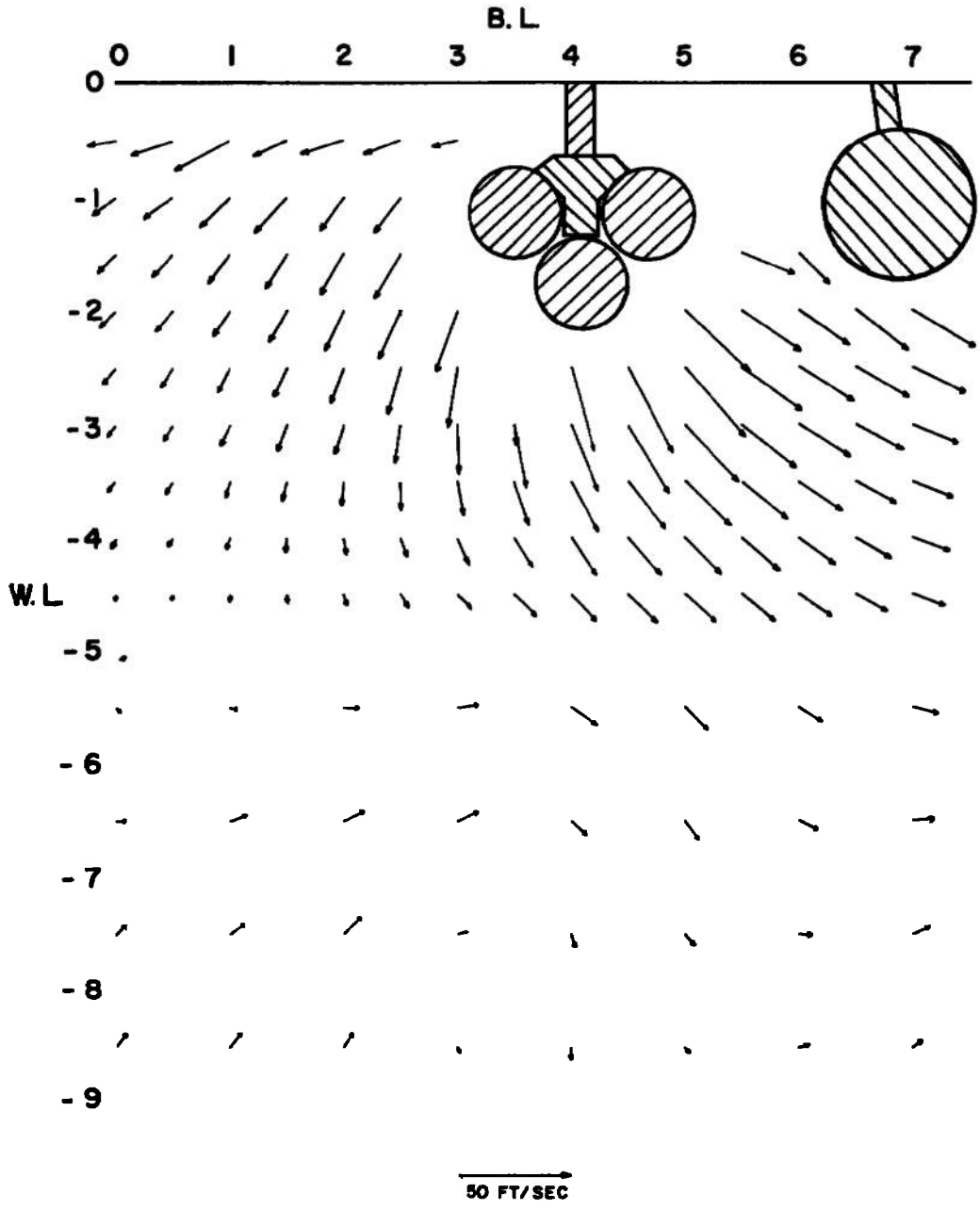

b. Configuration C
Fig. 16 Concluded

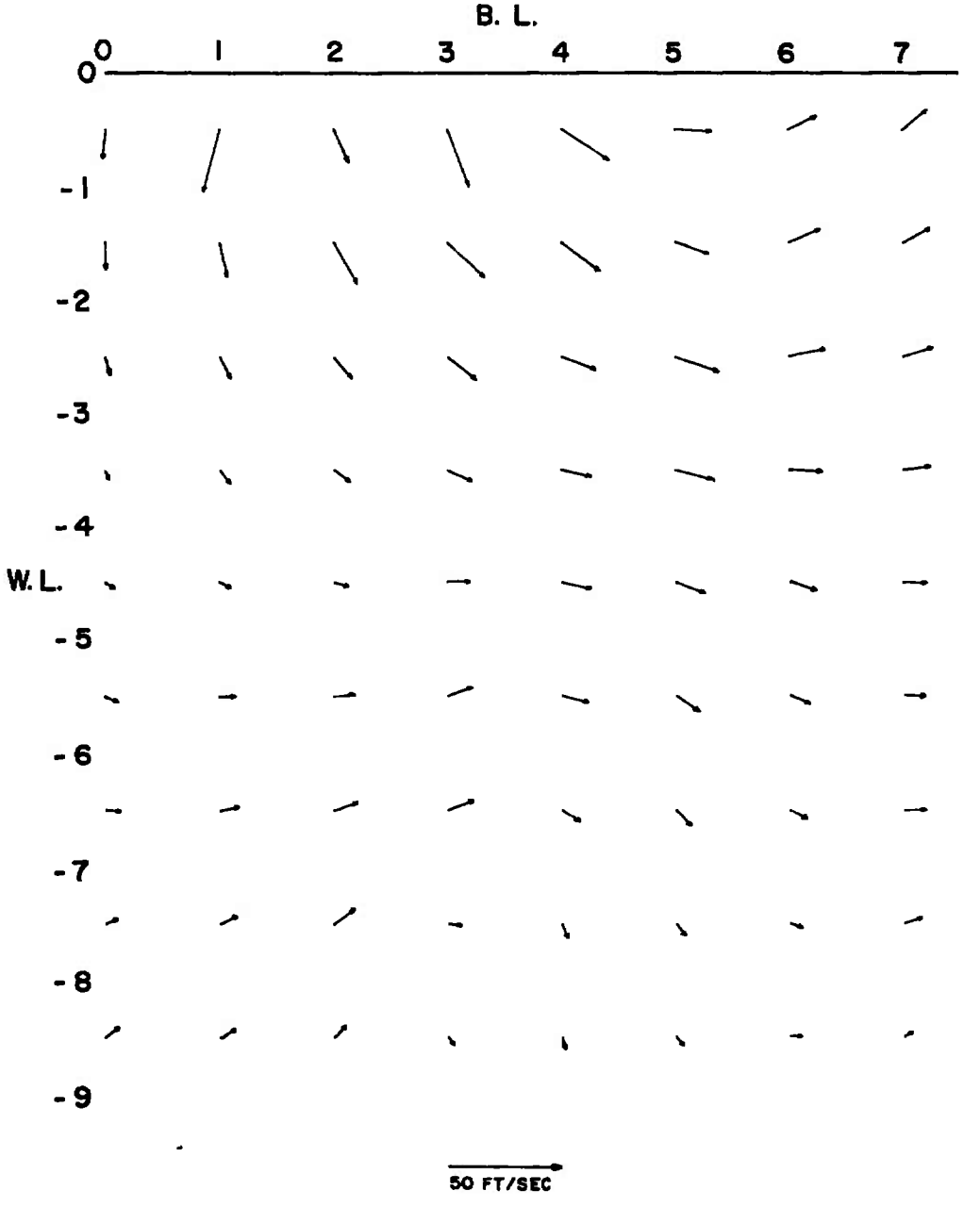

a. Configuration A

Fig. 17 Effect of External Stores on the Transverse Velocity Components of the Flow Field at M_∞ = 0.50, V_∞ = 578, MS 13

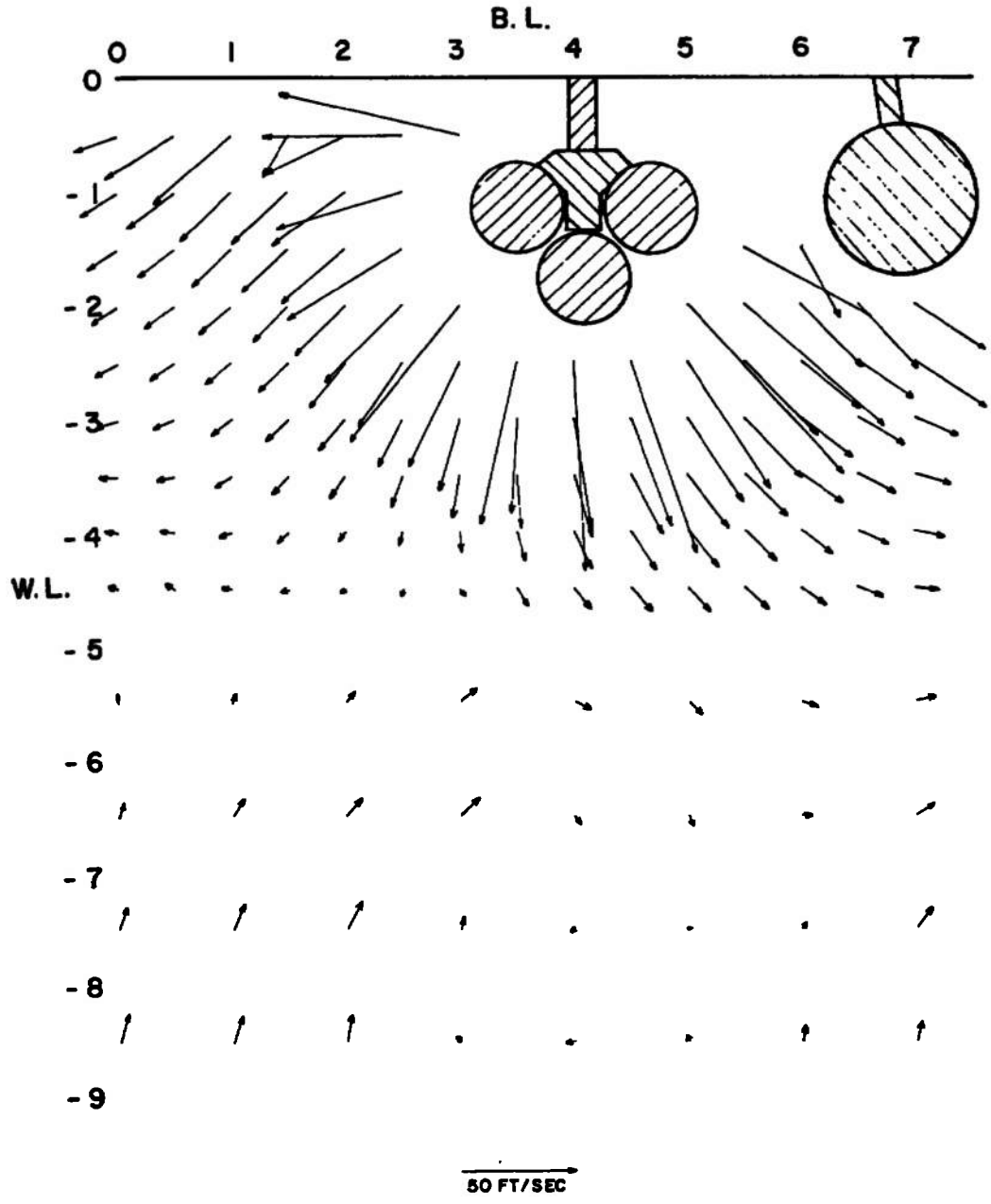

b. Configuration C
Fig. 17 Concluded

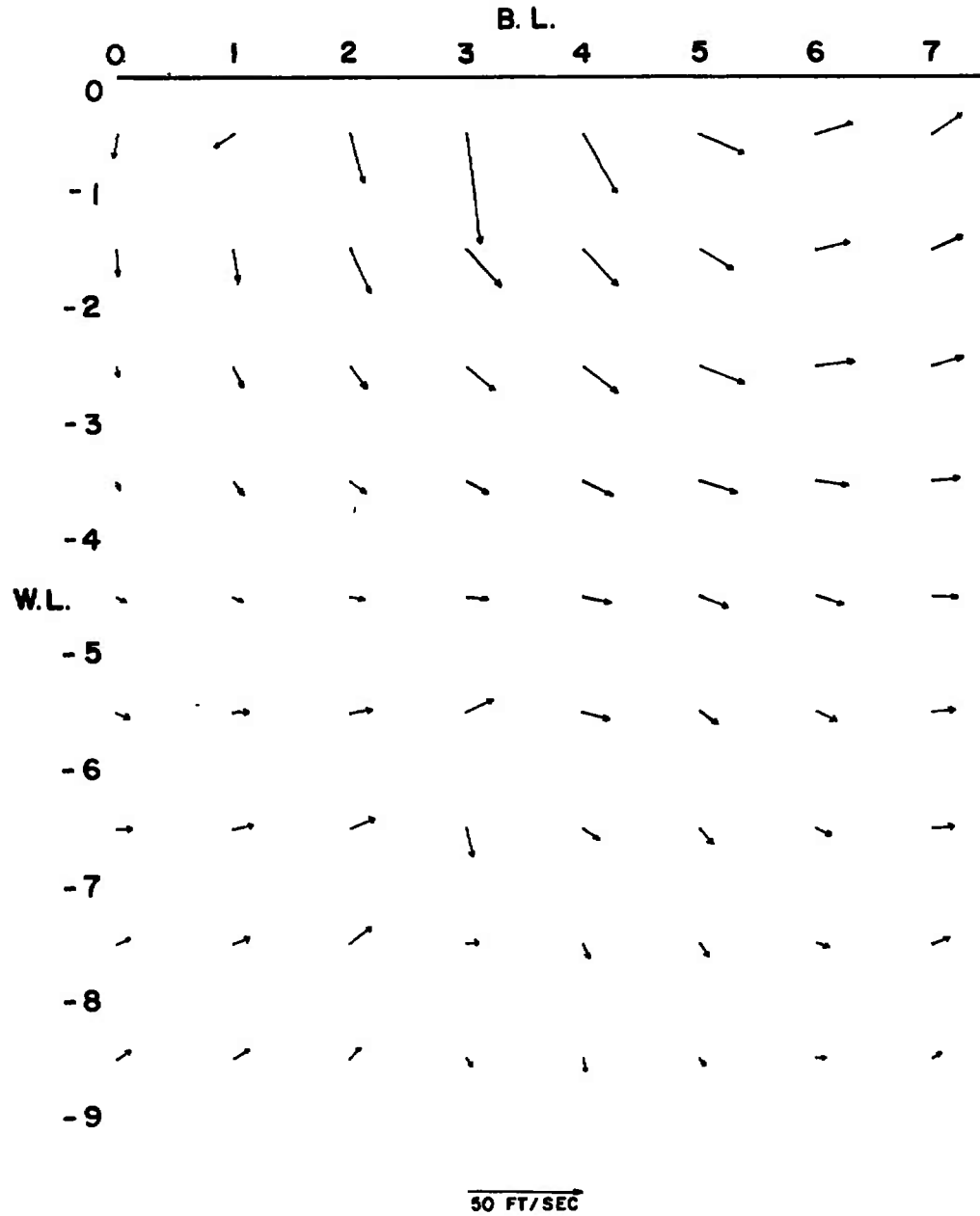

a. Configuration A

Fig. 18 Effect of External Stores on the Transverse Velocity Components of the Flow Field at M_∞ = 0.50, V_∞ = 578, MS 14

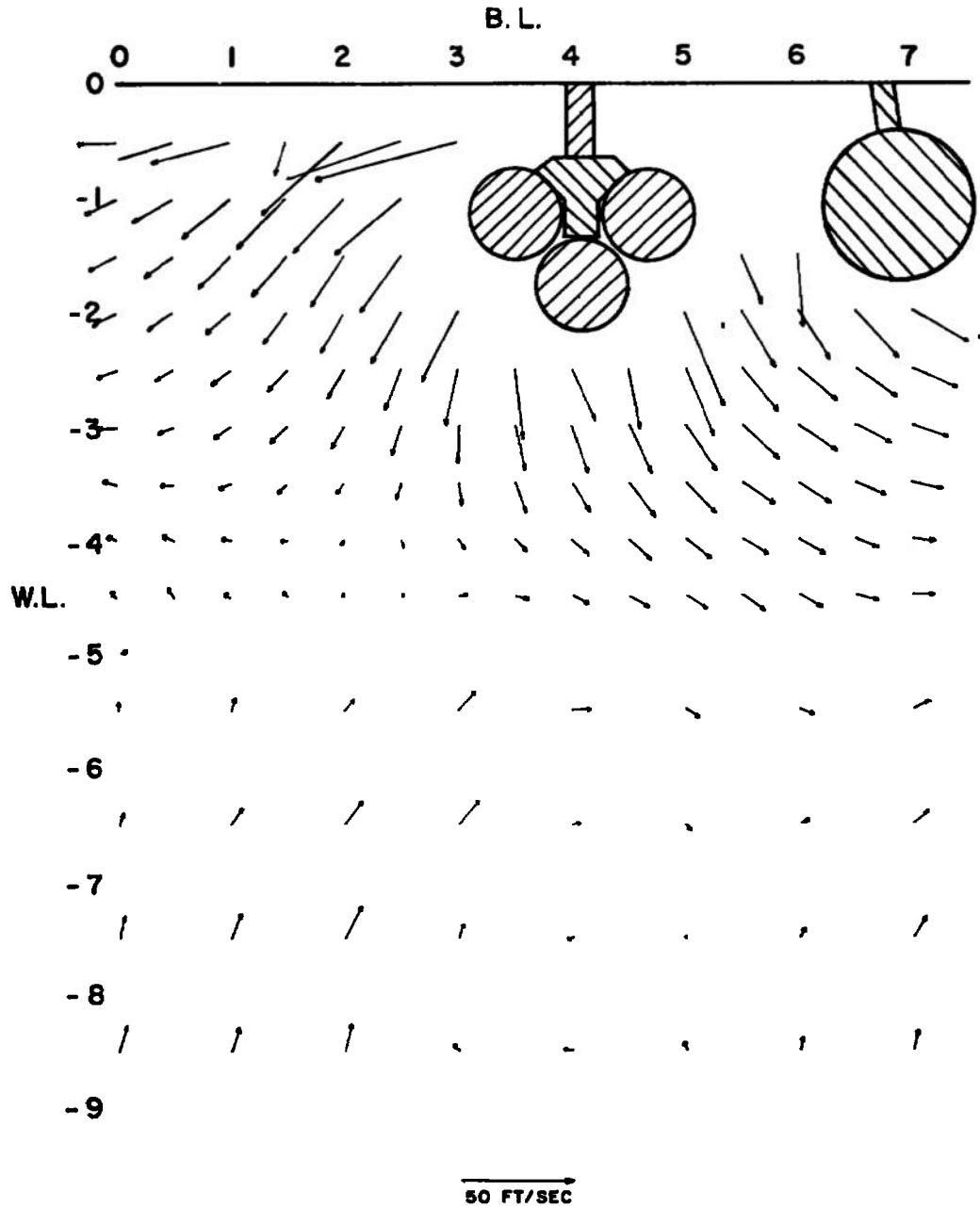

b. Configuration C
Fig. 18 Concluded

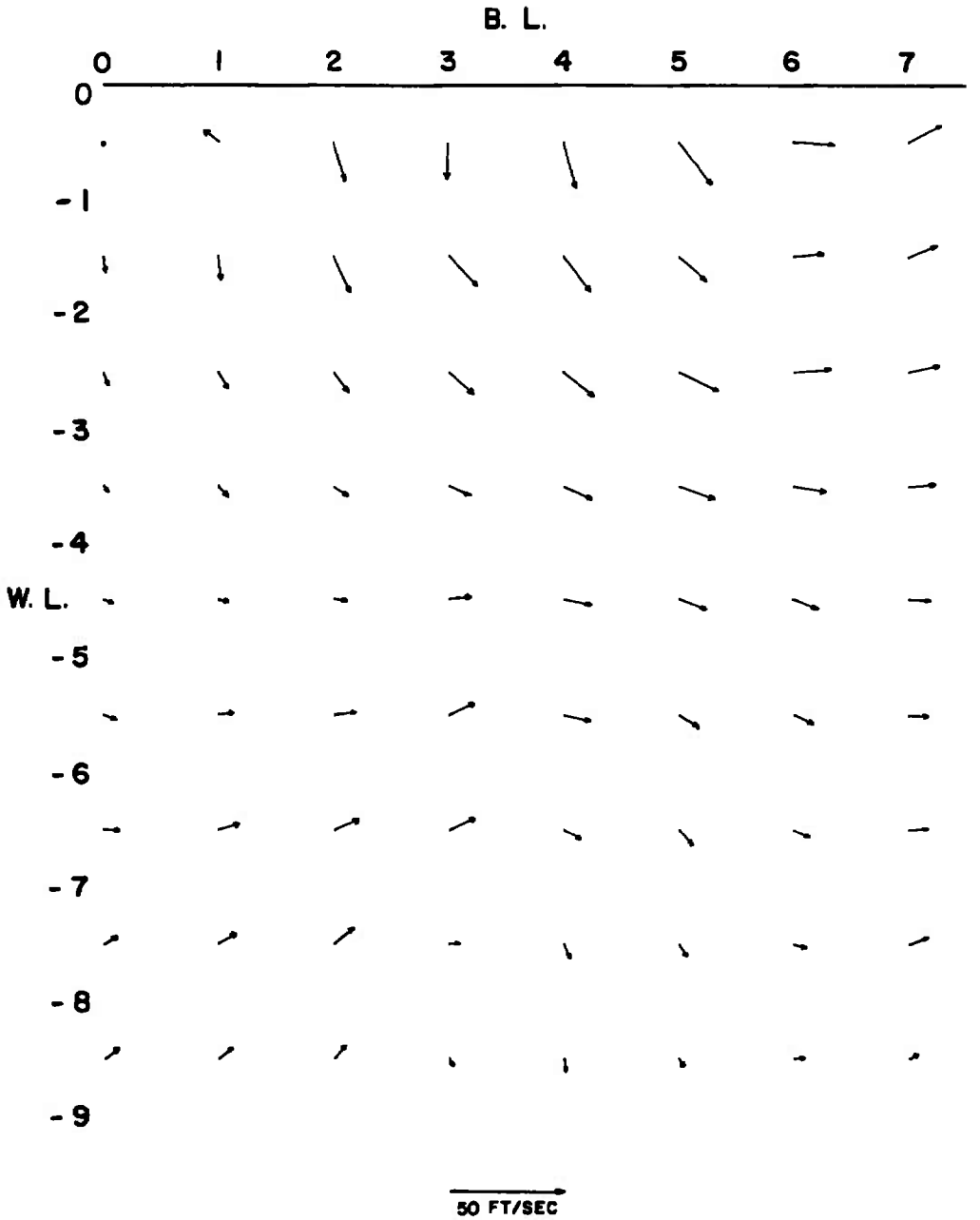

a. Configuration A

Fig. 19 Effect of External Stores on the Transverse Velocity Components of the Flow Field at M_∞ = 0.50, V_∞ = 578, MS 15

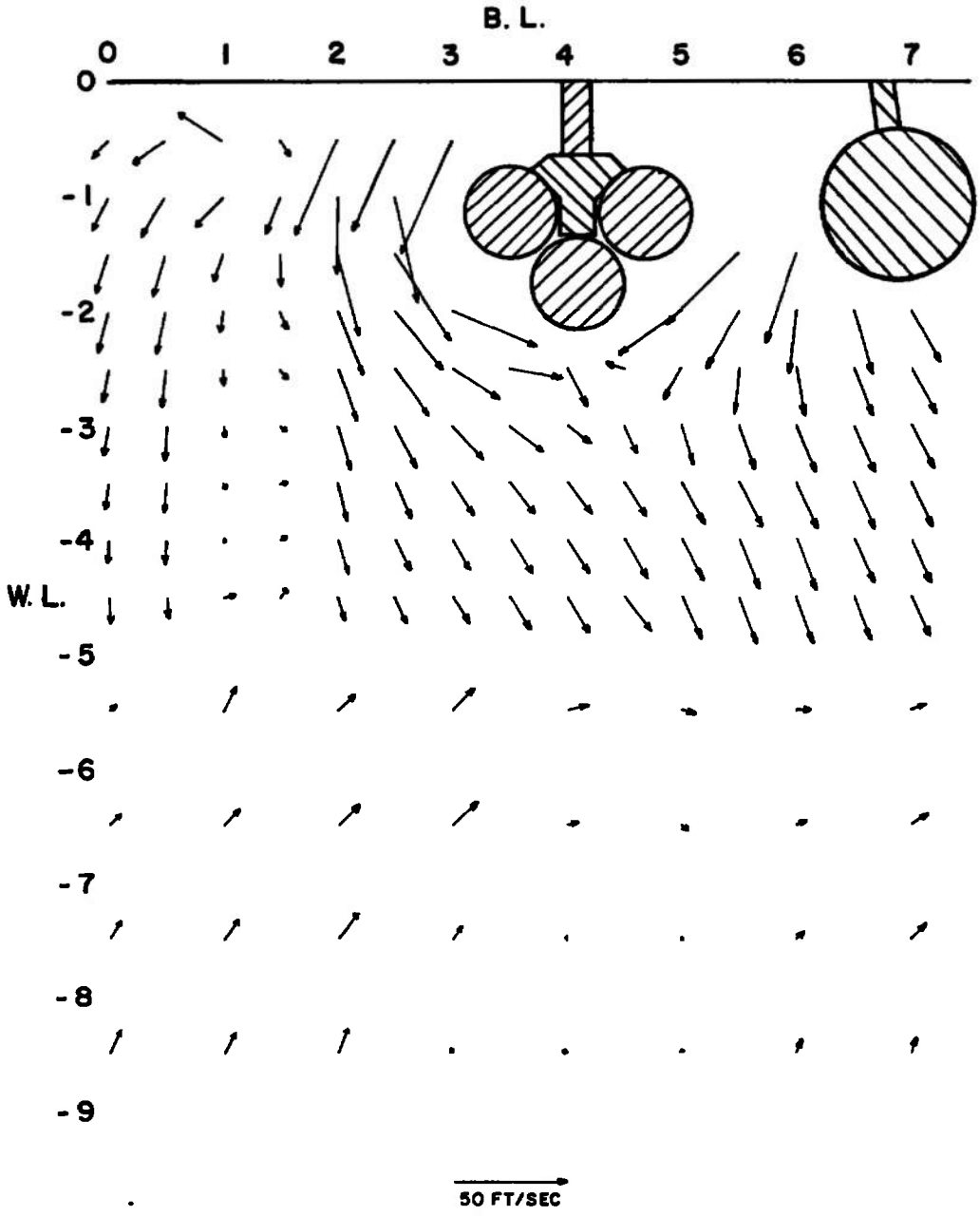

b. Configuration C
Fig. 19 Concluded

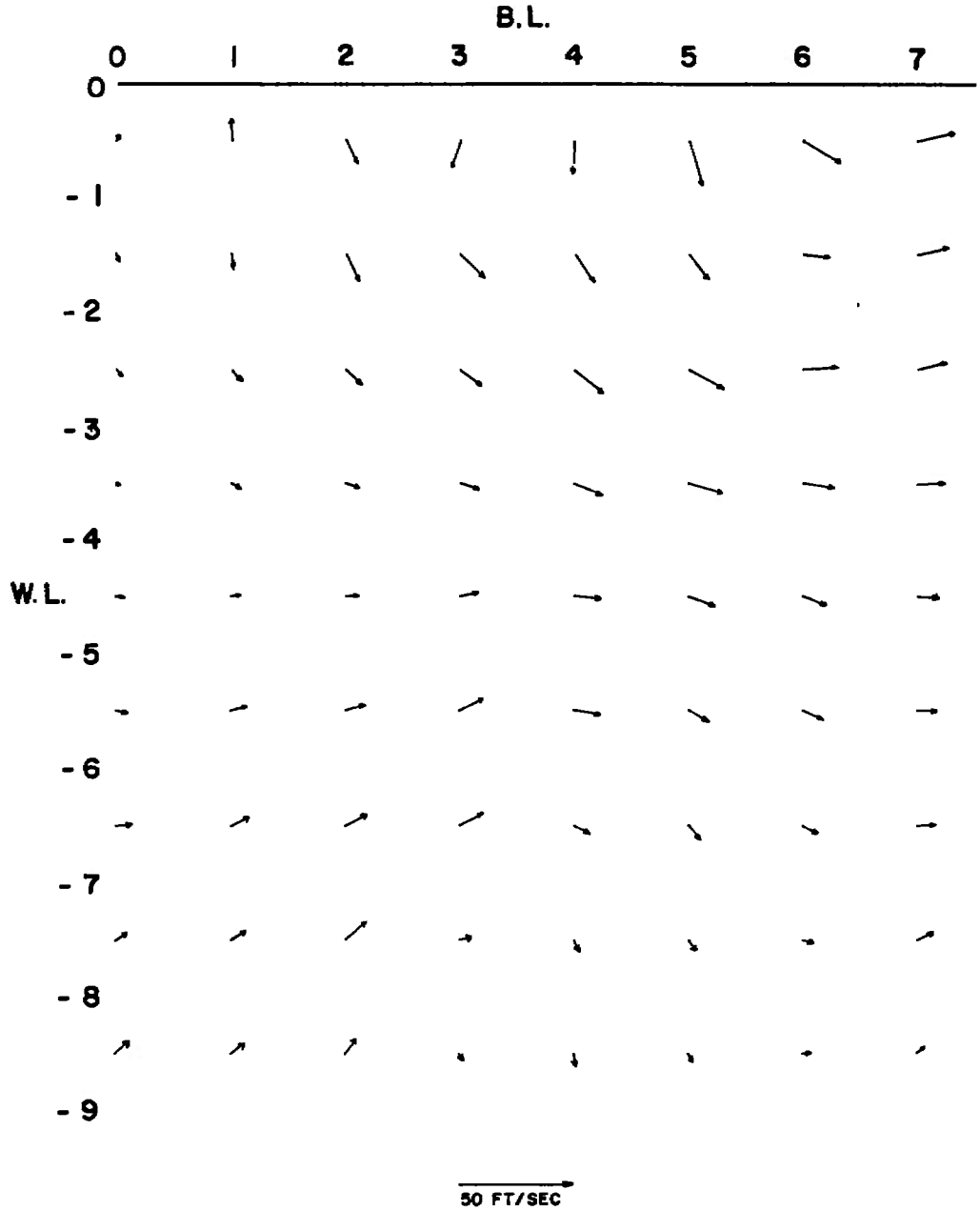

a. Configuration A

Fig. 20 Effect of External Stores on the Transverse Velocity Components of the Flow Field at $M_\infty = 0.50$, $V_\infty = 578$, MS 16

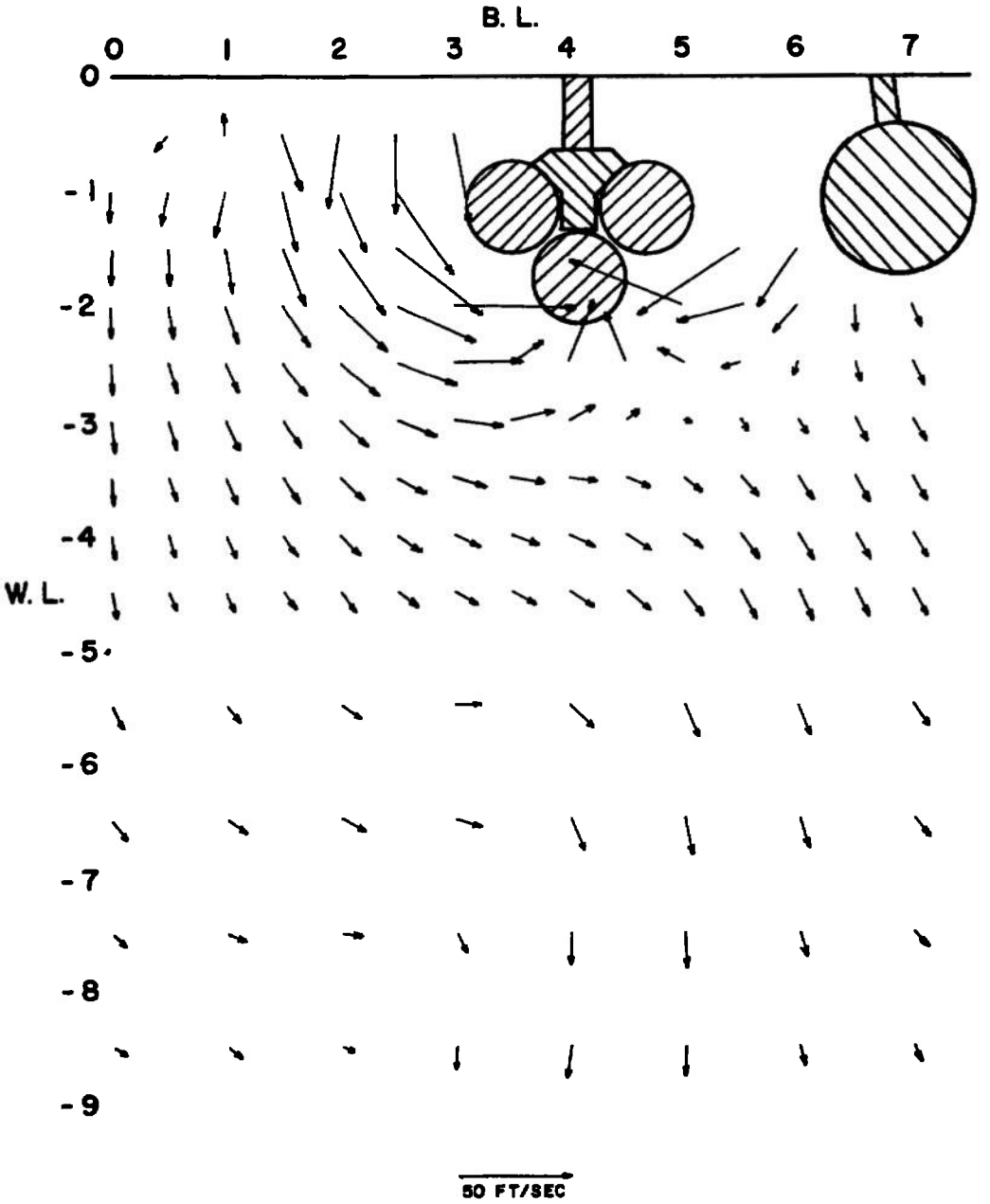

b. Configuration C
Fig. 20 Concluded

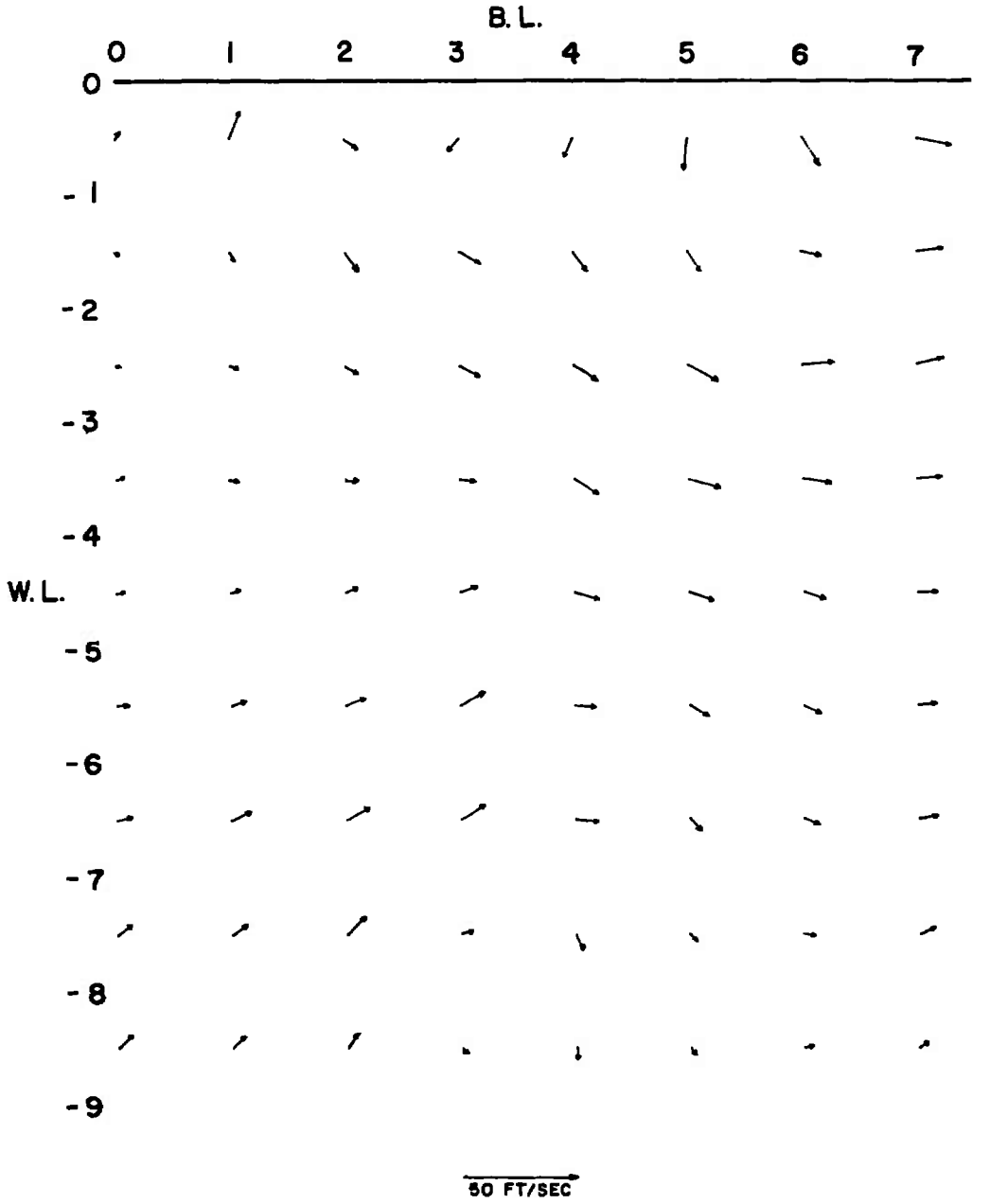

a. Configuration A

Fig. 21 Effect of External Stores on the Transverse Velocity Components of the Flow Field at $M_\infty = 0.50$, $V_\infty = 578$, MS 17

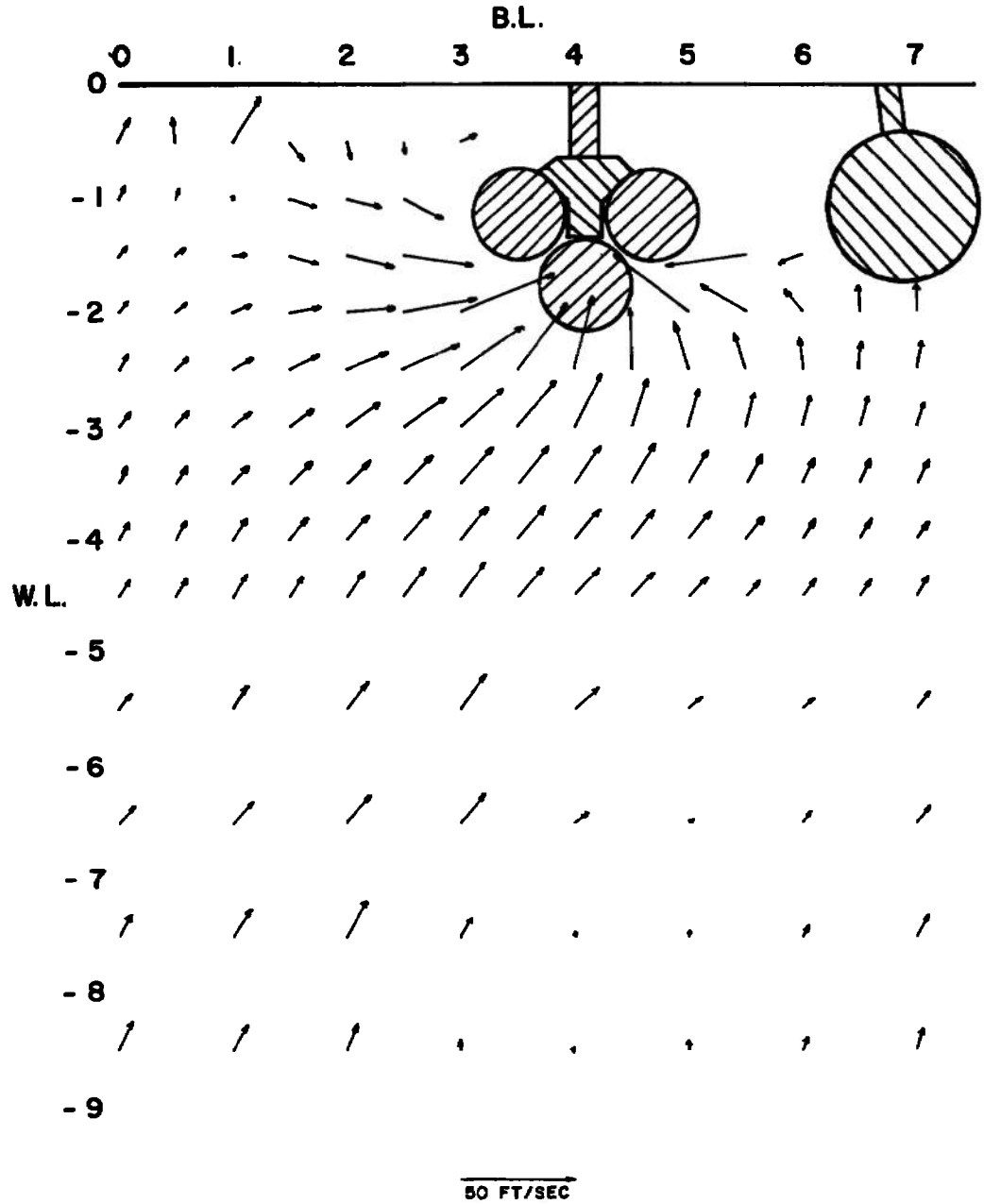

b. Configuration C
Fig. 21 Concluded

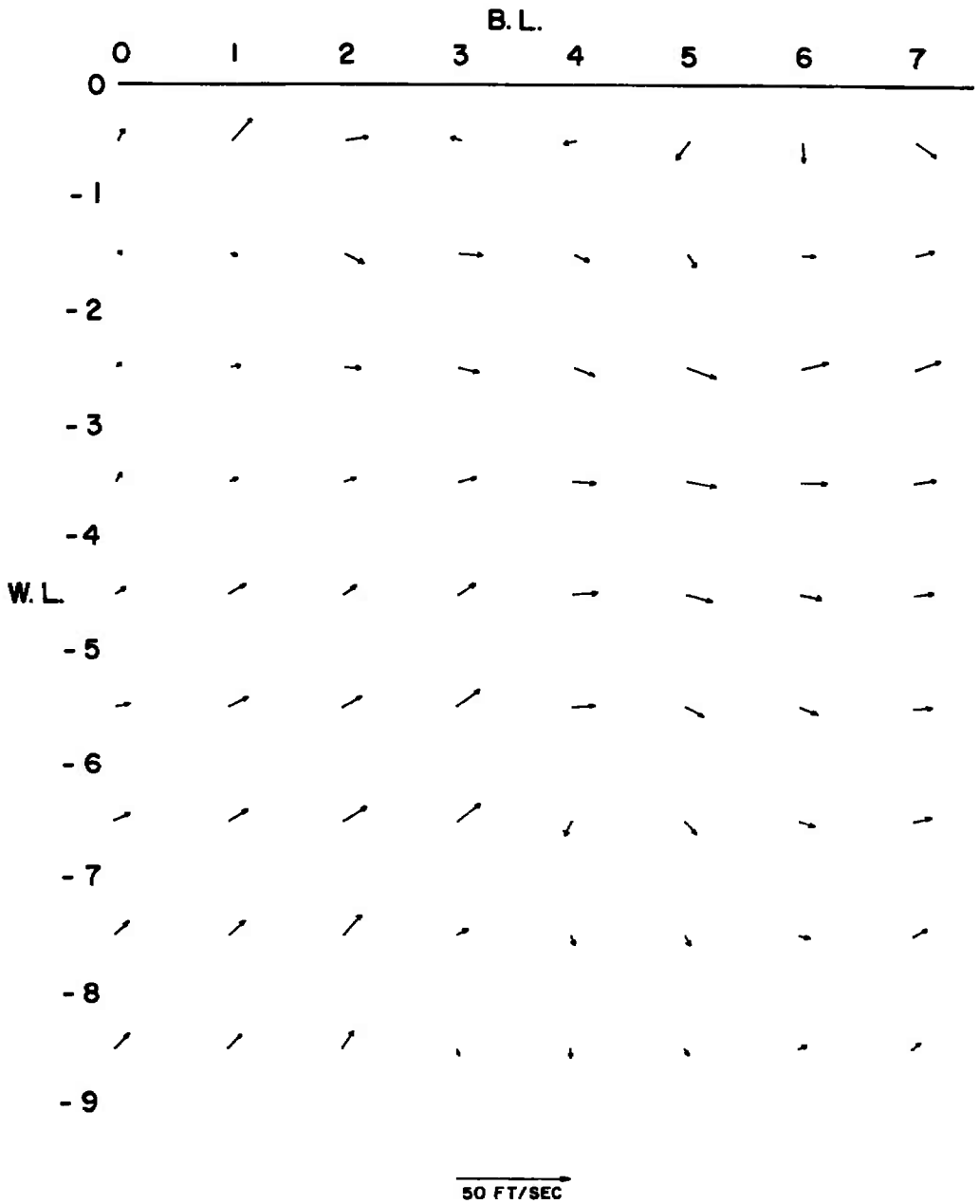

a. Configuration A

Fig. 22 Effect of External Stores on the Transverse Velocity Components of the Flow Field at M_∞ = 0.50, V_∞ = 578, MS 18

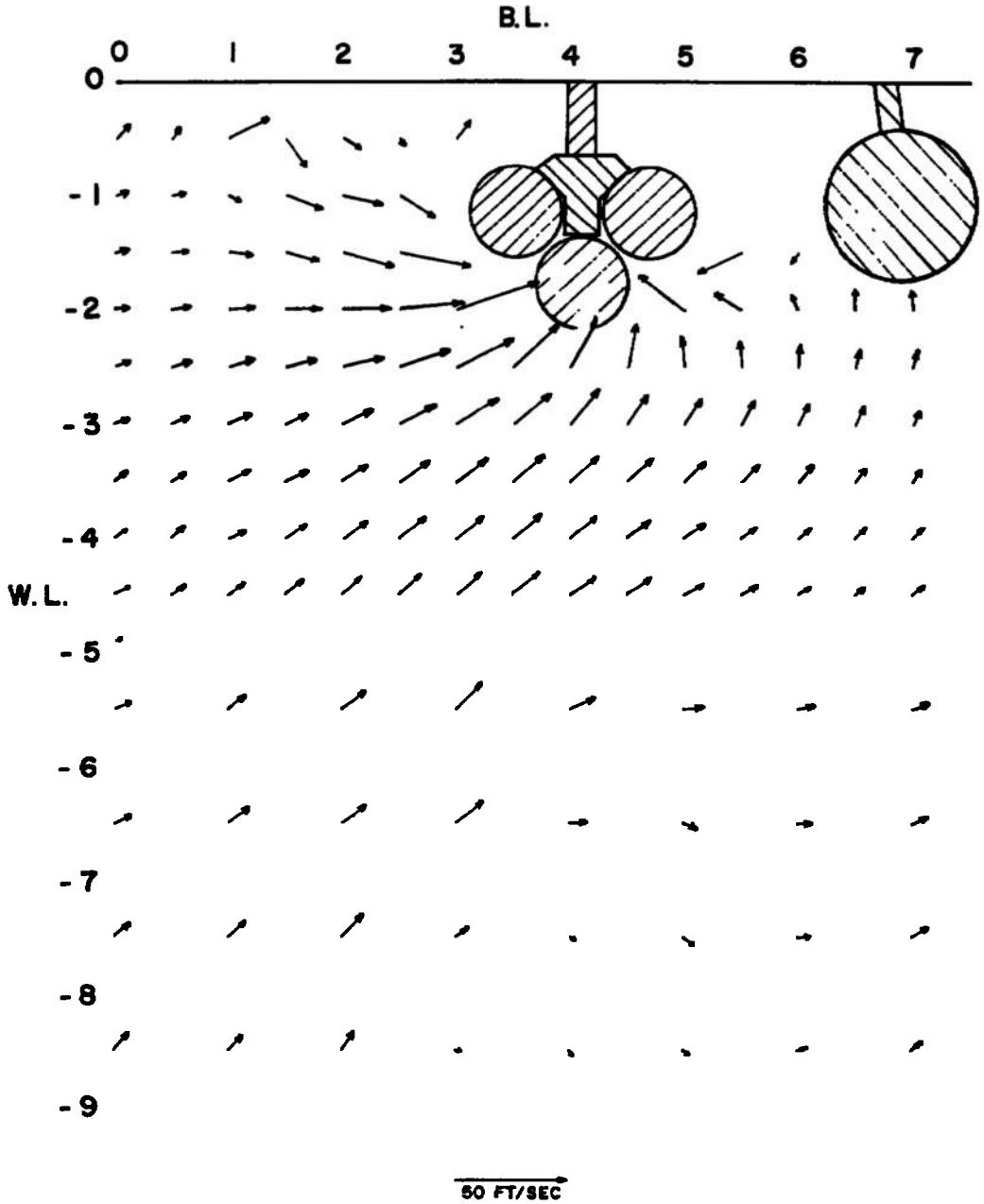

b. Configuration C
Fig. 22 Concluded

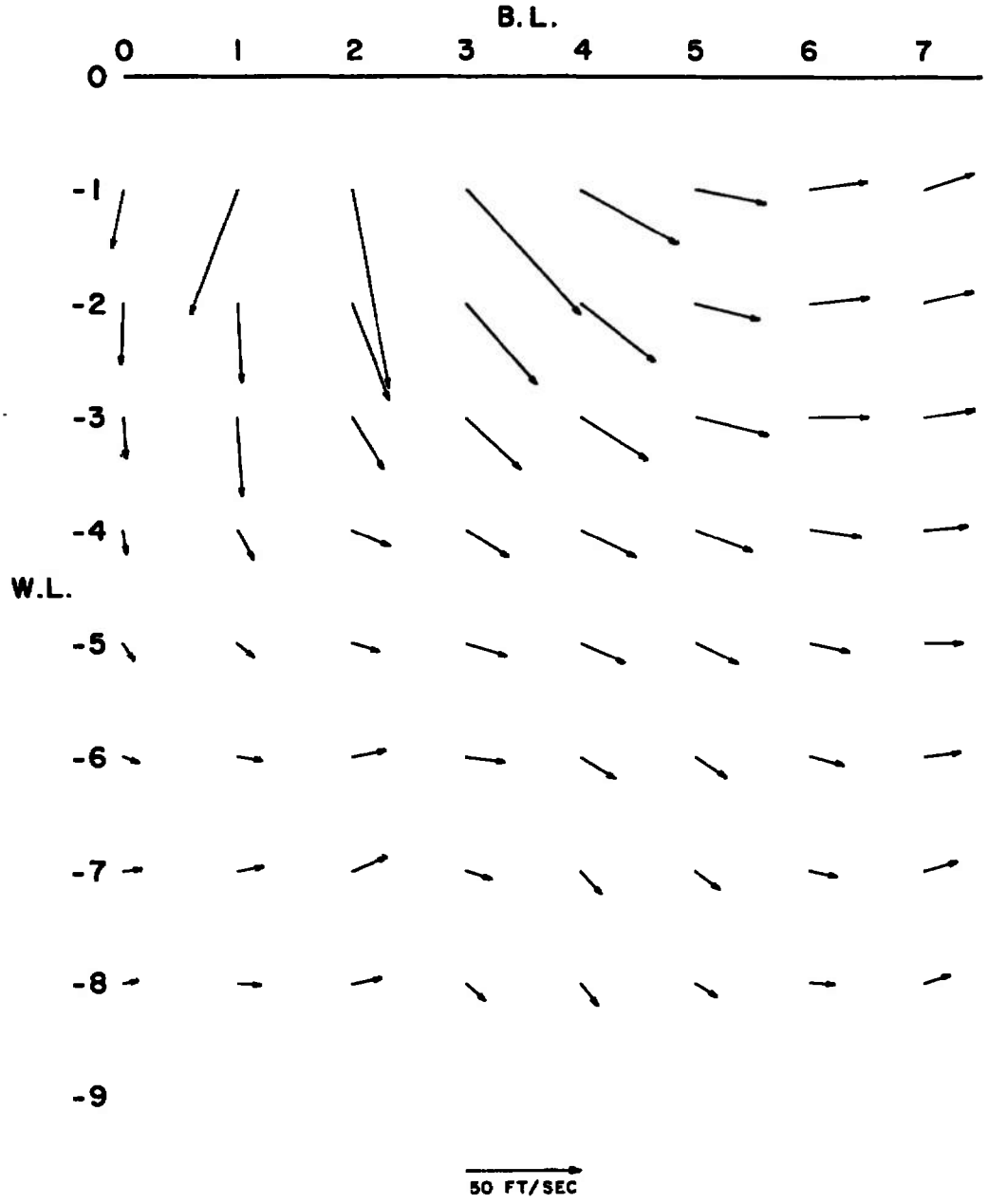

a. Configuration A

Fig. 23 Effect of External Stores on the Transverse Velocity Components of the Flow Field at M_∞ = 0.85, V_∞ = 940, MS 9

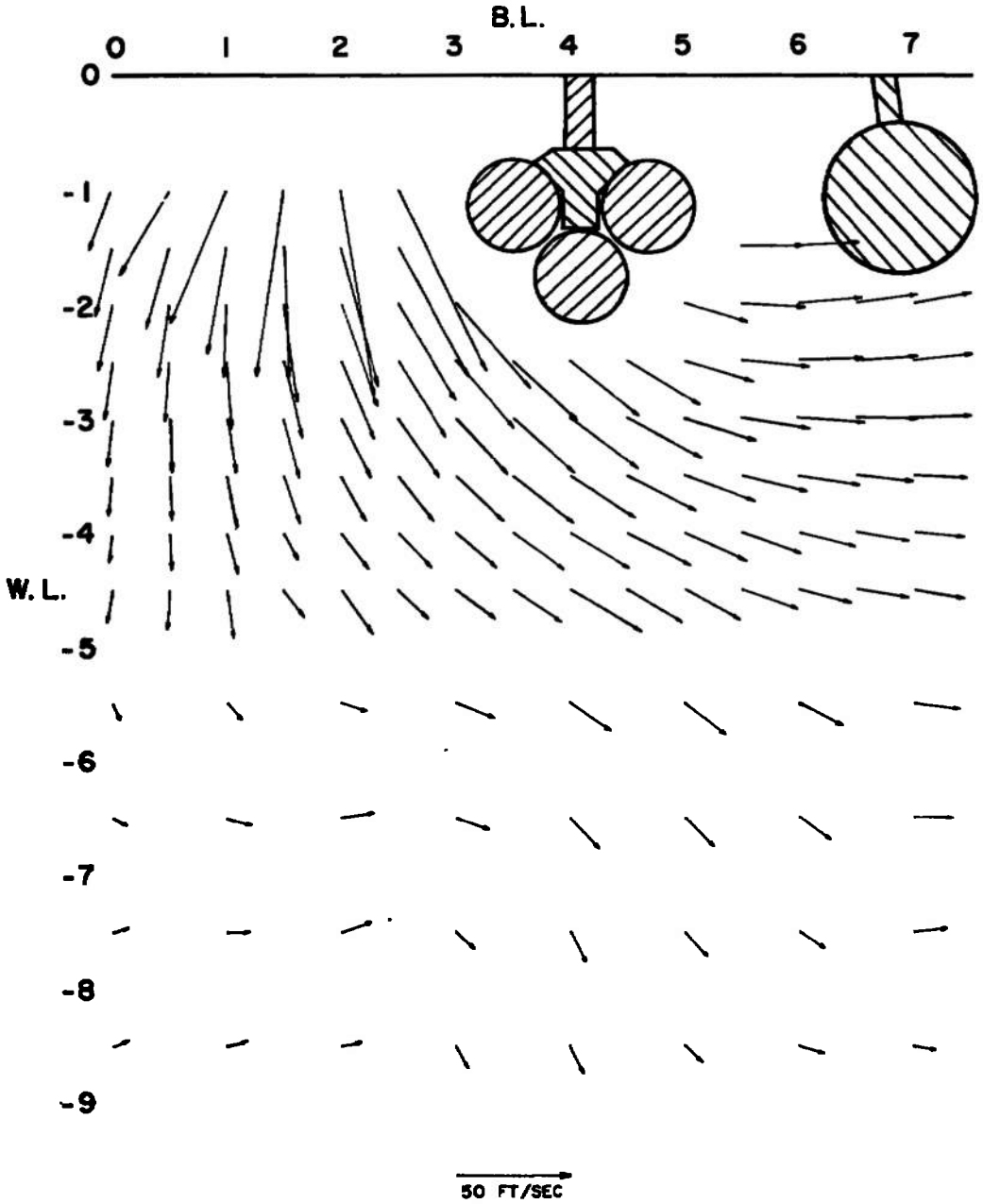

b. Configuration C
Fig. 23 Concluded

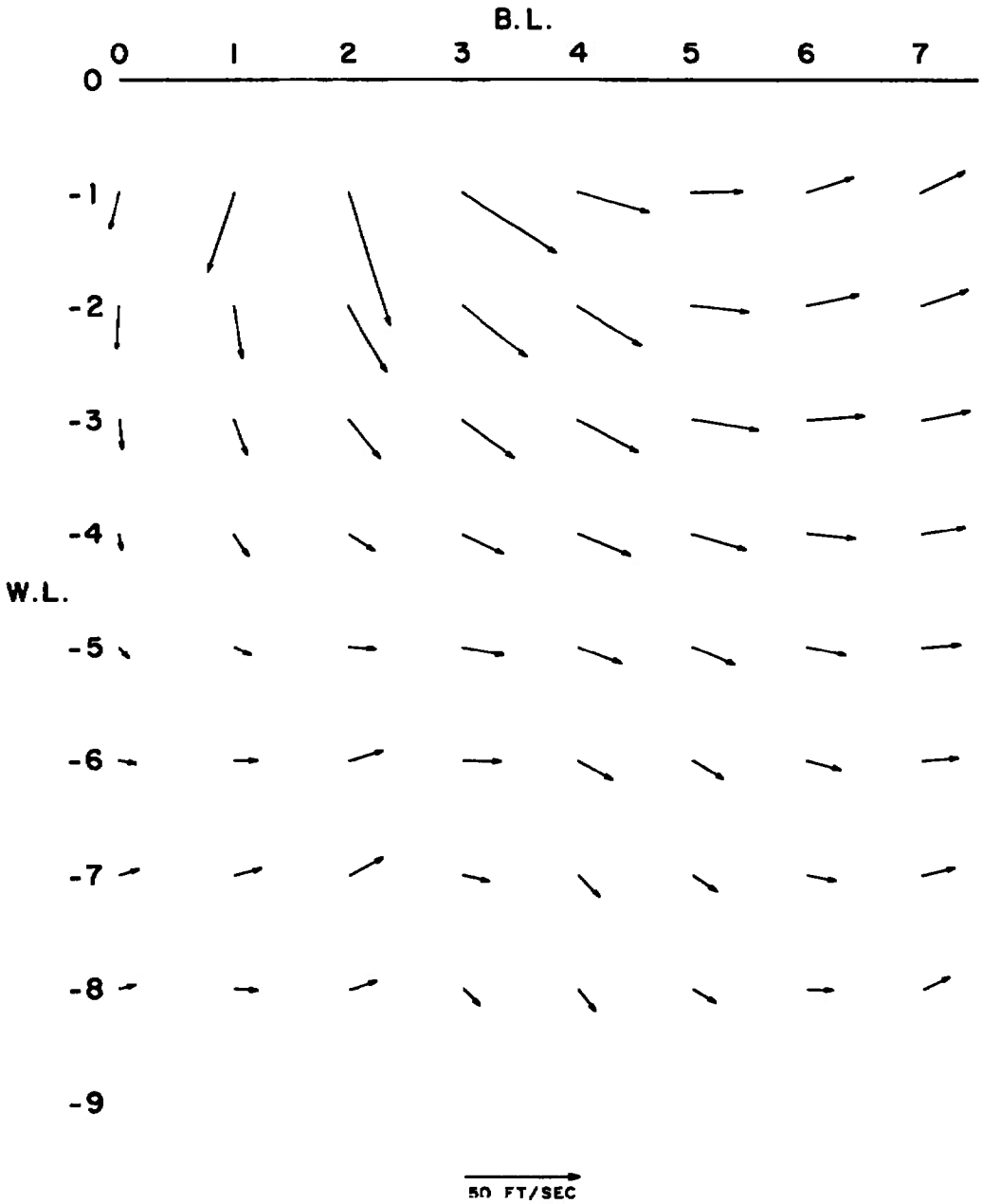

a. Configuration A

Fig. 24 Effect of External Stores on the Transverse Velocity Components of the Flow Field at M_∞ = 0.85, V_∞ = 940, MS 10

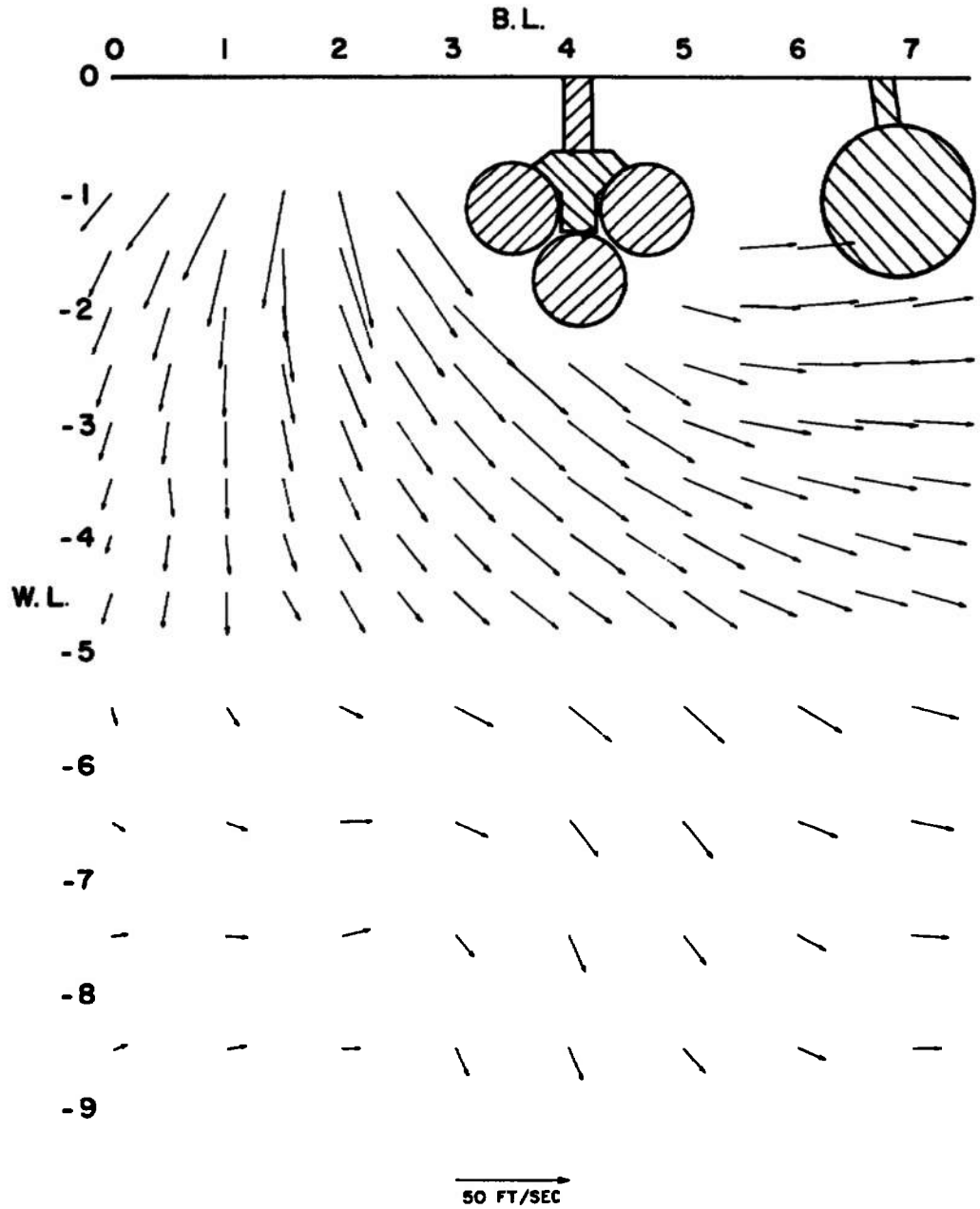

b. Configuration C
Fig. 24 Concluded

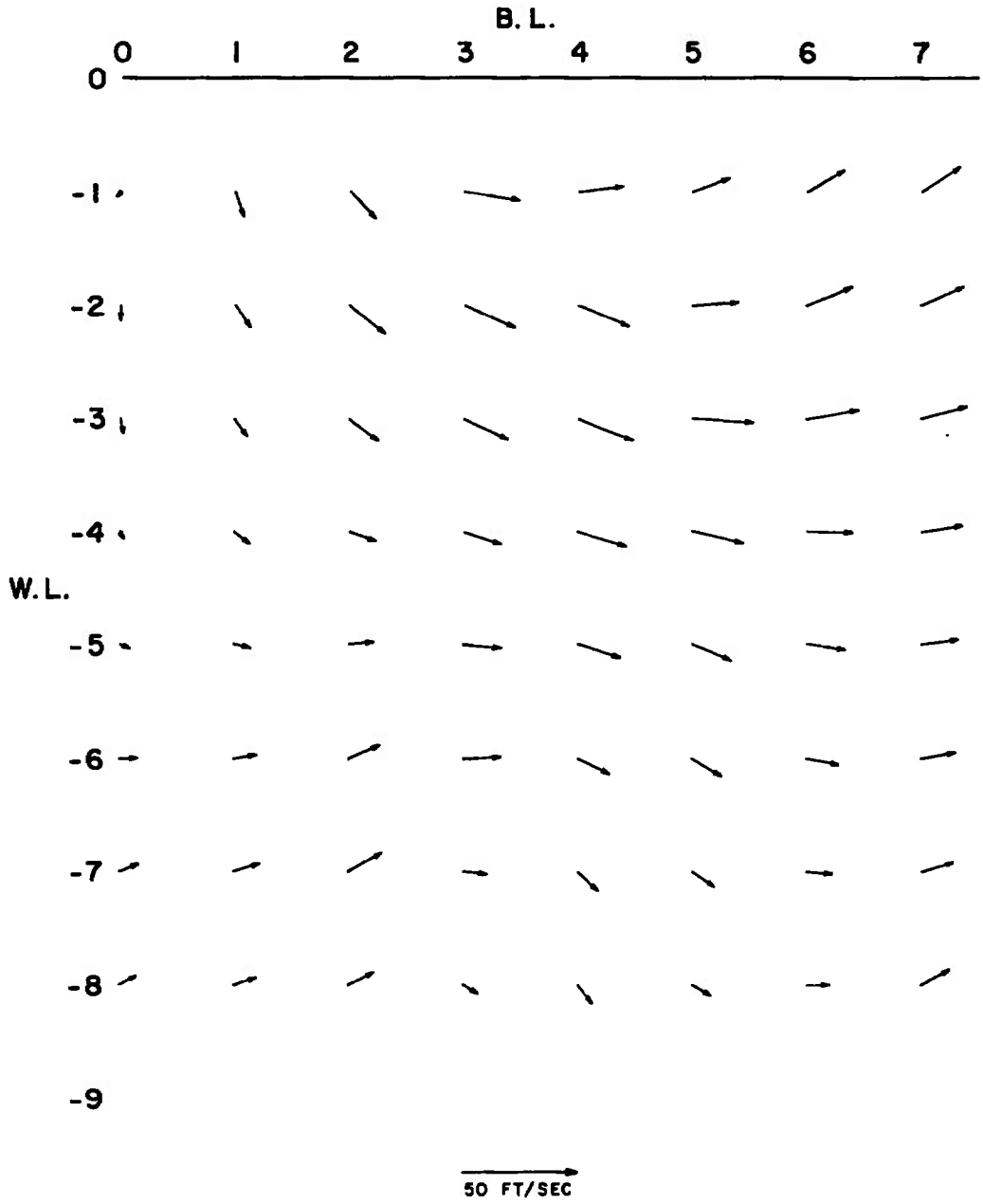

a. Configuration A

Fig. 25 Effect of External Stores on the Transverse Velocity Components of the Flow Field at M_∞ = 0.85, V_∞ = 940, MS 11

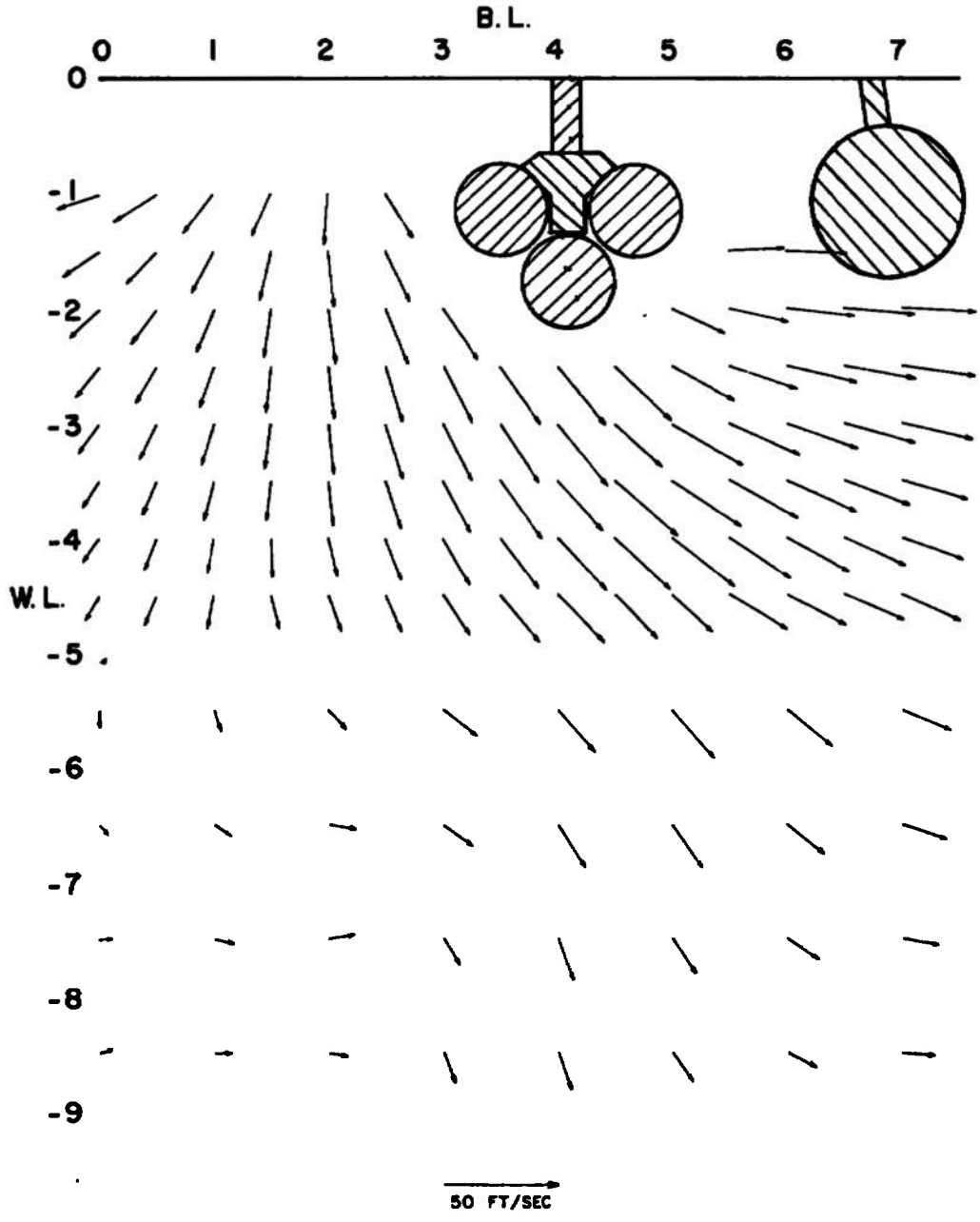

b. Configuration C
Fig. 25 Concluded

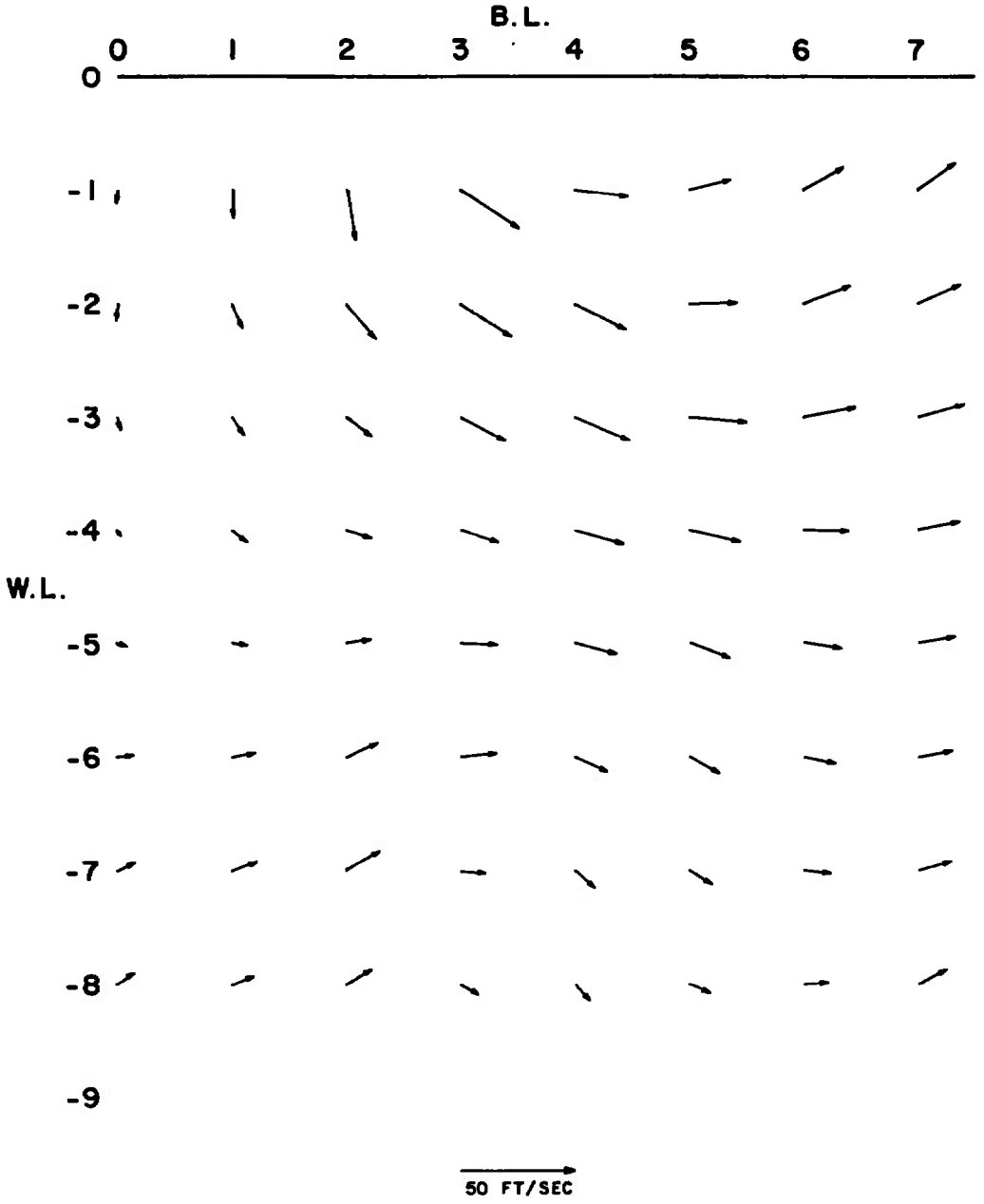

a. Configuration A

Fig. 26 Effect of External Stores on the Transverse Velocity Components of the Flow Field at $M_\infty = 0.85$, $V_\infty = 940$, MS 12

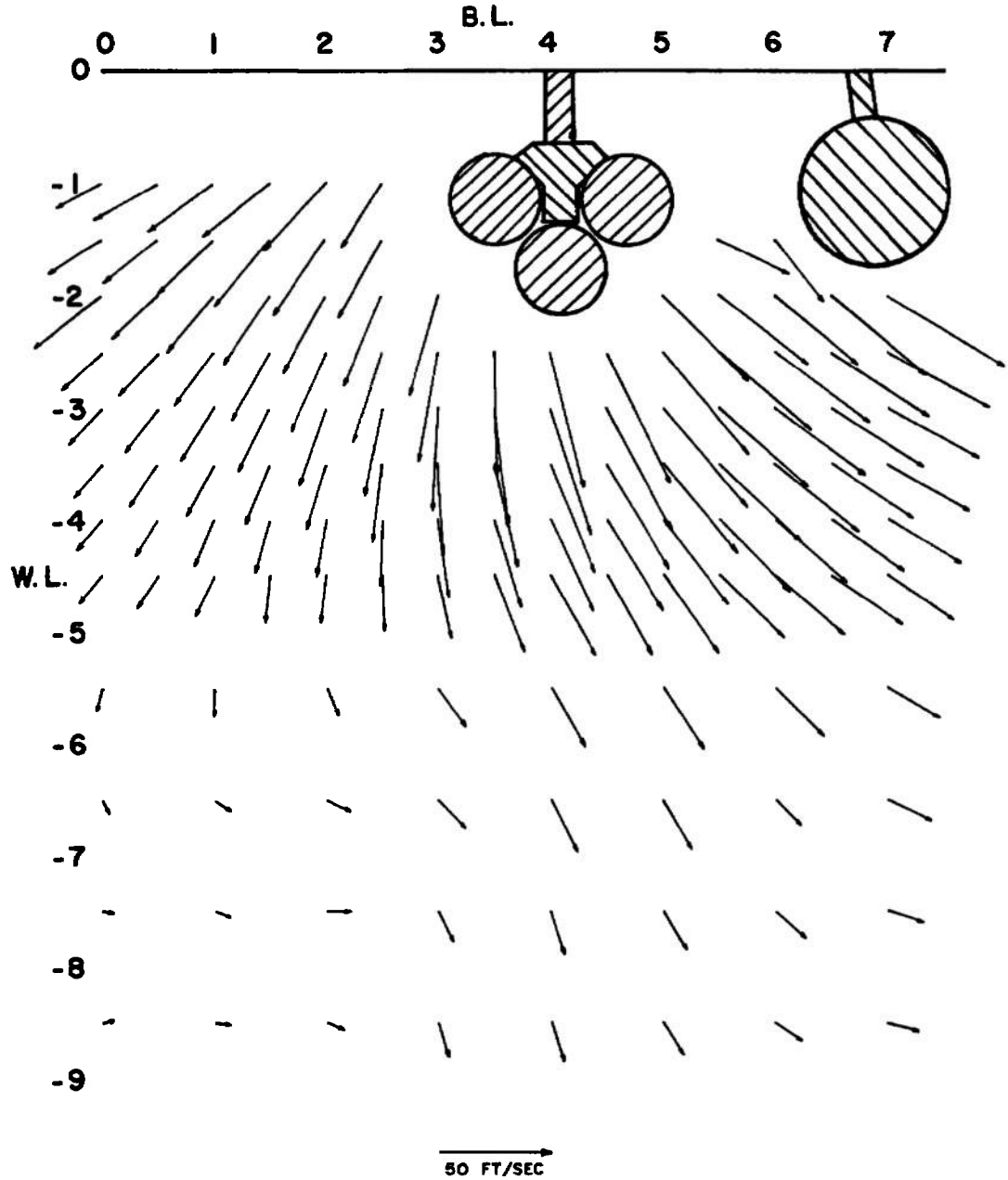

b. Configuration C
Fig. 26 Concluded

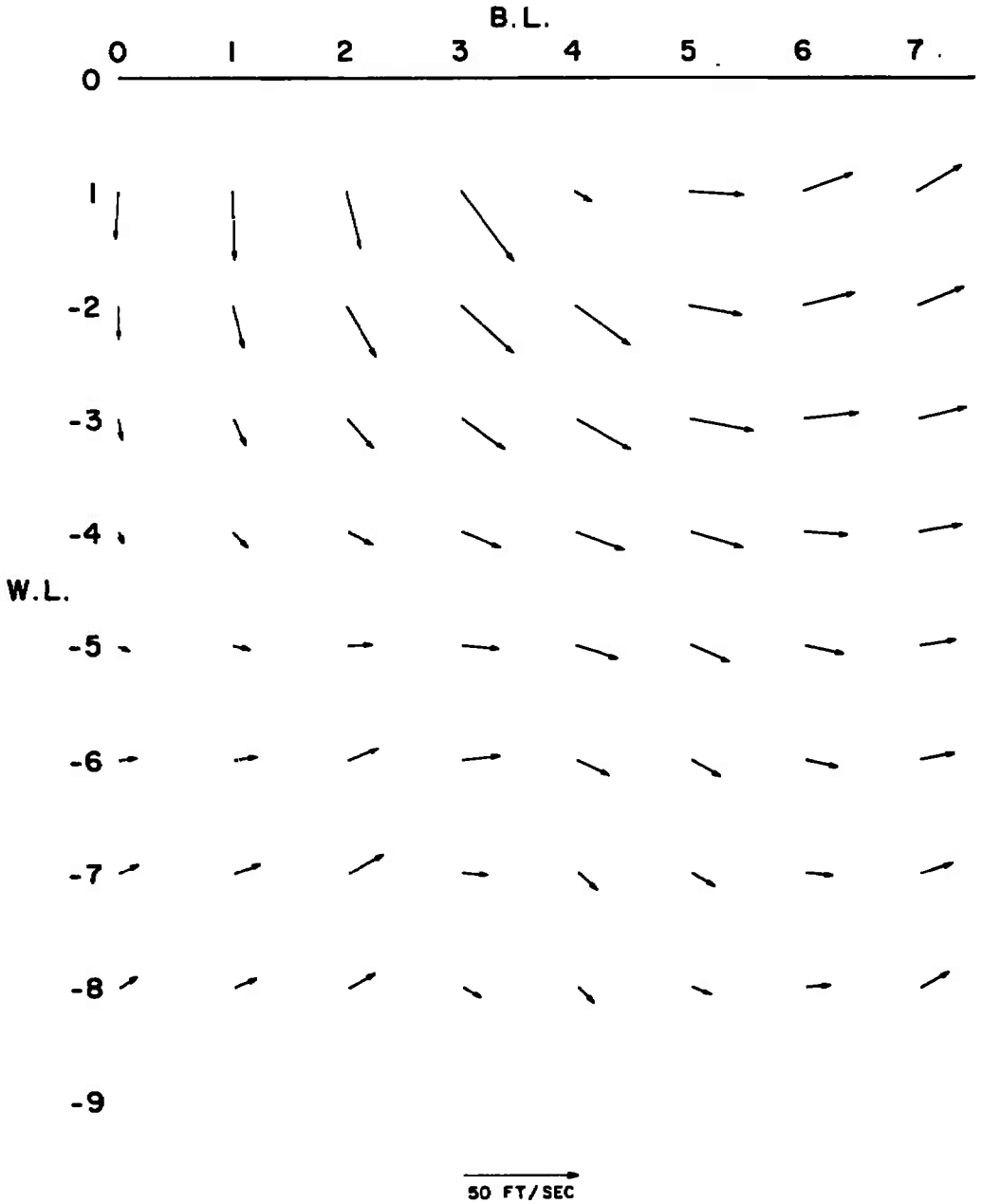

a. Configuration A

Fig. 27 Effect of External Stores on the Transverse Velocity Components of the Flow Field at $M_\infty = 0.85$, $V_\infty = 940$, MS 13

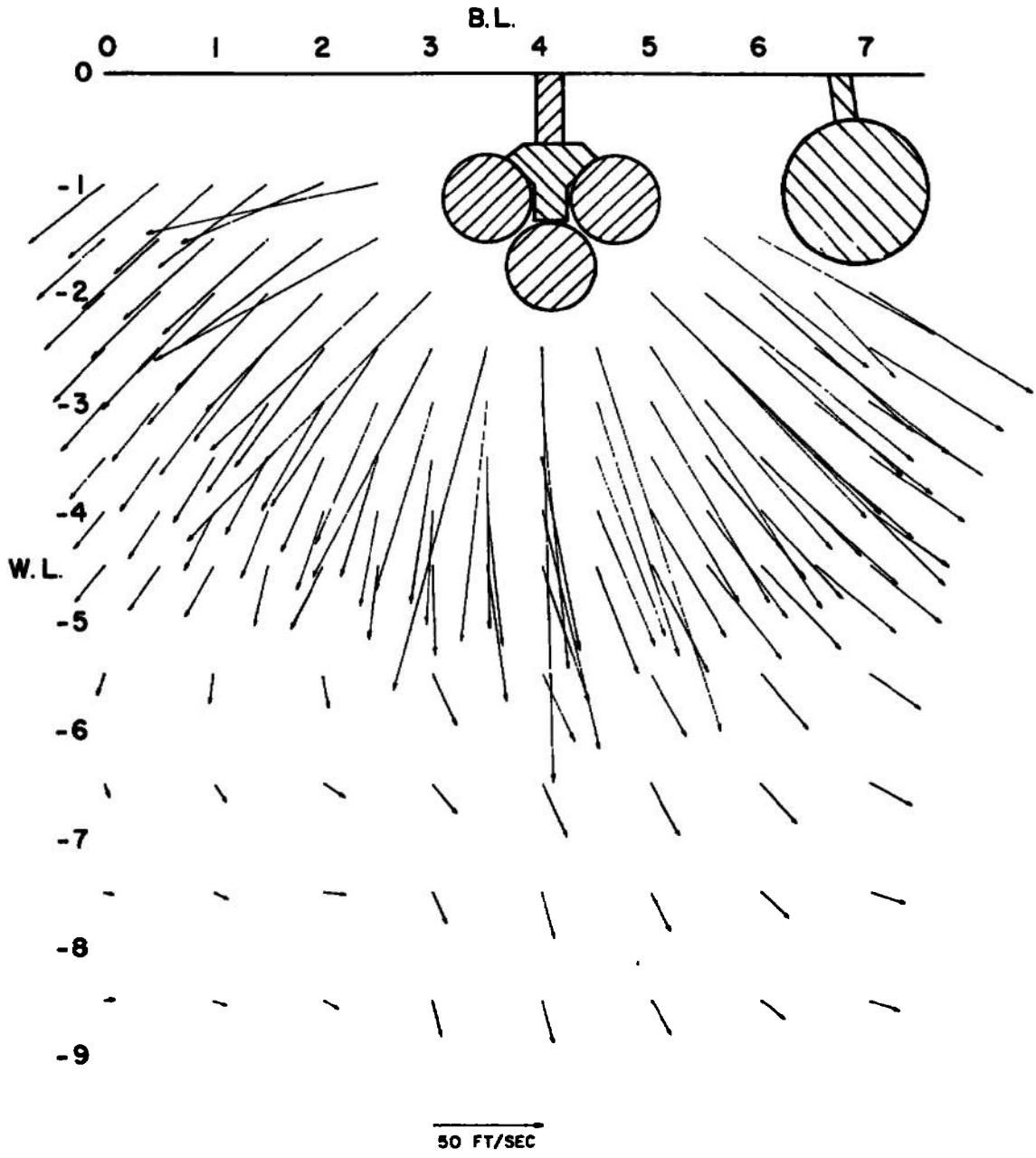

b. Configuration C
Fig. 27 Concluded

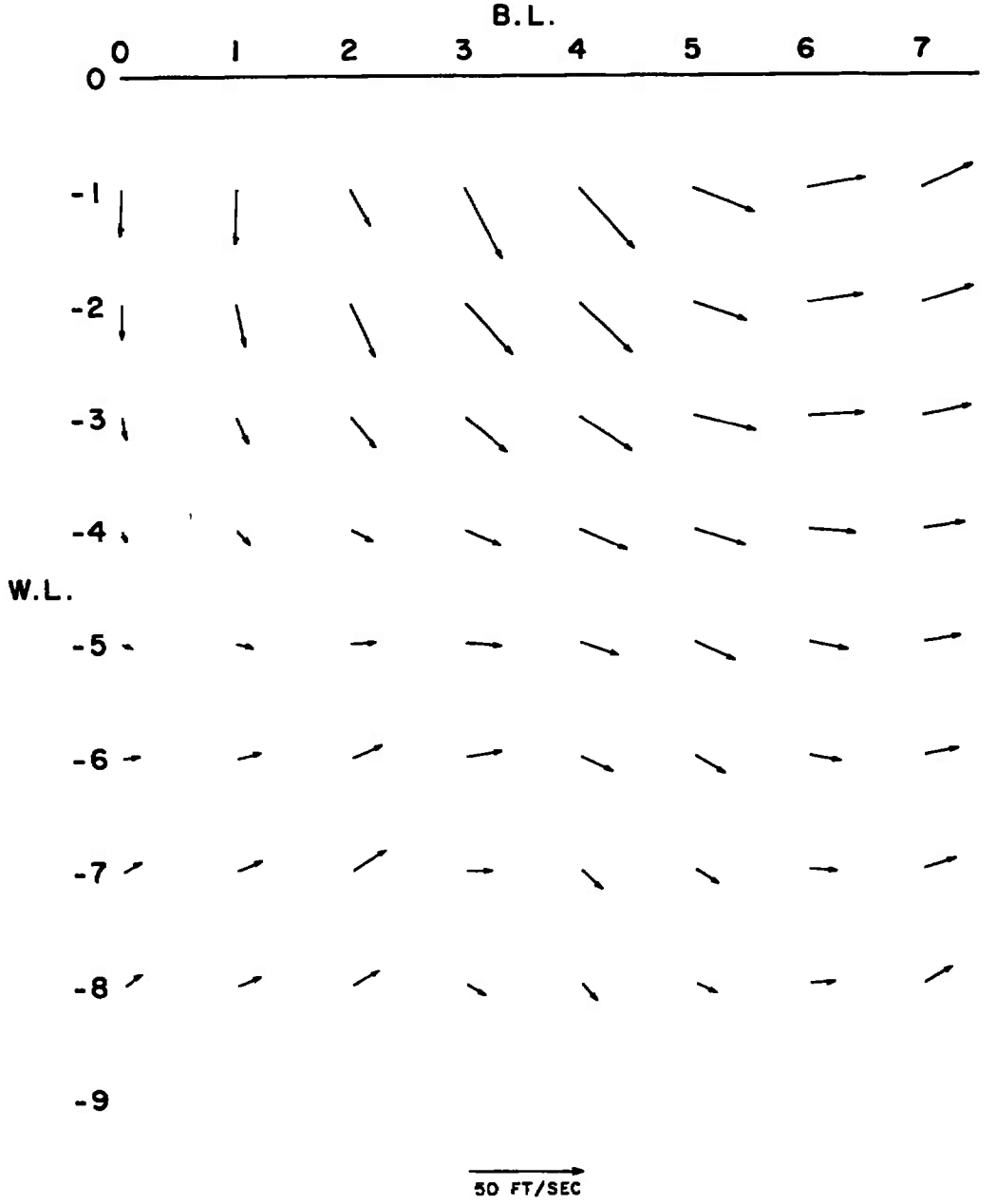

a. Configuration A

Fig. 28 Effect of External Stores on the Transverse Velocity Components of the Flow Field at M_∞ = 0.85, V_∞ = 940, MS 14

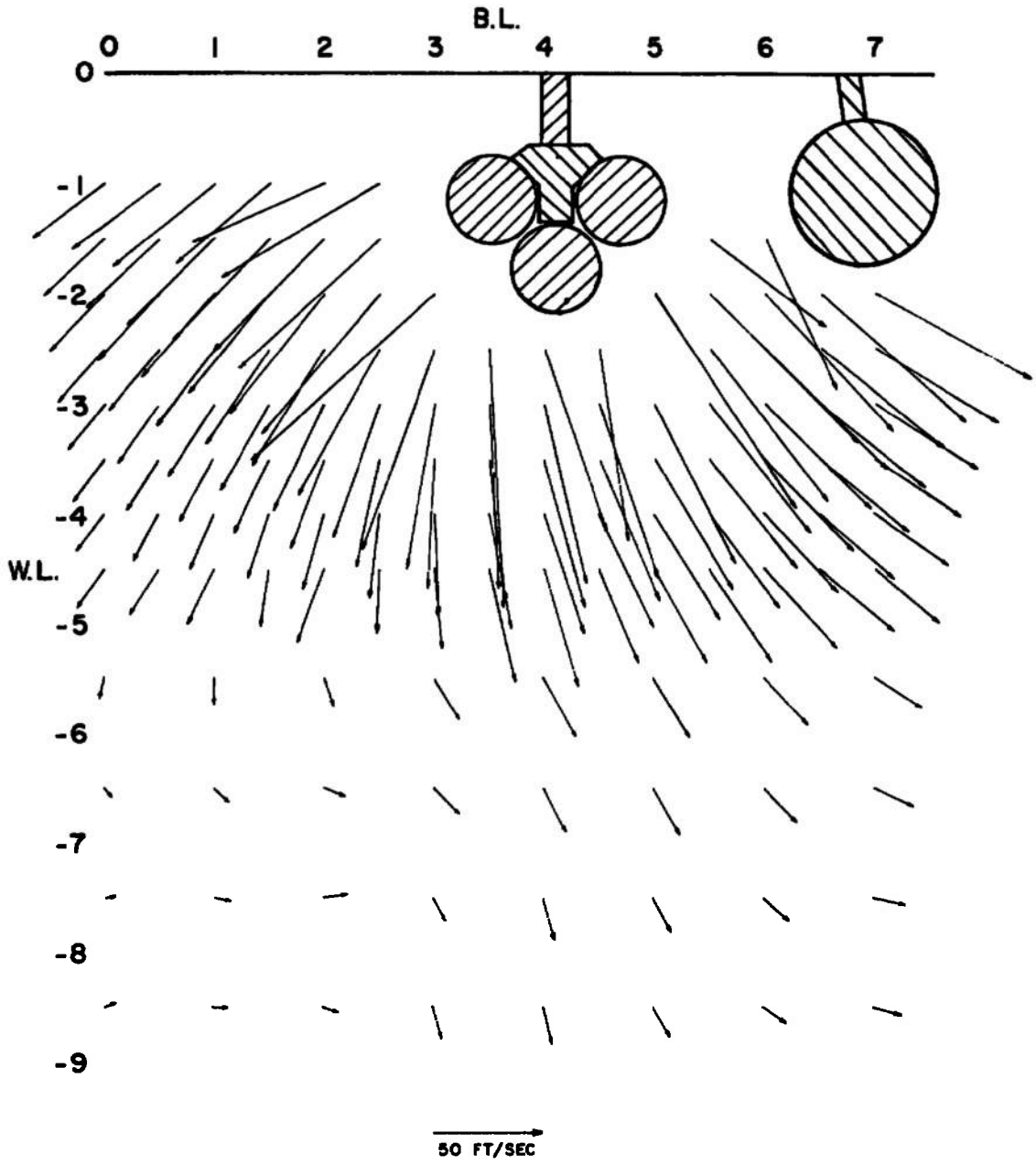

b. Configuration C
Fig. 28 Concluded

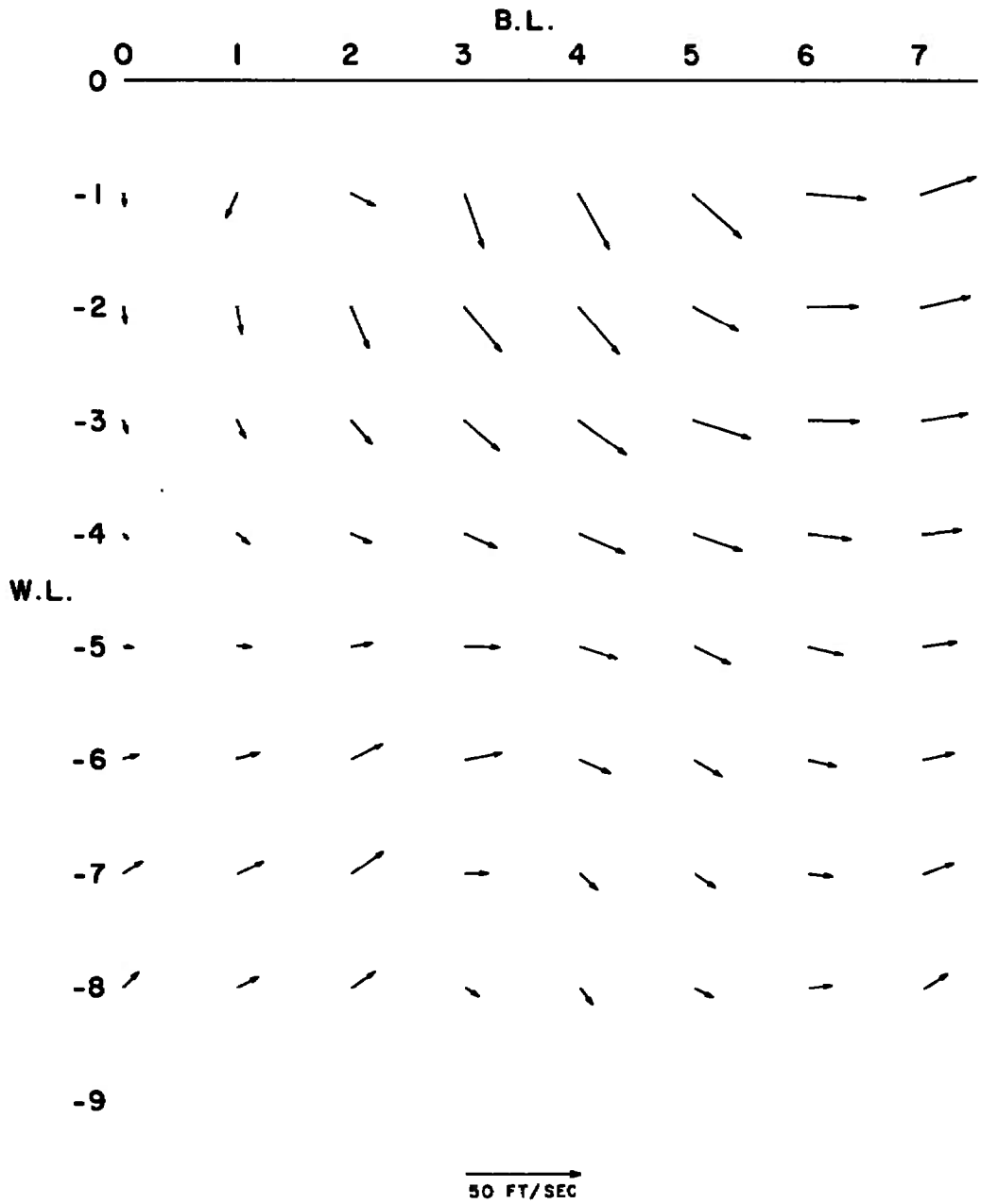

a. Configuration A

Fig. 29 Effect of External Stores on the Transverse Velocity Components of the Flow Field at M_∞ = 0.85, V_∞ = 940, MS 15

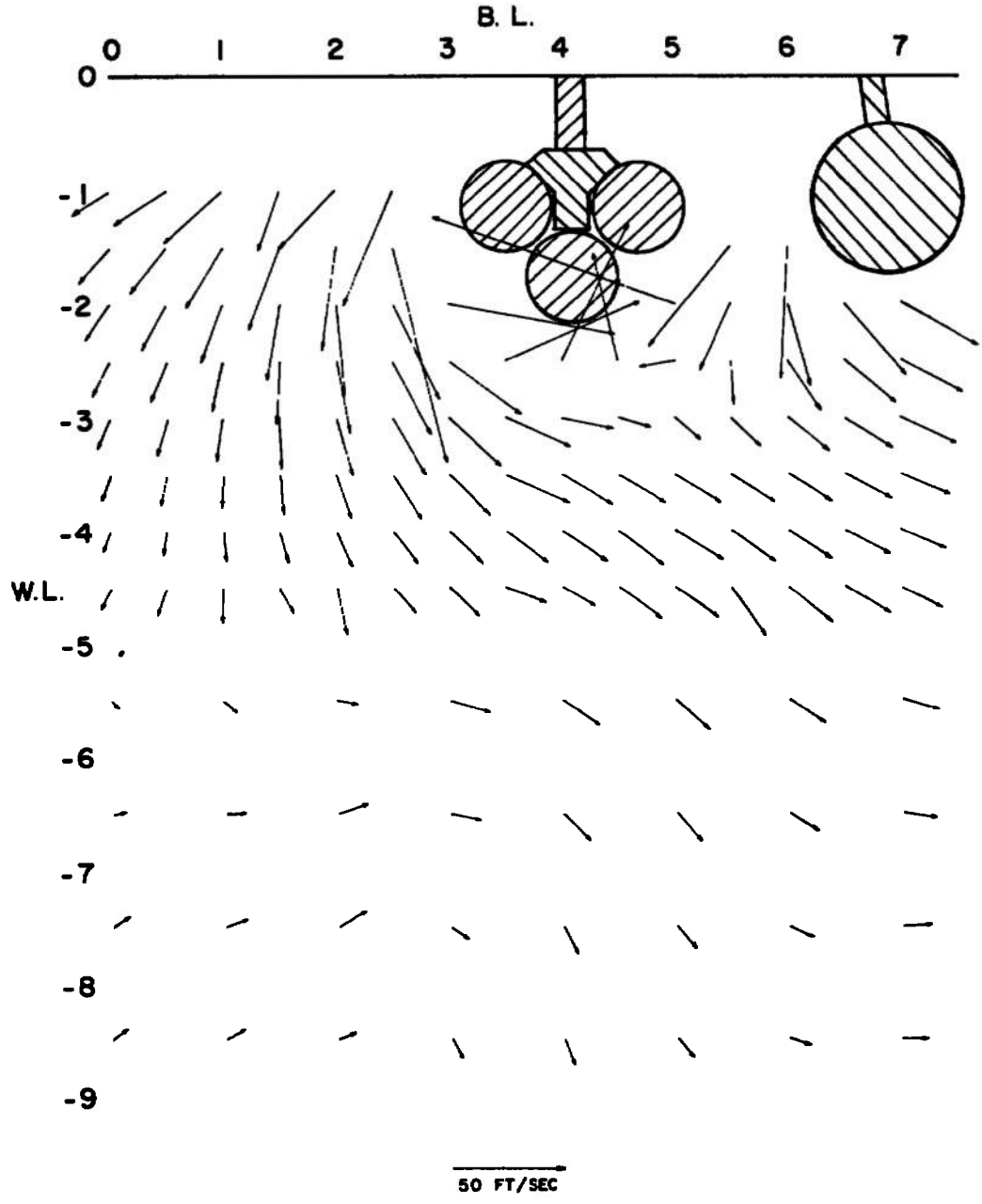

b. Configuration C
Fig. 29 Concluded

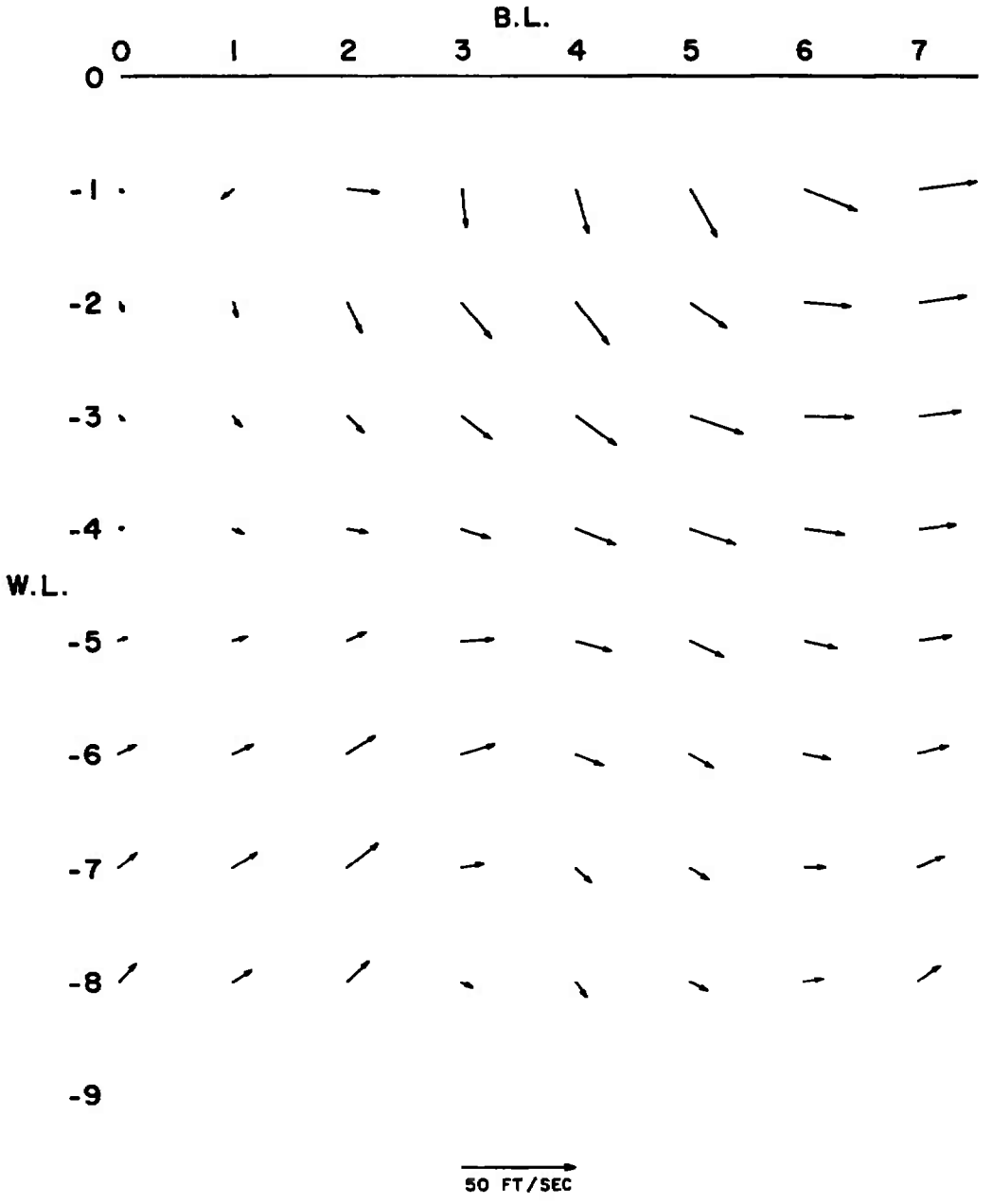

a. Configuration A

Fig. 30 Effect of External Stores on the Transverse Velocity Components of the Flow Field at $M_\infty = 0.85$, $V_\infty = 940$, MS 16

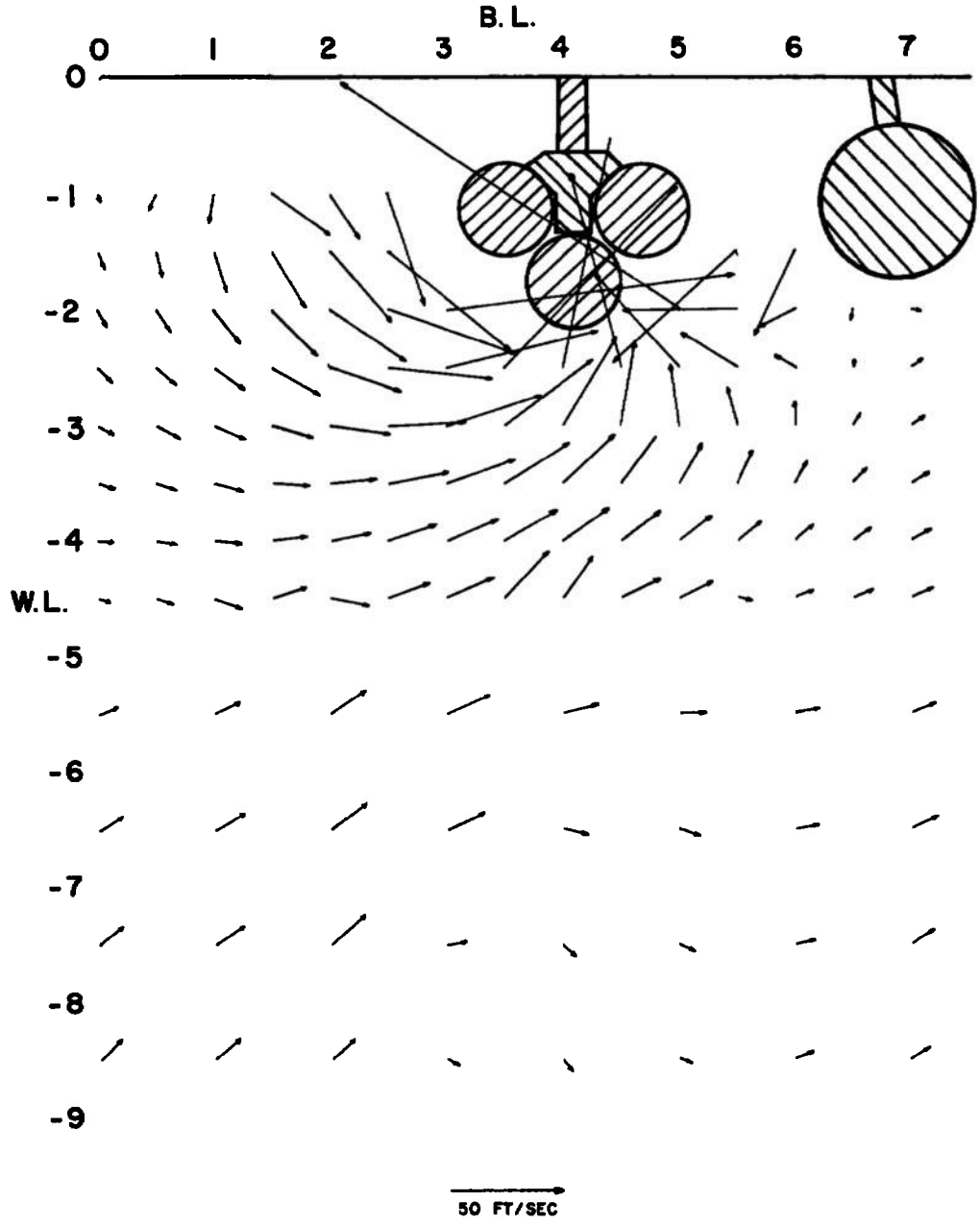

b. Configuration C
Fig. 30 Concluded

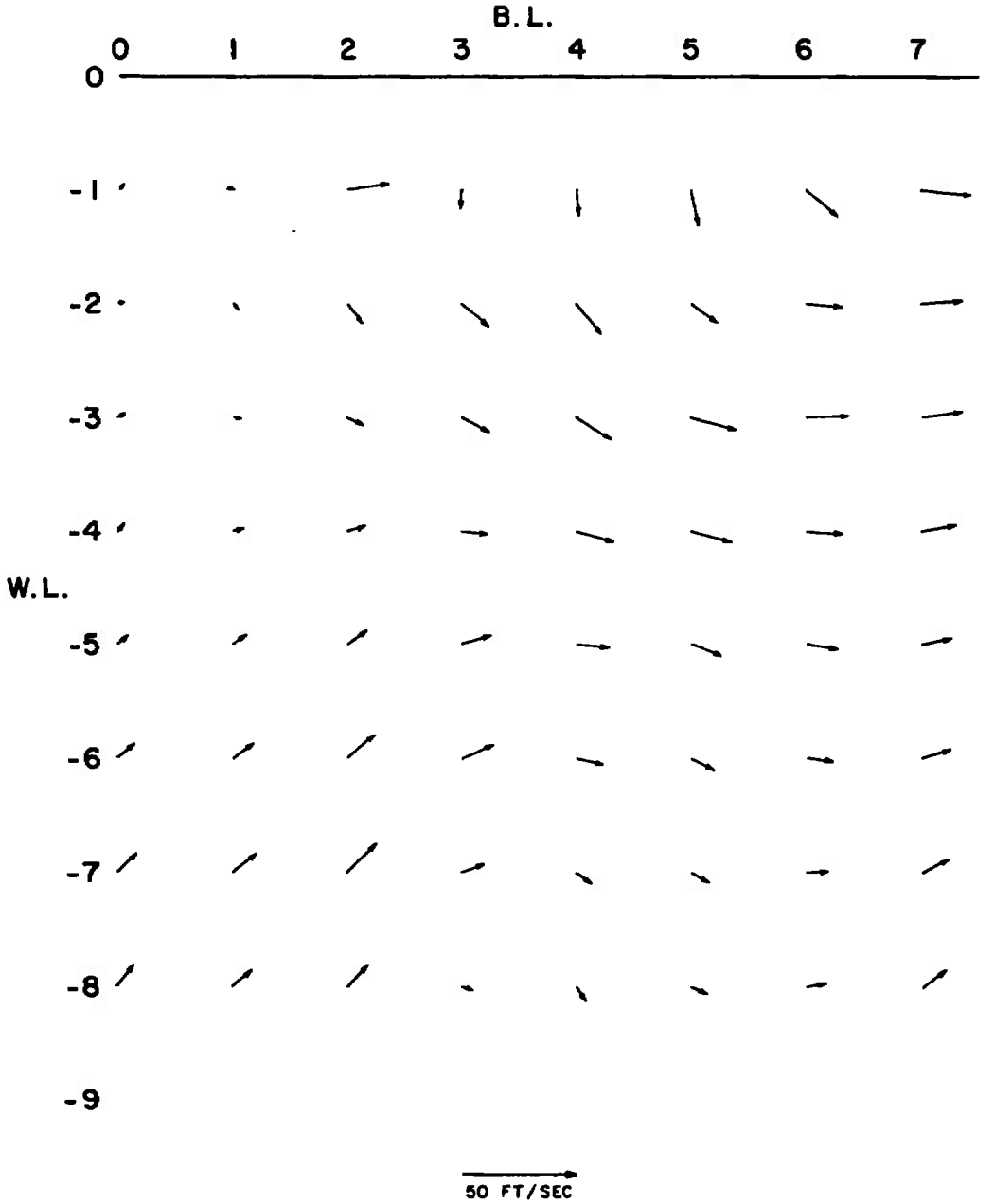

a. Configuration A

Fig. 31 Effect of External Stores on the Transverse Velocity Components of the Flow Field at $M_\infty = 0.85$, $V_\infty = 940$, MS 17

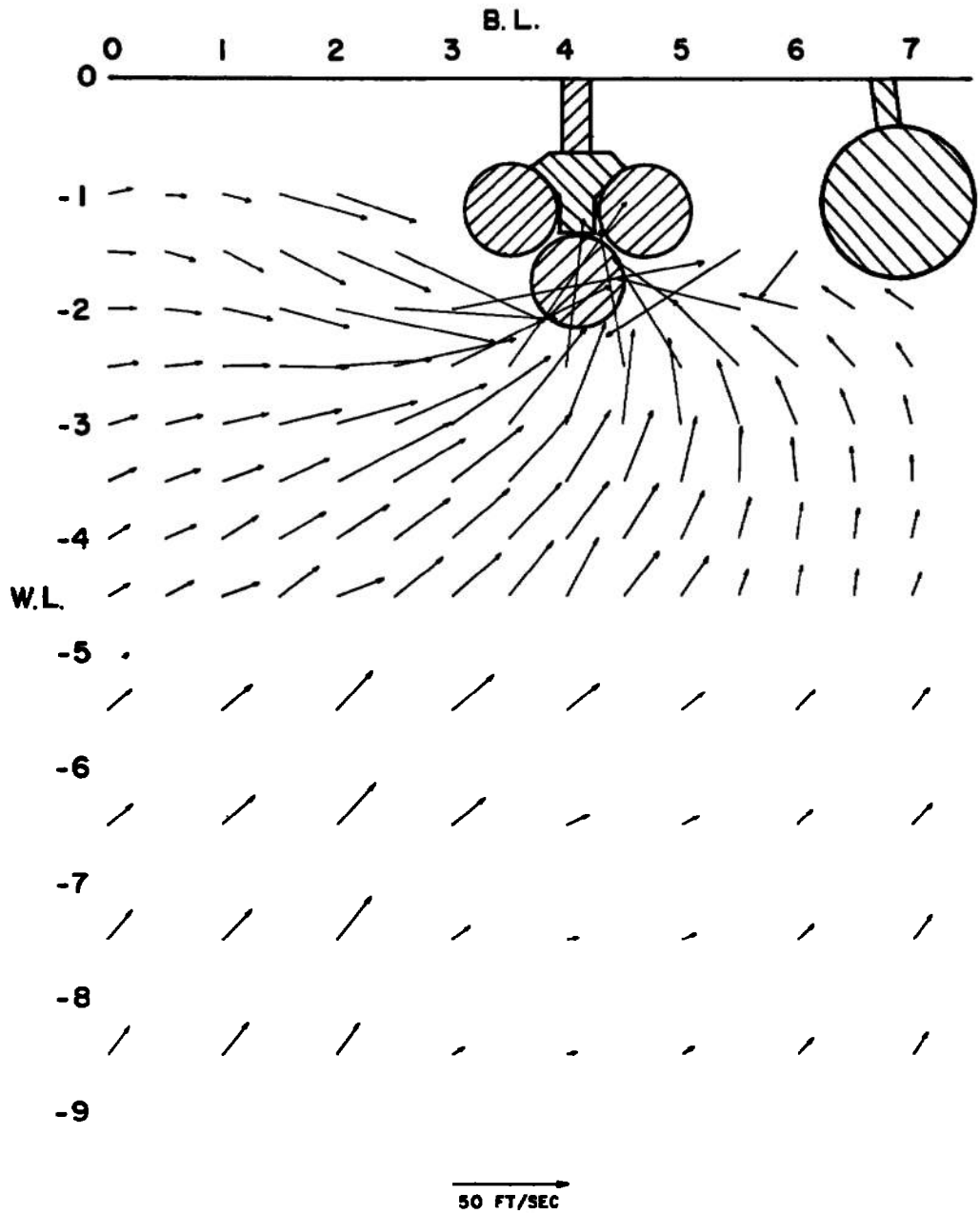

b. Configuration C
Fig. 31 Concluded

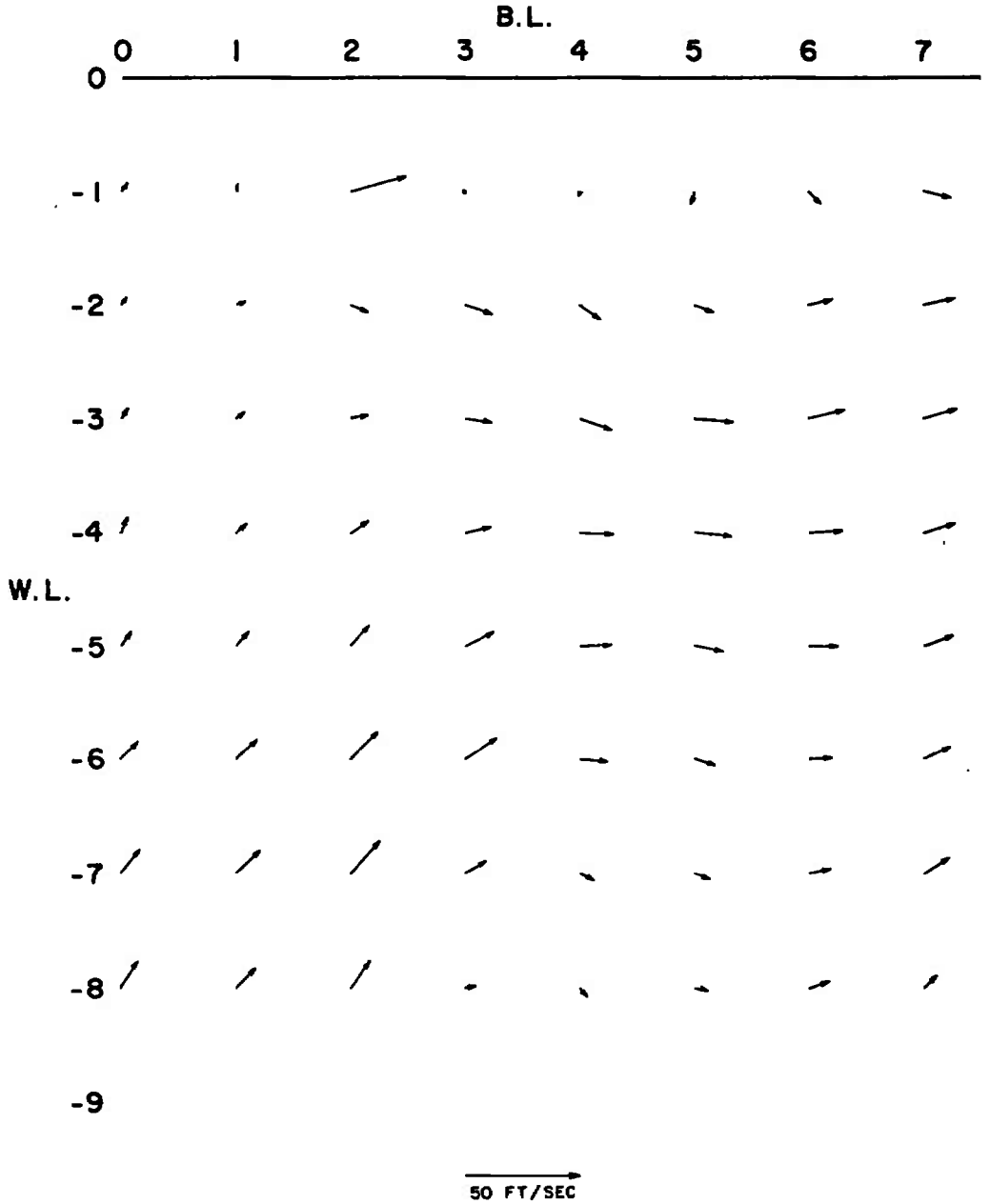

a. Configuration A

Fig. 32 Effect of External Stores on the Transverse Velocity Components of the Flow Field at M_∞ = 0.85, V_∞ = 940, MS 18

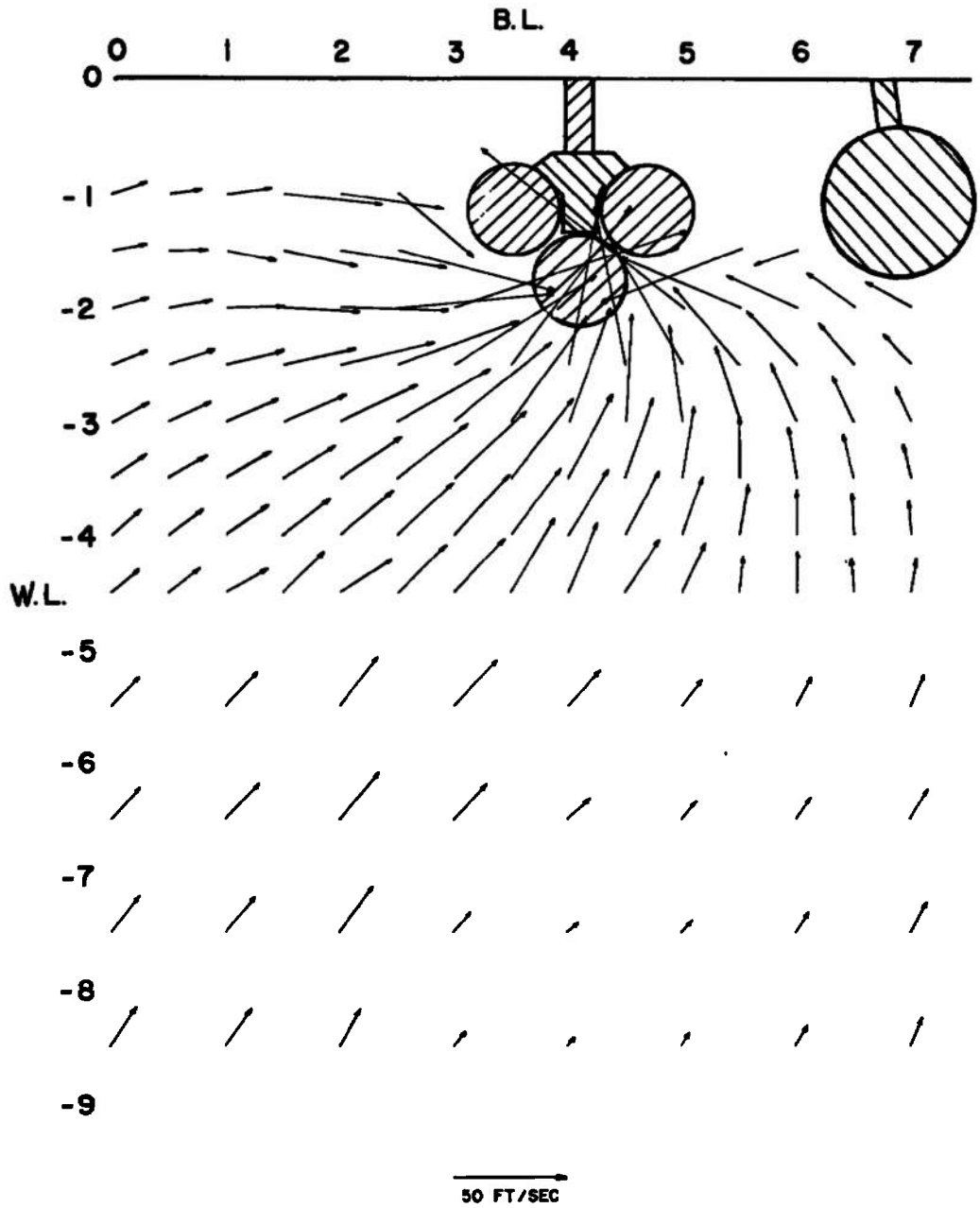

b. Configuration C
Fig. 32 Concluded

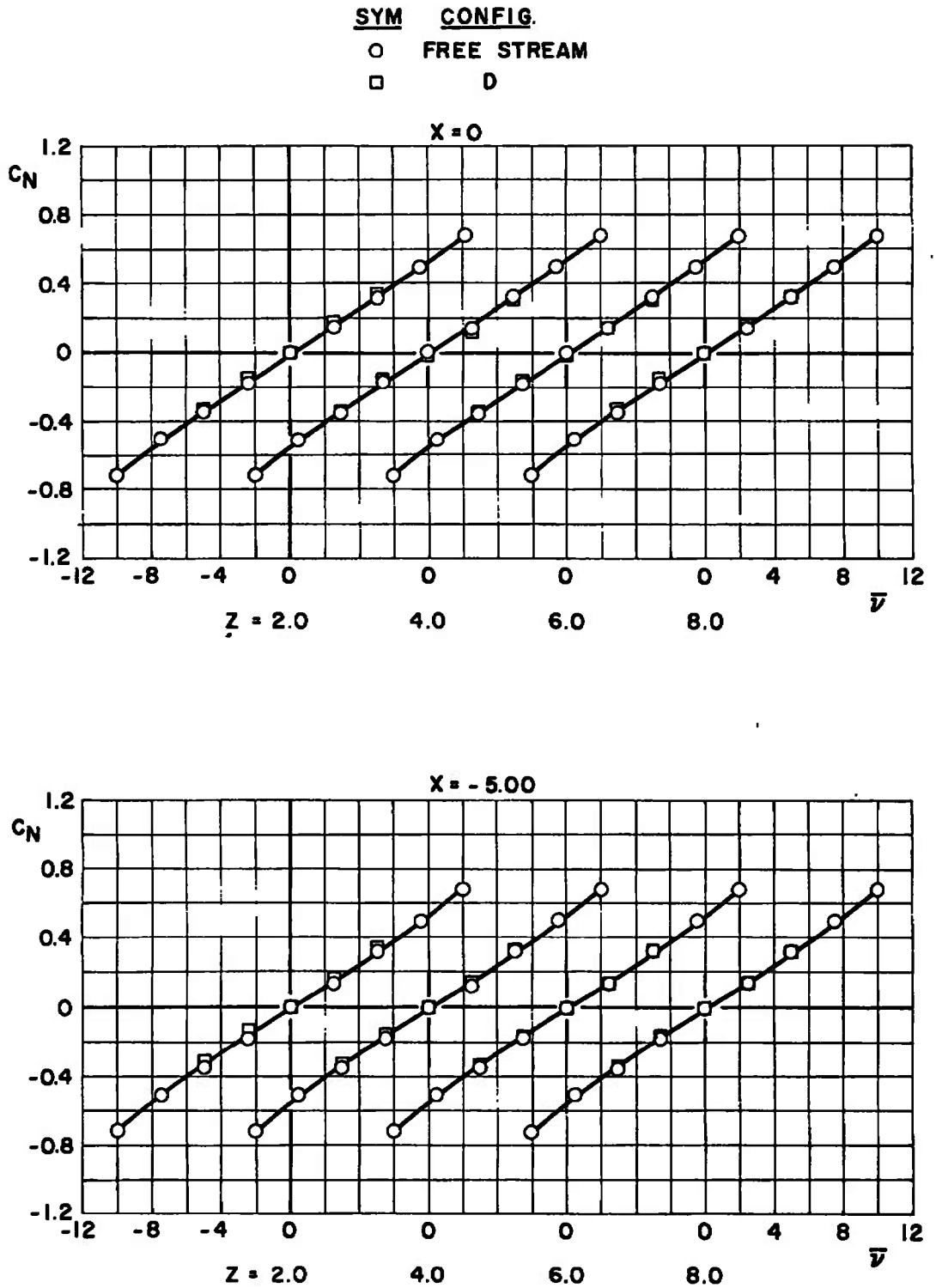

a. Y = -1.50

Fig. 33 Effect of Curvilinear Flow Field on M-117 Bomb Normal-Force Coefficient at M_∞ = 0.50

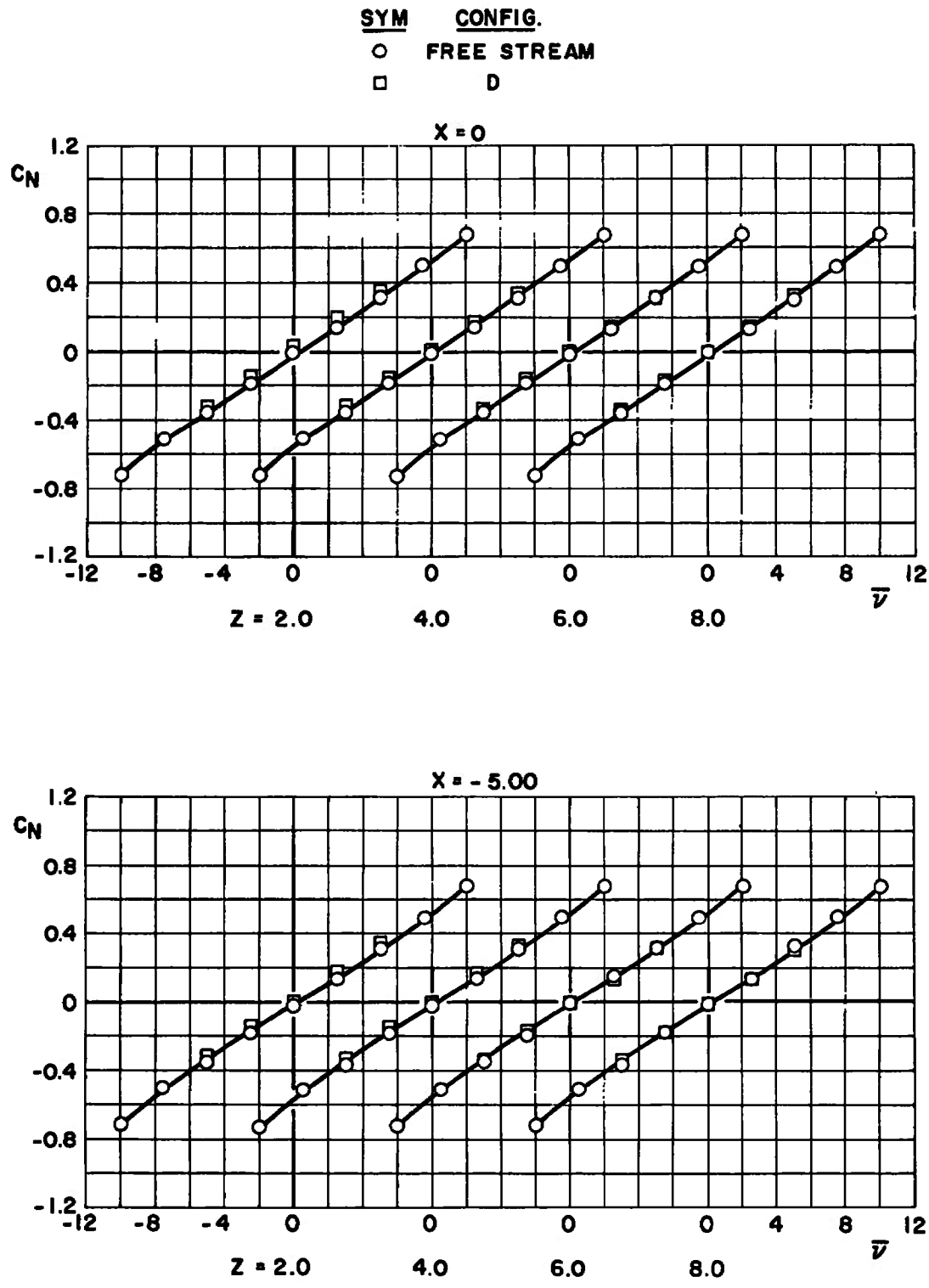

b. Y = 0
Fig. 33 Continued

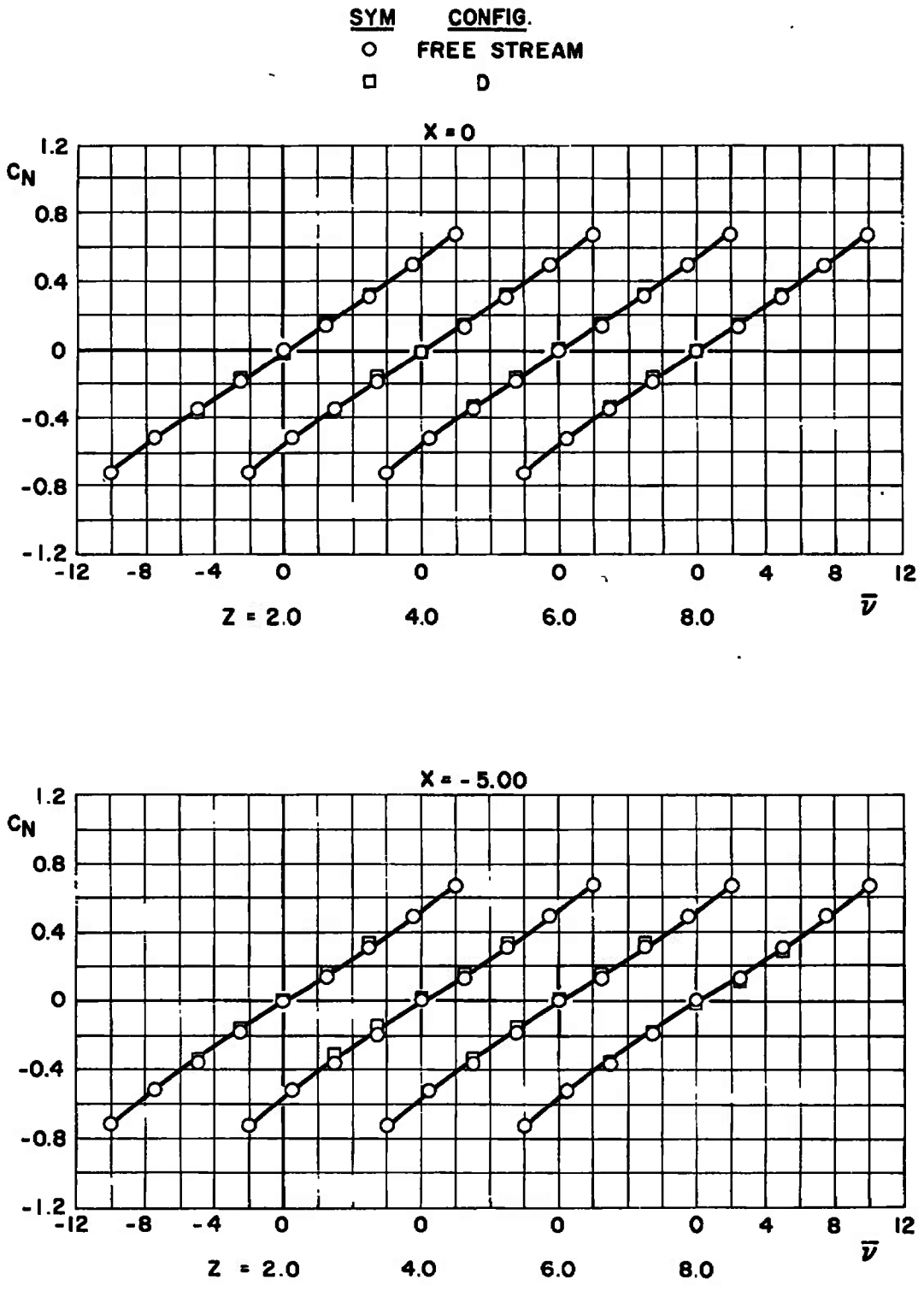

c. Y = 1.50

Fig. 33 Concluded

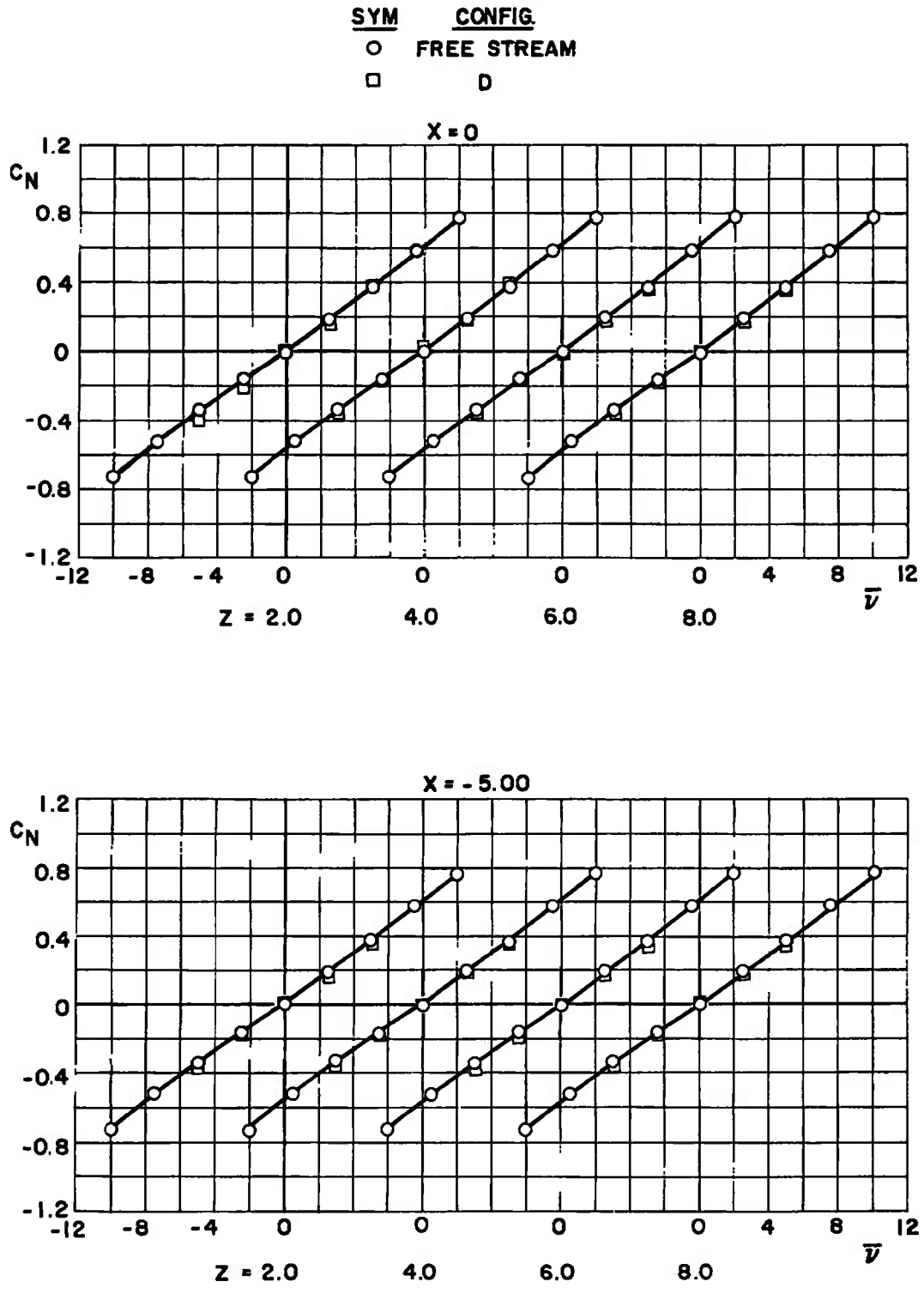

a. Y = -1.50

Fig. 34 Effect of Curvilinear Flow Field on M-117 Bomb Normal-Force Coefficient at M_∞ = 0.85

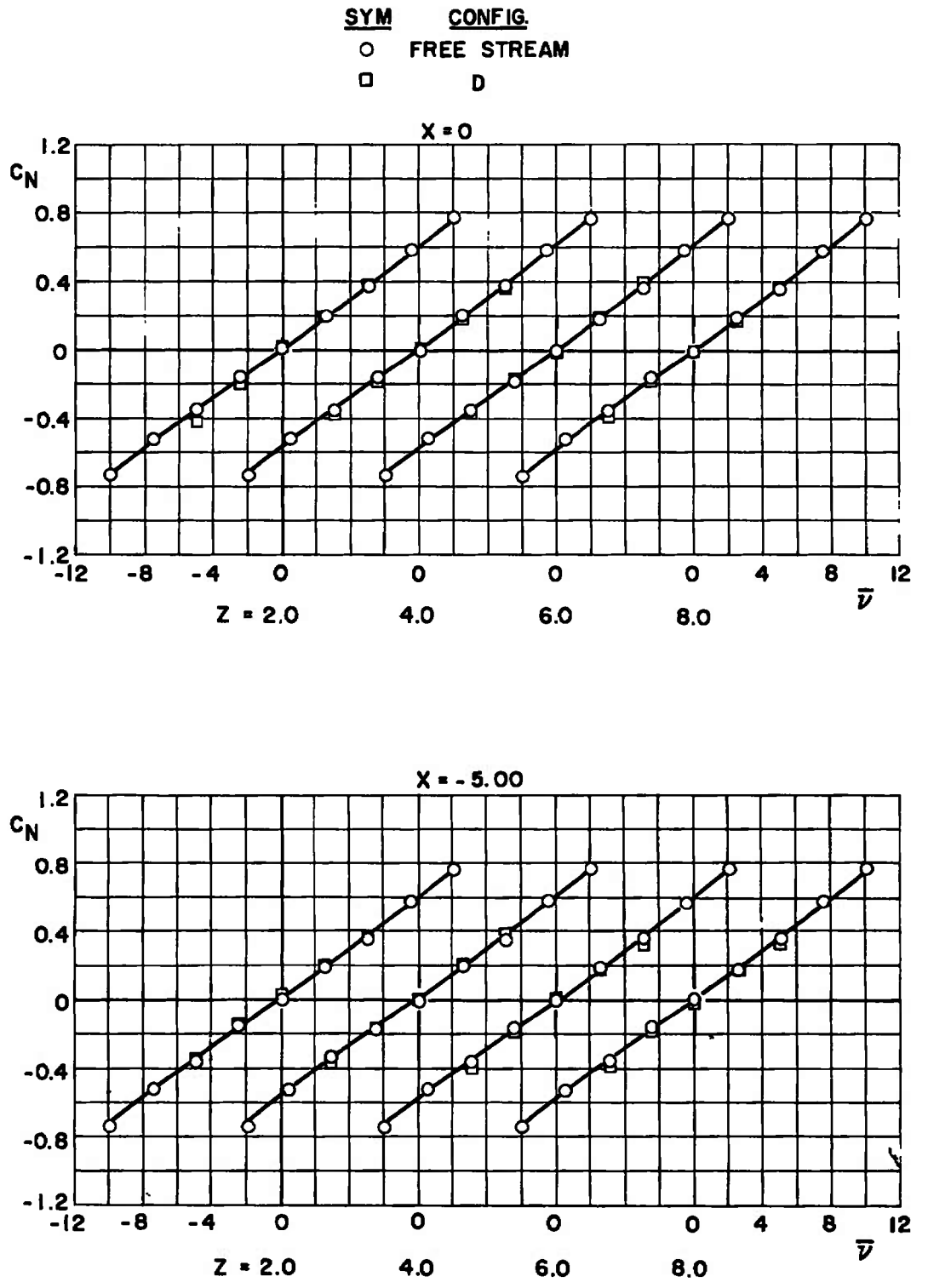

b. Y = 0
Fig. 34 Continued

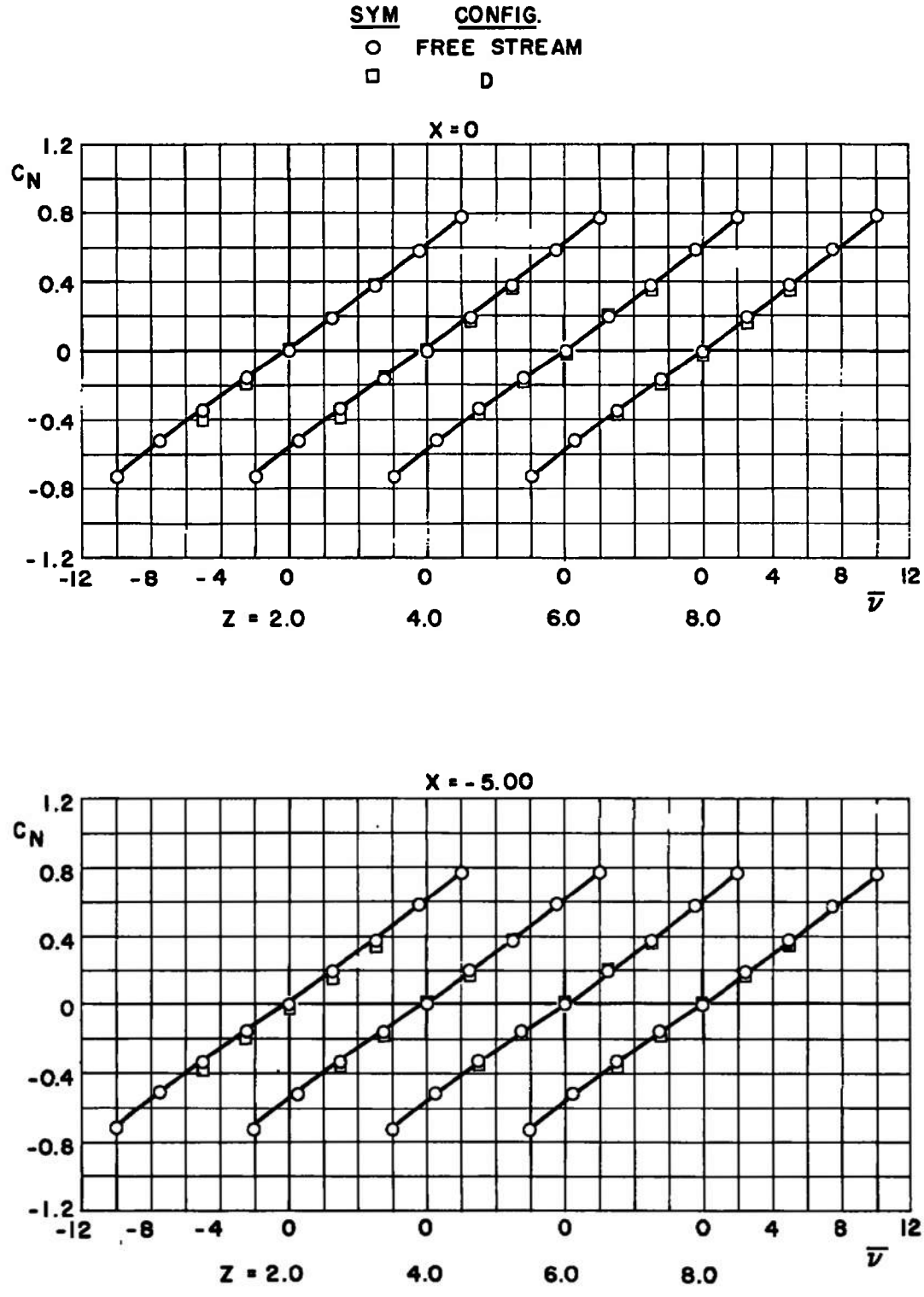

c. Y = 1.50

Fig. 34 Concluded

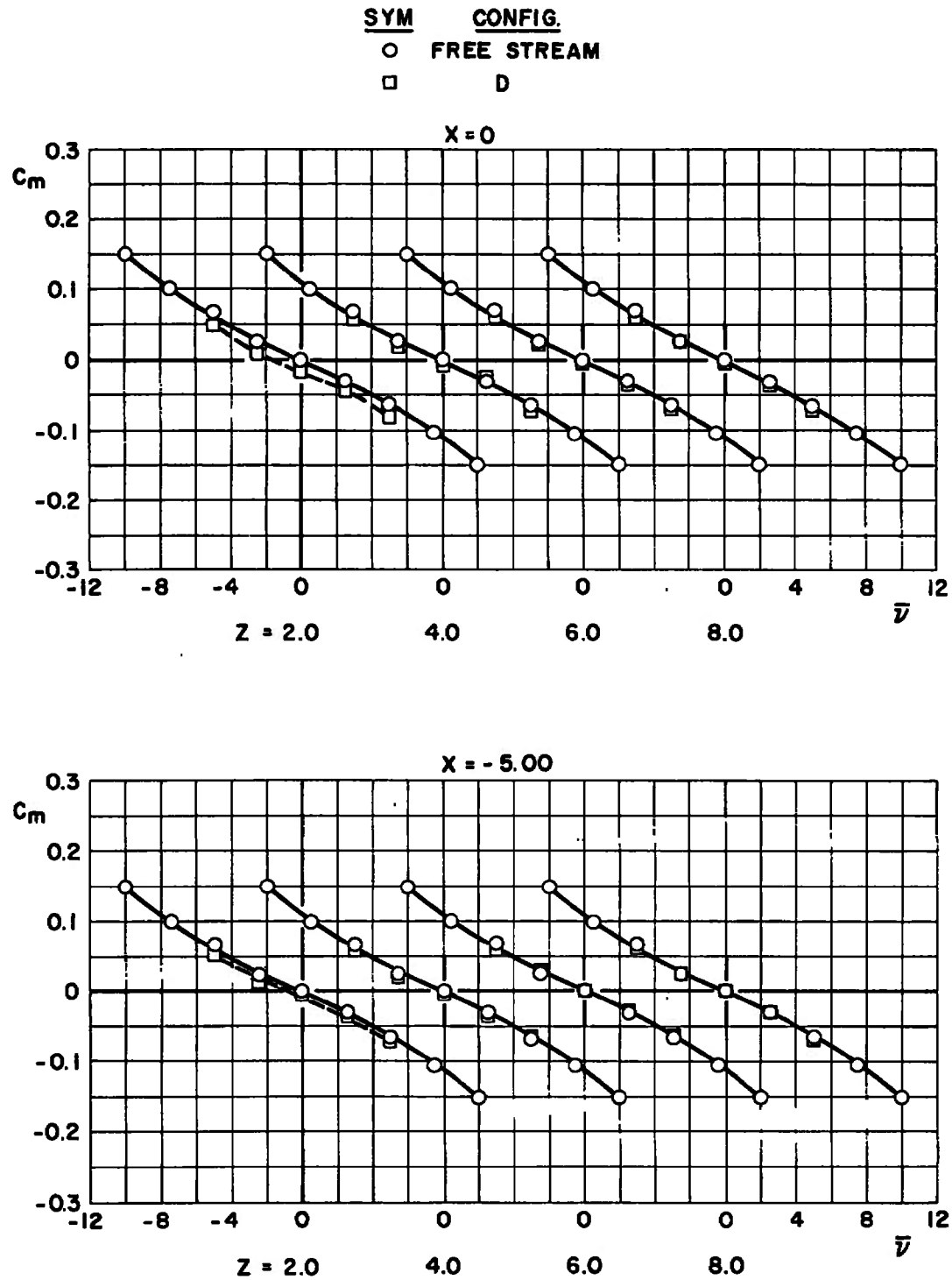

a. Y = -1.50

Fig. 35 Effect of Curvilinear Flow Field on M-117 Bomb Pitching-Moment Coefficient at M_∞ = 0.50

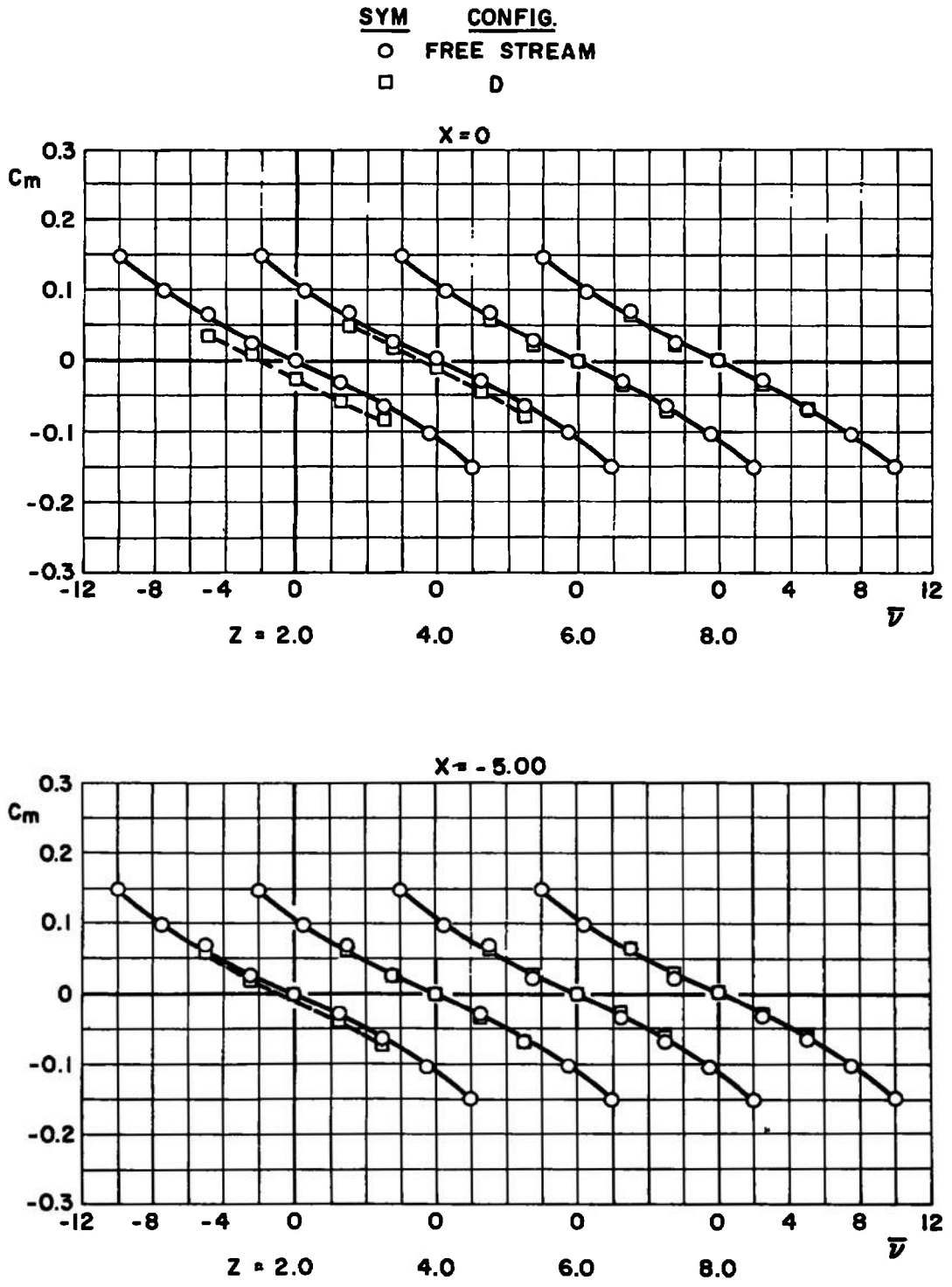

b. Y = 0

Fig. 35 Continued

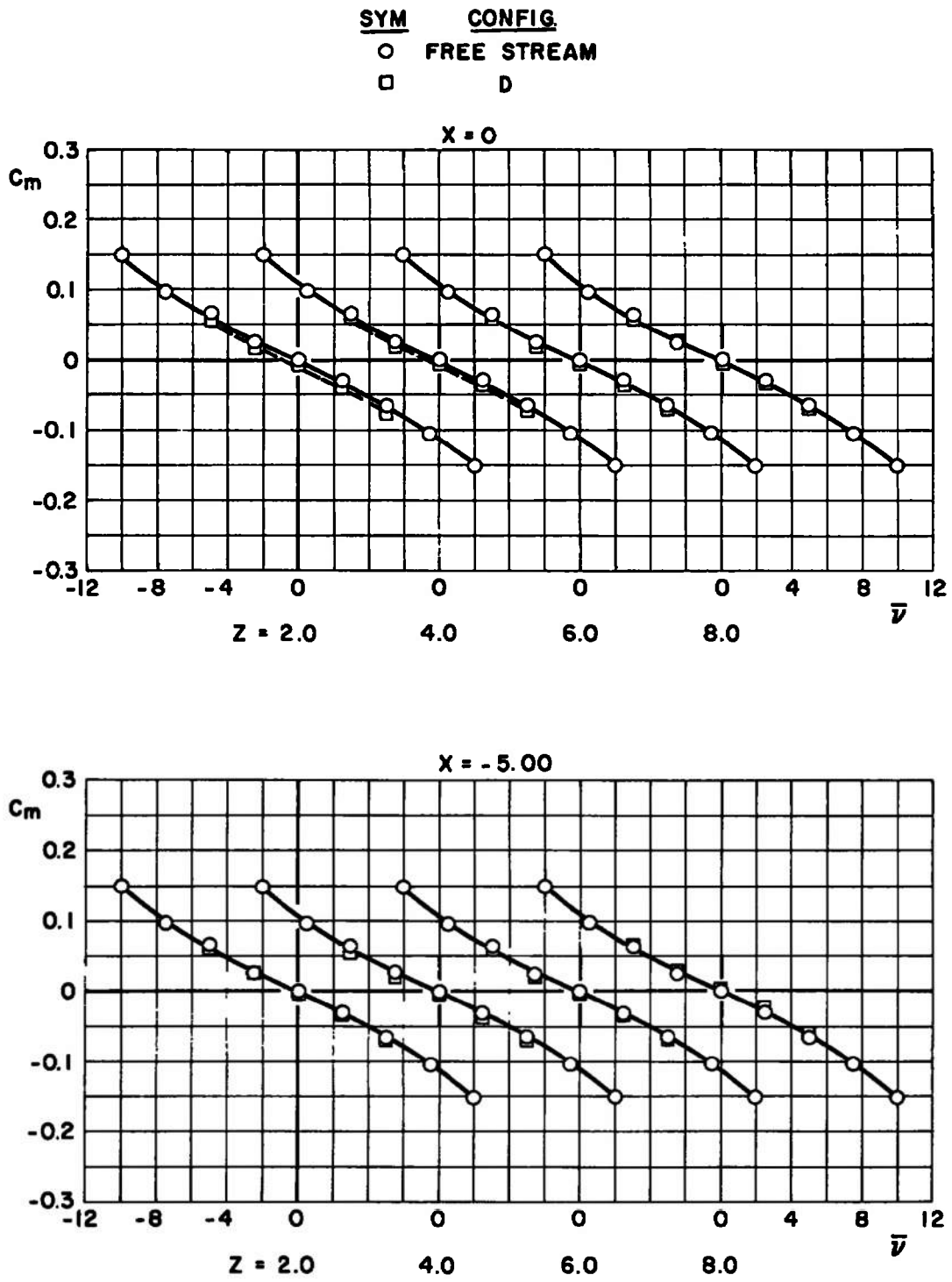

c. Y = 1.50
Fig. 35 Concluded

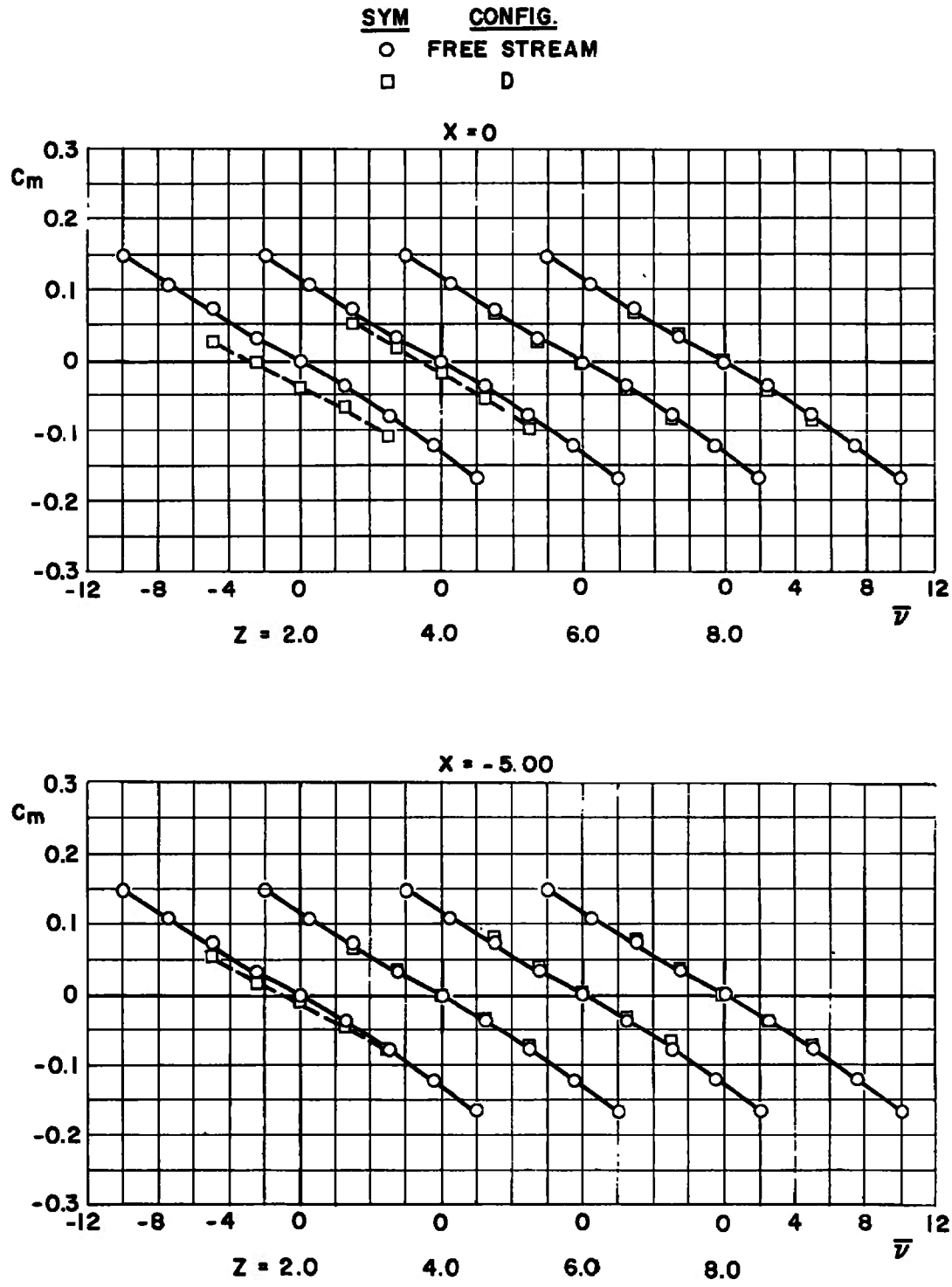

a. Y = -1.50

Fig. 36 Effect of Curvilinear Flow Field on M-117 Bomb Pitching-Moment Coefficient at M_∞ = 0.85

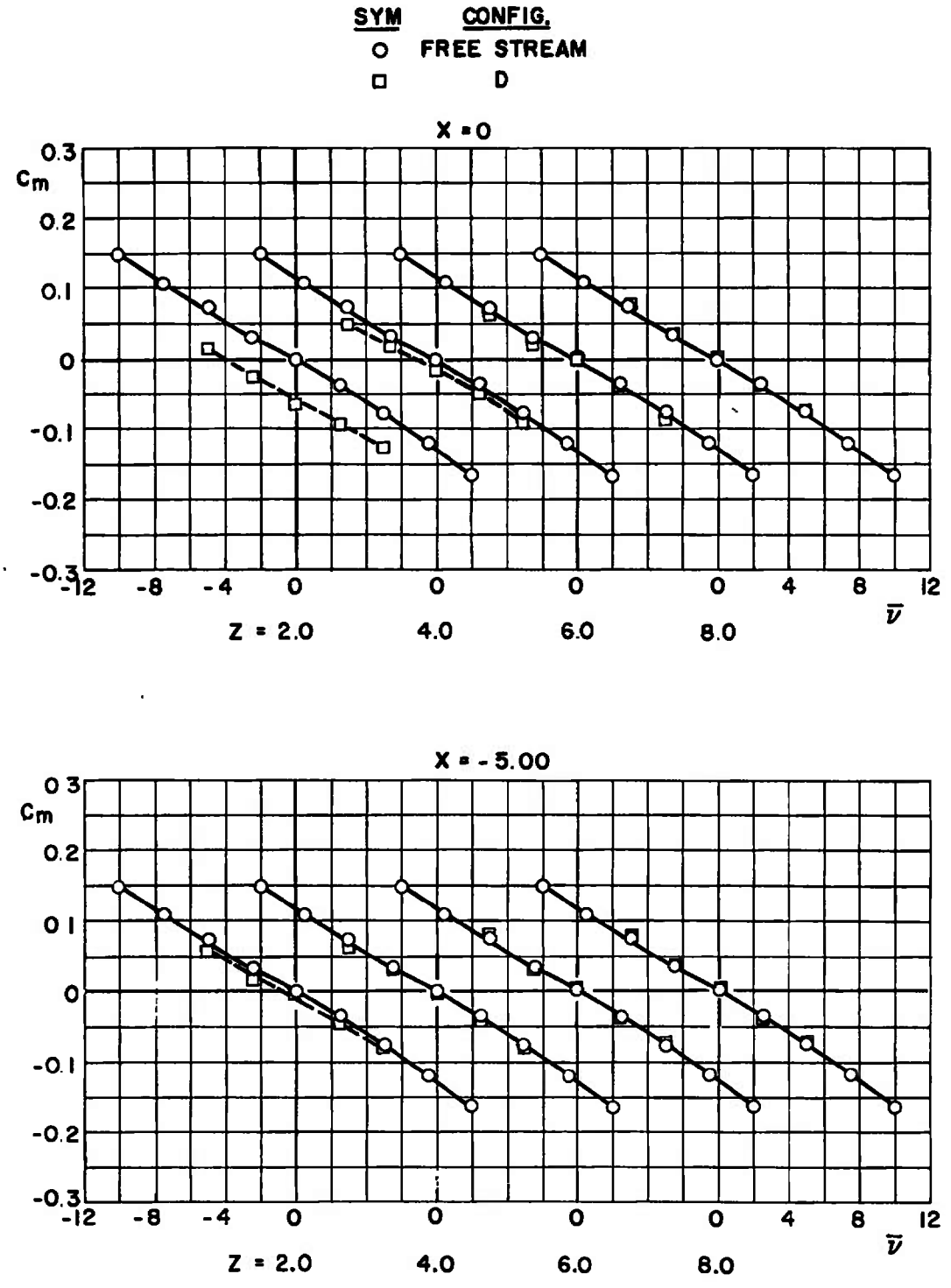

b. Y = 0
Fig. 36 Continued

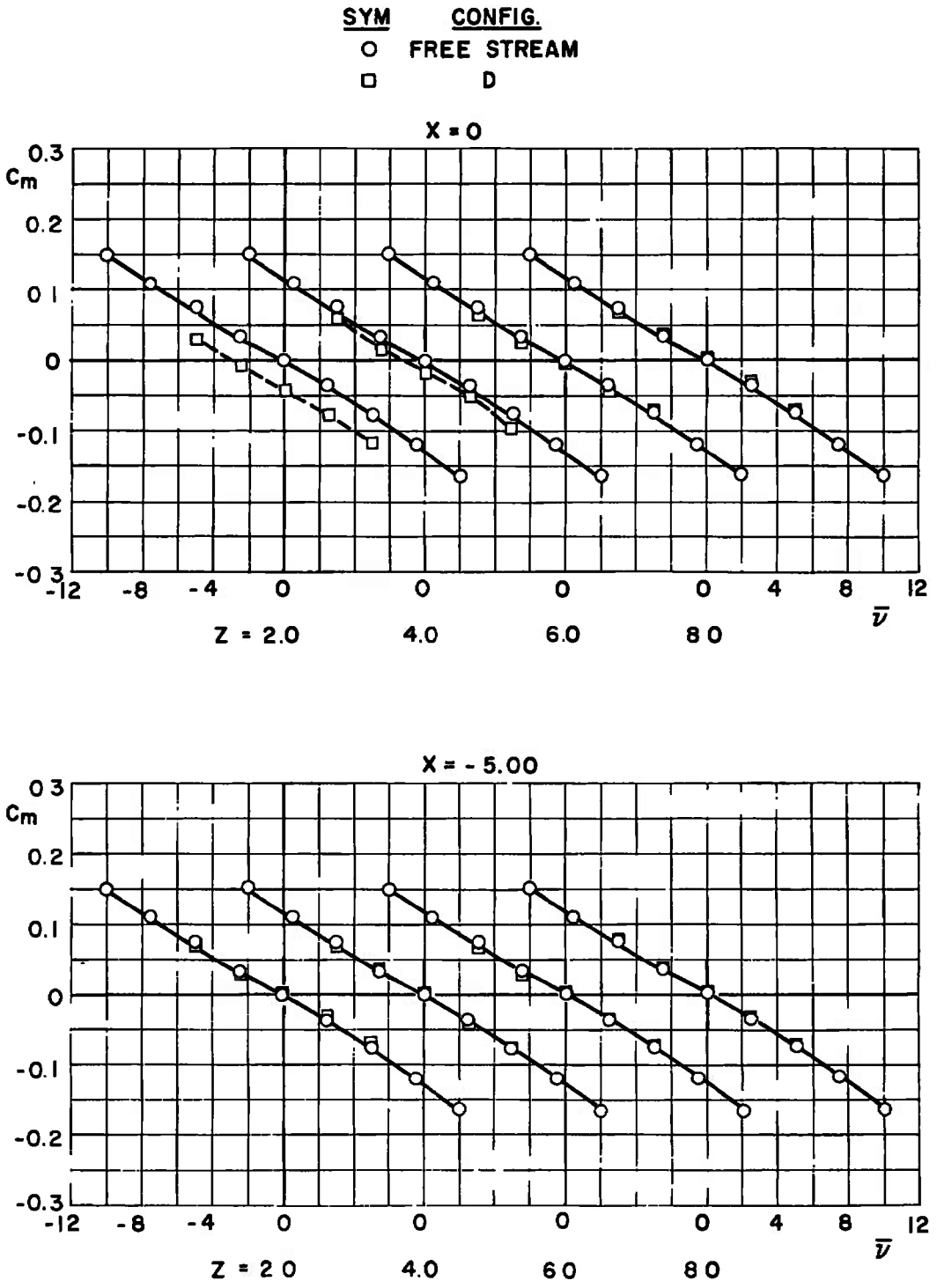

c. Y = 1.50
Fig. 36 Concluded

TABLE I
M-117 BOMB PITCH AND YAW NULL ANGLES FOR ZERO NORMAL AND SIDE FORCE IN PRESENCE OF F-4C MODEL

			Configuration							
			D				E			
			Mach Number							
			0.50		0.85		0.50		0.85	
X	Y	Z	ν_N	η_N	ν_N	η_N	ν_N	η_N	ν_N	η_N
0	-1.5	2.0	-0.38	0.12	-2.29	-0.41	0.17	1.42	0.49	0.94
		4.0	0.34	0.10	-0.52	-0.19	0.56	1.18	0.84	0.91
		6.0	0.35	-0.14	-0.31	-0.20	0.56	0.62	0.62	0.75
		8.0	0.35	-0.15	-0.81	-0.15	0.50	0.40	1.57	0.09
	0	2.0	-0.85	0.43	-3.25	0.80	0.56	1.46	0.53	0.67
		4.0	0.46	0.19	-1.34	0.54	0.72	1.32	0.76	0.90
		6.0	0.69	-0.25	-0.38	-0.06	0.85	0.64	0.99	0.50
		8.0	0.70	-0.23	-0.36	-0.02	0.86	0.46	1.02	0.30
	1.5	2.0	-0.71	0.72	-2.52	1.75	0.58	1.42	0.39	1.20
		4.0	-0.40	0.38	-1.89	0.88	0.40	1.40	0.40	0.55
		6.0	-0.06	0.30	-1.29	0.46	0.58	0.89	0.43	0.60
		8.0	0.59	-0.29	-0.85	0.20	0.77	0.61	0.91	0.22
-5.0	-1.5	2.0	-0.72	0.52	-2.54	0.68	-1.45	1.26	-2.52	0.41
		4.0	0.19	0.04	-1.53	0.35	0.36	1.01	-0.73	0.62
		6.0	0.19	-0.31	-1.53	0.53	0.54	0.73	-0.47	0.30
		8.0	0.20	-0.28	-1.53	0.38	0.54	0.51	-0.18	0.10
	0	2.0	-0.41	0.75	-1.99	1.23	0	1.90	-1.94	1.35
		4.0	-0.03	0.28	-1.53	0.67	0.42	1.51	-1.01	0.70
		6.0	0.31	-0.18	-1.29	0.33	0.81	0.69	-0.31	0.16
		8.0	0.32	-0.18	-1.28	0.38	0.84	0.48	-0.28	0.21
	1.5	2.0	-0.53	0.45	-2.23	1.13	0.04	1.82	-1.51	1.21
		4.0	-0.49	0.41	-2.19	0.95	0.08	1.43	-1.47	0.70
		6.0	-0.27	-0.09	-1.70	0.37	0.31	1.03	-1.07	0.41
		8.0	-0.10	-0.06	-1.4	0.31	1.05	0.59	-0.49	0.08

TABLE II
COMPARISON OF PROBE INDICATED FLOW ANGLE WITH M-117 BOMB ZERO NORMAL- AND SIDE-FORCE NULL ANGLES

Probe or M-117 Bomb cg Position						Mach Number							
Configuration													
B			E			0.50				0.85			
MS	BL	WL	MS	BL	WL	ν_N	ϵ	η_N	σ	ν_N	ϵ	η_N	σ
9.00	5.00	-3.00	14.63	4.66	-3.16	0.56	0.74	1.46	1.99	0.53	0.54	0.67	1.87
10.00	↓	↓	↓	↓	↓	↓	0.79	↓	1.89	↓	0.46	↓	1.73
11.00							1.02		1.80		0.54		1.55
12.00							1.43		1.69		1.13		1.44
13.00							1.80		1.66		1.97		1.54
14.00							1.58		1.52		1.75		1.37
15.00							1.05		1.31		0.78		1.00
16.00							0.35		0.91		0.28		0.91
17.00							0.13		0.63		0.21		1.02
18.00							0.21		1.32		-0.07		0.97
9.00		-5.00			-5.16	0.72	0.77	1.32	1.18	0.76	0.72	0.90	1.16
10.00		↓			↓	↓	0.85	↓	1.15	↓	0.73	↓	1.11
11.00							0.95		1.12		0.80		1.07
12.00							1.09		1.08		1.01		1.02
13.00							1.03		1.06		1.16		1.01
14.00							0.95		1.03		1.09		0.95
15.00							0.72		1.01		0.75		0.89
16.00							-0.35		0.87		0.48		0.81
17.00							-0.25		0.66		0.25		0.86
18.00							0.16		1.01		0.03		0.83
9.00		-7.00			-7.16	0.85	0.78	0.64	0.55	0.99	0.63	0.50	0.65
10.00		↓			↓	↓	0.79	↓	0.52	↓	0.59	↓	0.64
11.00							0.88		0.51		0.68		0.60
12.00							0.87		0.48		0.73		0.57
13.00							0.91		0.47		0.78		0.57
14.00							0.78		0.43		0.73		0.51
15.00							0.74		0.42		0.57		0.49
16.00							-0.36		0.87		0.39		0.46
17.00							-0.64		1.02		0.27		0.51
18.00	↓	↓	↓	↓	↓	↓	0.43	↓	0.41	↓	0.20	↓	0.49

UNCLASSIFIED

Security Classification

DOCUMENT CONTROL DATA - R & D

(Security classification of title, body of abstract and indexing annotation must be entered when the overall report is classified)

1. ORIGINATING ACTIVITY *(Corporate author)* Arnold Engineering Development Center, ARO, Inc., Operating Contractor, Arnold Air Force Station, Tennessee 37389	2a. REPORT SECURITY CLASSIFICATION UNCLASSIFIED 2b. GROUP N/A

3. REPORT TITLE

FLOW FIELD CHARACTERISTICS BENEATH THE F-4C AIRCRAFT AT MACH NUMBERS 0.50 AND 0.85

4. DESCRIPTIVE NOTES *(Type of report and inclusive dates)*

September 18 to 23, 1969 - Final Report

This document has been approved for public release its distribution is unlimited. Per A.A. letter dtd 26 Apr 73 signed by [illegible] J. Cole

5. AUTHOR(S) *(First name, middle initial, last name)*

Ronald E. Davis, ARO, Inc.

6. REPORT DATE	7a. TOTAL NO. OF PAGES	7b. NO. OF REFS
February 1970	84	2

8a. CONTRACT OR GRANT NO. F40600-69-C-0001	9a. ORIGINATOR'S REPORT NUMBER(S) AEDC-TR-70-8
b. System 670A	
c. Program Element 63716F	9b. OTHER REPORT NO(S) *(Any other numbers that may be assigned this report)* N/A
d.	

10. DISTRIBUTION STATEMENT This document is subject to special export controls and each transmittal to foreign governments or foreign nationals may be made only with prior approval of Air Force Armament Laboratory (ATII), Eglin Air Force Base, Florida 32542.

11. SUPPLEMENTARY NOTES Available in DDC.	12. SPONSORING MILITARY ACTIVITY Air Force Armament Laboratory (ATII), Eglin Air Force Base, Florida 32542

13. ABSTRACT

Tests were conducted to investigate the flow field characteristics beneath the F-4C aircraft at high subsonic speeds. A conical-tip probe was used to measure the velocity-vector components in the region near the aircraft at Mach numbers 0.50 and 0.85. Aerodynamic force and moment data were obtained on a model of the M-117 bomb both near the aircraft and in the free stream to further evaluate the flow field. Data were obtained with a clean-wing aircraft configuration and with several combinations of M-117 bombs on the inboard wing-pylon station plus a fuel tank on the outboard wing-pylon station. Results of the test indicated that a larger region of the flow beneath the F-4C model wing is affected by store addition at Mach number 0.85 than at Mach number 0.50. Also, in some regions of the curvilinear flow field near the wing, a pitching-moment couple was produced on the store model when the model was aligned for zero normal force.

This document is subject to special export controls and each transmittal to foreign governments or foreign nationals may be made only with prior approval of Air Force Armament (ATII), Eglin Air Force Base, Florida 32542.

DD FORM 1 NOV 65 1473

PC0017

UNCLASSIFIED

Security Classification

14. KEY WORDS	LINK A ROLE	LINK A WT	LINK B ROLE	LINK B WT	LINK C ROLE	LINK C WT
F-4C aircraft						
flow distribution						
subsonic flow						
M-117 bombs						
scale models						
aerodynamic configurations						
wind tunnels						

1. Airplane -- F-4C -- Subsonic flow
2. " -- Flow
3. Bombs -- Subsonic flow
4. " --
5. Stores -- Flow
6. "

1 2

AFSC
Arnold AFS Tenn